

Morse matchings and Khovanov homology of 4-strand torus links

Tuomas Kelomäki

July 22, 2025

Abstract

Given a link or a tangle diagram, we define algorithmic Morse theoretic simplifications on their Khovanov homology. In contrast to Bar-Natan's scanning algorithm, the cancellations are postponed until the end and performed in one go. Although our novel approach is computationally inferior to Bar-Natan's algorithm, it side-steps the need for a large amount of iterations, making it more fitting for theoretical analysis. Our main application is towards integral Khovanov homology of 4-strand torus links, for which we compute non-trivial Khovanov homology groups in all homological degrees and find an abundance of 4-torsion. At the limit $T(4, \infty)$, our computations agree with a conjecture of Gorsky, Oblomkov and Rasmussen. For finite n , we use the λ -invariant of Lewark, Marino and Zibrowius to derive lower bounds on proper rational Gordian distances from $T(4, n)$.

Contents

1	Introduction	2
2	Preliminaries	5
2.1	Algebraic discrete Morse theory	5
2.2	The Bar-Natan hypercube complex and delooping	6
2.3	Morse presentations of tangles	8
3	Algorithmic matchings for Khovanov complexes	8
4	Torus braids with 4 strands	16
4.1	Upper bounds on the homological dimensions	16
4.2	Homology results: recursions and vanishing of $\text{Kh}(T(4, -n))$	20
4.3	Comparison with GOR-conjecture	22
4.4	Rational replacements and $\mathbb{Z}[G]$ -complexes	24
5	Proof of Proposition 4.1	26
6	Proof of Proposition 4.4	30
6.1	Case \mathfrak{a}_n	31
6.2	Case \mathfrak{c}_n	32
6.2.1	Task 1: setting up Φ_n	33
6.2.2	Task 2: Φ_n is well defined and invariant under R	34
6.2.3	Task 3: (co)restrictions to Φ_n coincide with the differentials	40
7	Matchings on small braids: a numerical investigation	48
	Appendix A: $\text{Kh}^{i,j}(T(4, -n))$ in lowest and highest degrees	50

1 Introduction

Khovanov homology is a powerful link invariant which categorifies the Jones polynomial [Kho00]. Due to its combinatorial nature, it is readily computable for every link diagram and nowadays there are a number of computer programs which can compute Khovanov homology of diagrams with up to 50-100 crossings within minutes [BGM09] [LL16] [Sch25a] [Zib25]. The good computability of Khovanov homology is not just an algorithmic feat: a computer calculation played a crucial role in proving that the Conway knot is not smoothly slice [Pic20] and the efficient programs open up possibilities of discovering a counterexample to the smooth 4-dimensional Poincaré conjecture [Fre+10].

Despite the fact that for any ‘small’ link L its Khovanov homology, denoted $\text{Kh}(L)$, is easily obtainable, the list of infinite link families whose Khovanov homology is known remains short. Noteworthy infinite families for which Khovanov homology is well understood include alternating and quasi-alternating links [Lee05], [MO08], $T(2, m)$ and $T(3, m)$ torus links [Kho00], [Tur08], [Gil12], [Ben17], [Cha+22], 3-strand pretzel links [Man18] and closures of 3-braids [Sch25b]. Especially significant attention has been directed to torus links $T(n, m)$. Stošić computed some of the lowest and the highest nontrivial Khovanov homology groups of certain torus links [Sto07], [Sto09]. Furthermore, he showed that Khovanov homologies admit a stable limit $\lim_{m \rightarrow \infty} \text{Kh}(T(n, m))$ when renormalized correctly. These limits $\text{Kh}(T(n, \infty))$ were given conjectural descriptions as homologies of explicit Koszul complexes by Gorsky, Oblomkov and Rasmussen [GOR13].

While a complete picture of Khovanov homology of torus links remains elusive, some related invariants have been determined for all $T(n, m)$. The decategorification, Jones polynomial, admits a closed form [ILR93] and the triply graded Khovanov-Rozansky homology is also known for positive n, m [HM19]. Recently, the Lee degeneration of Khovanov homology was also computed for all $T(n, m)$ [Ren24]. The triply graded homology and the Lee degeneration are connected to Khovanov homology via a spectral sequences $\text{HHH}(L) \Rightarrow \text{Kh}(L)$ [Ras15] and $\text{Kh}(L) \Rightarrow \mathcal{H}_{\text{Lee}}(L)$ [Ras10].

In this article we do not aim to compute Khovanov homology using any of the spectral sequences involving it. Instead, we use a more elementary, combinatorial tool called discrete Morse theory. Originally, Forman developed a discretization of the classical Morse theory as a method to simplify cell complexes up to homotopy [For98]. Later Sköldberg formulated it purely in algebraic terms [Skö06] which is more suitable for our purposes. Roughly speaking, Sköldberg’s algebraic discrete Morse theory is Gaussian elimination for chain complexes employed at a larger scale. Assuming that certain combinatorial conditions are met, one can use the theory to simultaneously cancel many pairs of direct summands, each connected by an isomorphism. This way of packaging the data enables one to avoid a large number of iterations, which would be present, if one were to perform Gaussian elimination naively.

Algebraic discrete Morse theory has been previously employed for knot homologies only very recently. In [Mal24] Maltoni used discrete Morse theory to reduce the size of Rouquier complexes of braids which define the triply graded homology. Banerjee, Chakraborty and Das wielded it on a model of Khovanov homology [Weh08] which is based on the Tait graph of the link diagram [BCD25]. The author also applied it in his previous work to compute Khovanov homologies of certain families of links [Kel24] and this article aims to unify those ideas.

In the original article, Khovanov homology was obtained from a large, explicit chain complex of \mathbb{Z} -modules. A few year later, partly motivated by the search for an efficient algorithm, Bar-Natan formulated a local theory for Khovanov homology of tangles [Bar05]. In this paper, we employ discrete Morse theory on Bar-Natan’s local complexes over cobordism categories with a special focus on braids. Given a Morse presentation of a tangle diagram, we introduce two algorithmically defined ansätze of Morse matchings on the tangle complex: a *lexicographic matching* M_{lex} and a *greedy matching* M_{gr} . For every tangle diagram, we show that M_{lex} is Morse matching but strangely, there is exactly one counter-example in a database of 2977 braid diagrams, for which M_{gr} fails to generate a meaningful Morse complex. Nevertheless, M_{gr} seems to be a more useful tool than M_{lex} when performing concrete homology calculations for infinite link families.

Our main application is towards Khovanov homology of negative¹ 4-strand torus links $T(4, -n)$

¹Negative torus links are mirror images of positive ones and Khovanov homology of a mirror link can easily be

for which we show that M_{gr} is a Morse matching and thus can be applied. Working explicitly through graph theory and combinatorics, we obtain repetitions on the level of open braid Morse complexes which, when taking the braid closure, yield:

Theorem 1.1. *The unreduced and reduced Khovanov homology groups of negative 4-strand torus links admit recursions:*

$$\text{Kh}^{i,j}(T(4, -n)) \cong \text{Kh}^{i,j-12}(T(4, -n-4)), \quad \overline{\text{Kh}}^{i,j}(T(4, -n)) \cong \overline{\text{Kh}}^{i,j-12}(T(4, -n-4))$$

for all $n, i, j \in \mathbb{Z}$ such that $n \geq 0$ and $-2n + 2i - j \geq 14$. They also admit recursions:

$$\text{Kh}^{i,j}(T(4, -n)) \cong \text{Kh}^{i-8,j-24}(T(4, -n-4)), \quad \overline{\text{Kh}}^{i,j}(T(4, -n)) \cong \overline{\text{Kh}}^{i-8,j-24}(T(4, -n-4))$$

for all $n, i, j \in \mathbb{Z}$ such that $n \geq 0$ and $-9n + 4i - 3j \geq 41$.

Combining Theorem 1.1 with some vanishing results and a hefty amount of computer base cases for induction, we obtain:

Theorem 1.2. *For $n \geq 28$, the integral Khovanov homology of negative 4-strand torus links $\text{Kh}^{i,j}(T(4, -n))$ of a certain range are displayed in Figures 1, 16 and 17. Figure 1 partially describes the middle homological degrees whereas Figures 16 and 17 fully describe the lowest and highest homological degrees respectively.*

Our results in Figure 1 also give out infinitely many $\mathbb{Z}/4\mathbb{Z}$ torsion groups in the limit $\text{Kh}(T(4, \infty))$ and arbitrarily many $\mathbb{Z}/4\mathbb{Z}$ given $T(4, n)$ with large n . Over the integers, similar 4-torsion is also present in the conjecture of Gorsky, Oblomkov and Rasmussen and when taken with \mathbb{F}_2 coefficients our calculations for $\text{Kh}(T(4, \infty); \mathbb{F}_2)$ agree with the conjecture. In addition to the two recursion of Theorem 1.1, our computations also suggest a third one which would be able to completely describe $\text{Kh}^{i,j}(T(4, n))$ for all i, j, n . While we do have a rigorous construction for the third correspondence on the level of chain spaces of the open braid complexes, we are unable to prove that it commutes with the differentials. Hence we do not manage to construct a third recursion on the level of homology groups.

Not long after Khovanov's original work, Lee showed that Khovanov homology carries an endomorphism which is also a link invariant [Lee05]. The endomorphism takes slightly different forms depending on the coefficients and whether one considers the unreduced or the reduced Khovanov homology [Ras10], [Bar05], [Tur06]. A unified approach to this array of homology theories can be taken by associating to a knot K a homotopy class of chain complexes $\text{BN}(K)$ of graded $\mathbb{Z}[G]$ -modules where G is a formal variable [Nao06]. From this $H(\text{BN}(K) \otimes_{\mathbb{Z}[G]} \mathbb{Z}[G]/(G))$ recovers the reduced Khovanov homology $\overline{\text{Kh}}(K)$ and the unreduced one can be also retrieved as well. Although we are unable to completely compute the whole Khovanov homology of 4-strand torus knots, let alone $\text{BN}(T(4, 2n+1))$, we manage to show in Proposition 4.10 that an indecomposable subcomplex of the form:

$$\begin{array}{ccccc} & & \mathbb{Z}[G] & & \\ & \nearrow^{G^2} & & \searrow^2 & \\ \mathbb{Z}[G] & & \oplus & & \mathbb{Z}[G] \\ & \searrow_{2G} & & \nearrow_{-G} & \\ & & \mathbb{Z}[G] & & \end{array} \quad (1)$$

splits from $\text{BN}(T(4, 2n+1))$ in the highest non-trivial homological degrees when $n \geq 2$.

The majority of geometric applications of Khovanov homology stem from the Rasmussen s -invariants. These integers $s_{\mathbb{F}}(K)$ can be recovered from quantum grading of the free part of $\text{BN}(K) \otimes_{\mathbb{Z}[G]} \mathbb{F}[G]$. In Rasmussen's original paper, $s_{\mathbb{Q}}(K)$ was computed for all positive knots K which gave a combinatorial proof for the slice genus and unknotting numbers of all torus knots $T(n, m)$.

taken from the dual chain complex. We follow the conventions of [Cha+22] except that we enforce that $T(4, -n)$ has negative crossings and thus its Khovanov homology is supported on the non-positive homological degrees for $n > 0$.

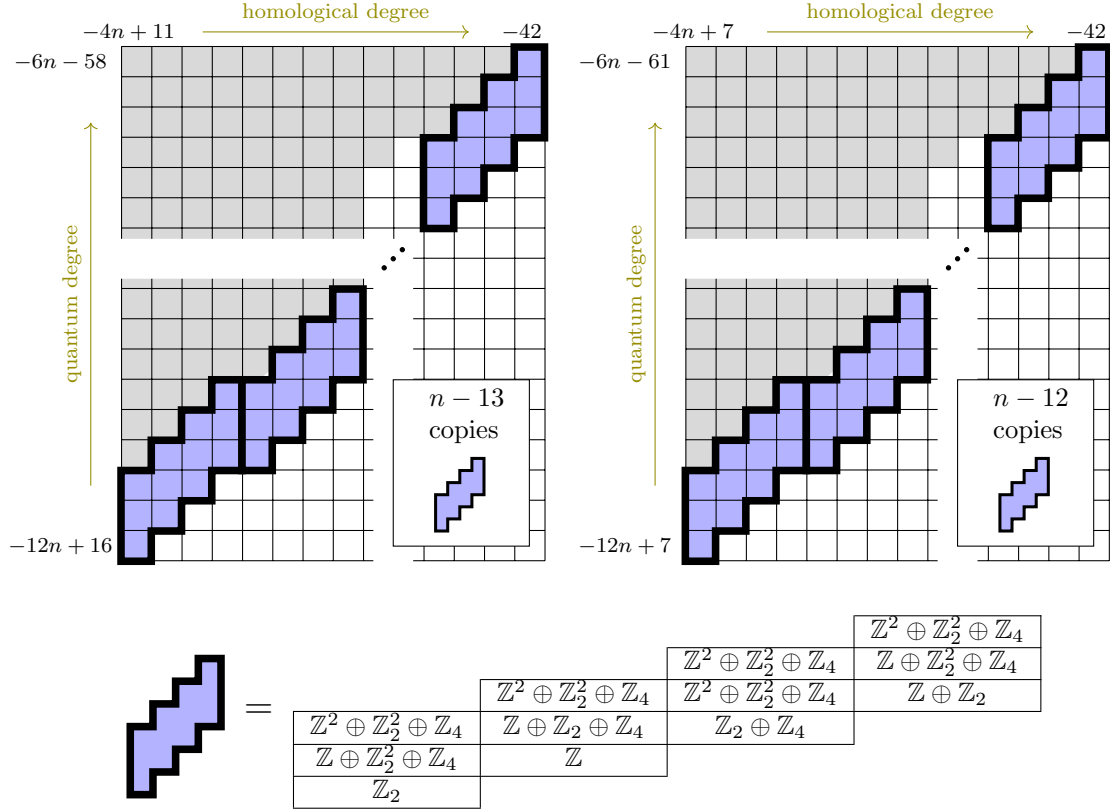


Figure 1: For $n \geq 14$, the unreduced integer Khovanov homology $\text{Kh}^{i,j}(T(4, -2n))$ (top left) and $\text{Kh}^{i,j}(T(4, -2n-1))$ (top right) and the reoccurring block (bottom). The homology remains unknown in the gray area above the purple blocks and it vanishes below them. More precisely, the top left table describes $\text{Kh}^{i,j}(T(4, -2n))$ only when $i \in [-4n+11, -42]$ and $j \leq \frac{3}{2}i - 6n + 5$. The top right table describes $\text{Kh}^{i,j}(T(4, -2n-1))$ when $i \in [-4n+7, -42]$ and $j \leq \frac{3}{2}i - 6n + 2$. Outside these homological degrees $\text{Kh}^{i,j}(T(4, -2n))$ and $\text{Kh}^{i,j}(T(4, -2n-1))$ are described completely in Figures 16 and 17 in Appendix A.

Another source of geometric applications of Khovanov homology come from the G -torsion part of $\text{BN}(K)$. In the first edition of these G -torsion invariants, Alishahi and Dowlin showed that $u_{\mathbb{F}_2}(K) \leq u(K)$ where $u_{\mathbb{F}_2}(K)$ is the maximum order of G -torsion in $\text{BN}(K) \otimes_{\mathbb{Z}[G]} \mathbb{F}_2[G]$ and $u(K)$ is the unknotting number of K [Ali19], [AD19]. Iltgen, Lewark and Marino refined $u_{\mathbb{F}_2}(K)$ to $\lambda(K)$ which works over the integers and includes the information carried by the chain homotopy type of $\text{BN}(K)$. Moreover, they showed that λ defines pseudo metric on knots and that $\lambda(K_1, K_2) \leq u_q(K_1, K_2)$ where u_q denotes the rational Gordian distance, that is, the minimum number of proper rational tangle replacements needed to go from K_1 to K_2 . The invariant λ was further refined in [LMZ24] to accommodate for grading shifts.

Since $s_{\mathbb{F}}(K)$ has already been computed for torus knots, we will rely on the λ to make a modest new geometric application of our homology computations: The following proposition, which mimics Theorem 1.4 and Proposition 4.6 from [LMZ24], can be obtained as a corollary of (1).

Proposition 1.3. *Suppose K is a knot which admits a diagram with c_+ positive crossings. If $n \geq 2$ and $c_+ \leq 4n$ then $u_q(T(4, 2n+1), K) \geq 2$. Distinct 4-strand torus knots are at least 2 rational replacements from each other: $u_q(T(4, n), T(4, m)) \geq 2$ whenever $n, m \in 2\mathbb{Z}+1$, $n \neq m$ and $|n|, |m| \geq 5$.*

To prove (1) and thus Proposition 1.3 we first computed the reduced non-equivariant Khovanov

homology $\overline{\text{Kh}}(T(4, 2n+1))$ using Theorem 1.1. Since the homology is reasonably ‘thin’ in the highest degrees, we can guess the G -action on the homology, essentially by using the fact that the reduced Lee spectral sequence converges to 0 in those degrees. It is noteworthy that this tactic would not have sufficed had we done our main Khovanov homology computations over any one field, instead of over the integers. With field coefficients, the necessary G -action for λ could not be determined from the non-equivariant homology alone.

Structure of the paper. In Section 2 we introduce discrete Morse theory and our encoding of tangles and their Khovanov complexes. Section 3 lays out our protagonists M_{lex} and M_{gr} . Almost all results of this paper are contained in Section 4 where homological recursions are derived from the open braid complex ones. The proofs of these braid recursions take up the next two sections. Finally in Section 7, we numerically examine the effectiveness of our Morse theoretic simplifications and display the curious braid diagram, where M_{gr} breaks down.

Computer assistance in this paper. The following computer tools have been used in deriving the main mathematical results:

- **Khoca**[LL16], was used to compute the reduced and unreduced integer Khovanov homologies which played the role of base cases in the proofs of Theorem 1.2 and Proposition 4.10.
- Simple custom made **Python** program **basecases.py** was used to verify base cases for inductions in Lemmas 4.5, 5.3 and 6.2. It evaluates rational valued functions on specific sets of formal strings. **Python** was also used to verify that Theorem 1.2 holds for $n = 28, \dots, 82$ before the induction kicks in.
- **Lean**’s linarith tactic [MU21] was used to deduce linear inequalities from sets of linear inequalities in the proofs of Theorem 1.2, Corollary 4.2, Proposition 4.10 and Lemma 6.2.
- **Mathematica** was used in Proposition 4.9 to extract power series coefficients from an expansion of a rational function related to the the GOR-conjecture.

Additionally to obtain numerical results in Section 7, a software written by the author **braidalgo.py**, which computes the greedy matching for any braid diagram, and **kht++** [Zib25] were utilized. The data of the base cases and the aforementioned code can be found in [Kel25].

Acknowledgments. The author was supported by the Väisälä Fund of the Finnish Academy of Science and Letters. The author would like to thank Gregory Arone, Jouko Kelomäki, Oscar Kivinen, Kalle Kytölä, Lukas Lewark, Milo Orlich, Dirk Schütz and Claudius Zibrowius for useful discussions and technical and moral support.

2 Preliminaries

In this section we lay out the main tool, discrete Morse theory, and our conventions for local Khovanov complexes.

2.1 Algebraic discrete Morse theory

Let \mathbf{C} be an additive category. A *based* chain complex C is a chain complex over \mathbf{C} with a fixed *basis*, that is, fixed direct sum decomposition $C^i = \bigoplus_{j \in J_i} C_j^i$ on every *chain space* C^i . A *matrix element* of a based complex C is

$$d_{C_k^{i+1}, C_j^i} : C_j^i \rightarrow C_k^{i+1}, \quad d_{C_k^{i+1}, C_j^i} = \pi d^i \iota$$

where ι and π are the canonical inclusion and projection morphisms associated to the direct sums. A based complex induces a simple directed graph $G(C) = (V, E)$ whose vertices are the summands C_j^i and directed edges are non-zero matrix elements. Choosing a subset of edges $M \subset E$ generates another directed graph $G(C, M) = (V', E')$ by reversing the edges of M , that is, $V' = V$ and

$$E' = (E \setminus M) \cup \{b \rightarrow a \mid (a \rightarrow b) \in M\}.$$

We call the set of edges M a *Morse matching* on $G(C)$, if

1. M is finite.
2. M is a matching, i.e., its edges are pairwise non-adjacent.
3. For every edge $f \in M$, the corresponding matrix element f is an isomorphism in \mathbf{C} .
4. $G(C, M)$ has no directed cycles.

We often do not distinguish between vertices of $G(C)$ and $G(C, M)$ and the summands of C and refer to all of them as *cells* and denote the collection of all of them by $\text{cells}(C)$. A cell x is called *unmatched* if x is not the domain or the codomain of any $f \in M$. Abusing the notation slightly, we can consider the graph $G(C, M)$ as a category, whose morphisms are paths and identity morphisms are paths of length 0. This allows one to define a *remembering functor* $R: G(C, M) \rightarrow \mathbf{C}$ which maps an edge $f \in E \setminus M$ to the corresponding matrix element f in \mathbf{C} and a reversed edge g of M to $-g^{-1}$ in \mathbf{C} . (Naturally, the functor R depends heavily on C and M .)

We can now define the based *Morse complex* (MC, ∂) whose basis is given by the unmatched cells of C . The matrix elements of MC are given by

$$\partial_{b,a} = \sum_{p \in \{\text{paths: } a \rightarrow b\}} R(p)$$

which completely define the differentials ∂^i . As a sanity check, the empty matching $M = \emptyset$ recovers the original complex $C = MC$ and matching of one edge $M = \{f\}$ recovers Gaussian elimination of chain complexes, Lemma 3.2 from [Bar06]. A consequence of Condition 2 is that only those paths which zig-zag between two adjacent homological degrees will end up contributing to ∂ .

Theorem 2.1 (Sköldberg [Skö06]). *If M is a Morse matching on $G(C)$, then $C \simeq MC$.*

Although we will not need them in this article, the explicit chain maps of Theorem 2.1 can also be written as sums of paths: the maps $f: C \rightarrow MC$ and $g: MC \rightarrow C$ are defined by their matrix elements with

$$\pi_b f \iota_a = \sum_{p \in \{\text{paths: } a \rightarrow b\}} R(p), \quad \pi_d g \iota_c = \sum_{p \in \{\text{paths: } c \rightarrow d\}} R(p)$$

where ι_a, ι_c, π_b and π_d are again the canonical projection and inclusion morphisms with respect to C and MC . The map g could be used to track back a homology cycle of MC to a cycle of C . Explicit homology cycles are important in Khovanov homology since they are needed to evaluate the induced homomorphisms which in turn can be used to distinguish exotically embedded smooth surfaces in B^4 , see [HS24]. Recently this strategy was used in [BCD25], where discrete Morse theory was employed on a graph theoretic model of Khovanov homology to obtain explicit homology cycles which were used to obtain a new family of exotic surfaces.

2.2 The Bar-Natan hypercube complex and delooping

In [Bar05] Bar-Natan constructed from a tangle diagram T with $2n$ endpoints a local Khovanov complex $\llbracket T \rrbracket$ over the category $\text{Mat}(\text{Cob}_{\bullet}^3(2n))$ which we will review here. The building blocks of this category are of the form $c\{m\}$ where c is a crossingless planar diagrams and $m \in \mathbb{Z}$ is a quantum grading shift. Furthermore, one adds finite formal direct sums to the mix, so that a generic object in $\text{Mat}(\text{Cob}_{\bullet}^3(2n))$ is written as $\bigoplus_i c_i\{m_i\}$. The morphisms of $\text{Mat}(\text{Cob}_{\bullet}^3(2n))$ are matrices whose entries are of formal sums of dotted cobordisms. These formal sums of cobordisms are considered up to boundary preserving isotopy, moving the dots around and the “dotted” relations depicted in Figure 2. The morphisms are graded, so that if $f: c_1\{m_1\} \rightarrow c_2\{m_2\}$ is a cobordism, then $\deg(f) = \chi(f) - 2 \cdot \#(\text{dots in } f) + n + m_2 - m_1$ where $\chi(f)$ is the Euler characteristic of the underlying cobordism f . We will only consider morphisms of degree 0.

Due to the relations imposed on cobordisms, the category $\text{Mat}(\text{Cob}_{\bullet}^3(2n))$ admits a local delooping isomorphism Ψ depicted in Figure 3. Iteratively removing loops with Ψ , one obtains a global isomorphism

$$\Psi_{c\{m\}}: c\{m\} \rightarrow \bigoplus_{K \subset L_c} c'\{m + 2 \cdot \#K - \#L_c\}$$

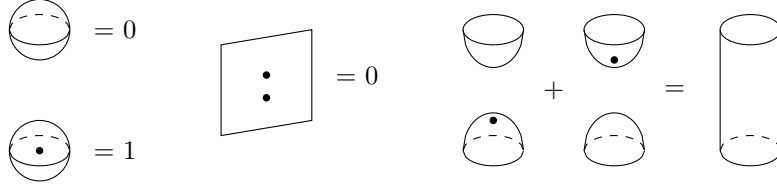


Figure 2: The dotted relations of $\text{Mat}(\text{Cob}^3_\bullet(2n))$.

where L_c is the set of loops in c and c' is the planar diagram of c with all of the loops removed. We denote Ψc for the codomain of Ψc and graphically represent a direct summand of Ψc by coloring the loops contained in K with red and those in $L_c \setminus K$ blue. By acting diagonally, Ψ can be extended to formal direct sums and for any object a .

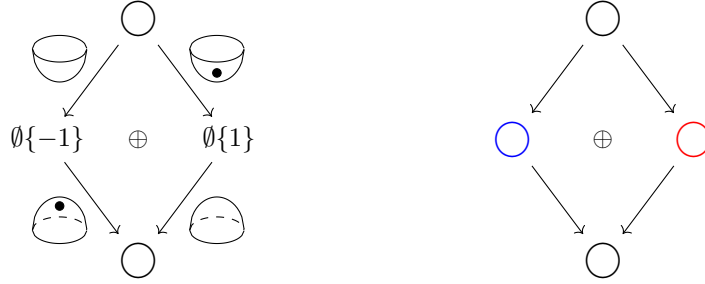


Figure 3: For a diagram which consists of only a single circle: delooping isomorphism Ψ and its inverse Ψ^{-1} . The cobordism of the matrix elements of Ψ and Ψ^{-1} are displayed on the left and our diagrammatic convention for the delooped objects is shown on the right.

The standard Bar-Natan hypercube complex $(\llbracket T \rrbracket, d)$ is generated from the tangle diagram T by resolving every crossing \times with either a 0-smoothing \smile or a 1-smoothing \frown . If a single crossing is 0-smoothed in c_0 and 1-smoothed in c_1 and the diagrams c_0 and c_1 coincide otherwise, then the matrix element d_{c_1, c_0} is the simplest saddle cobordism between c_0 and c_1 with a sign $s \in \{-, +\}$ which is explained later. Suppose that T has n_+ and n_- positive and negative crossings, see Figure 4 for conventions, and c is a diagram with k number of 1-smoothings, then c will have homological degree $k - n_-$ and quantum degree shift $k + n_+ - 2n_-$.

In the hypercube complex $(\llbracket T \rrbracket, d)$, all of the morphisms are saddles which in particular means that there are no isomorphisms and discrete Morse theory will not make a dent on $\llbracket T \rrbracket$. Instead we work with $\Psi\llbracket T \rrbracket$ whose the chain spaces are defined as $\Psi(\llbracket T \rrbracket^i)$ and the differential are pulled back from d and defined as $\Psi d^i \Psi^{-1}$. The basis of $\Psi\llbracket T \rrbracket$ consists of diagrams with black line segments from the boundary to the boundary accompanied with red and blue colored circles. The following lemma allows us to classify the matrix elements of $\Psi\llbracket T \rrbracket$ in a local manner. Its proof is a case-by-case application of the relations in Figure 2 and we omit it.

Lemma 2.2. *Let T be tangle diagram and suppose $d_{b,a}$ is a matrix element of $\Psi\llbracket T \rrbracket$ where a, b are completely smoothed pictures with red/blue colored loops. If a and b agree everywhere except for a local change displayed in Figure 5, pictures i)-vi), then $d_{b,a}$ is an isomorphism. If a and b agree everywhere except for a local change of pictures vii)-ix), then $d_{b,a}$ is neither a zero morphism nor an isomorphism. Otherwise $d_{b,a} = 0$.*

The cells of $\Psi\llbracket T \rrbracket$ are large pictures, but often we only care about some of their local aspects. In particular, when drawing local diagrams we are typically very interested in the colors of some loops, but less concerned whether other components in the global picture form red or blue loops, or whether they are connected to the boundary and are thus colored black. In these cases, we draw the less important components with green as to say that a local phenomenon can be lifted into any of the global pictures of $\Psi\llbracket T \rrbracket$ that are obtained by replacing the green color with red, blue or black

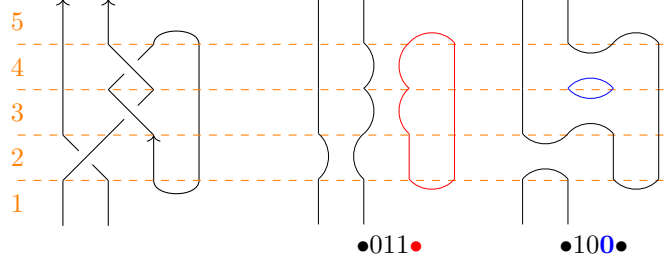


Figure 4: Morse presentation of an oriented tangle with 5 Morse layers. On layer 2 we see a positive crossing and on layers 3 and 4 we see negative ones. On the right we see 2 examples of cells in $\Psi[[T]]$ with their symbolic encodings.

individually in each component. As an example, the isomorphisms of Figure 5 can be divided into two classes: *merge-type* and *split-type*, see Figure 6.

2.3 Morse presentations of tangles

Topologically, a tangle T is an embedded smooth 1-manifold in B^3 with possibly a non-empty boundary which intersects $S^2 = \partial B^3$ transversally. Two tangles are equivalent, if they are related by a boundary fixing ambient isotopy. In this paper, we will work with (highly non-unique) combinatorial descriptions of tangles as *Morse presentations*. They consist of a strings at top and b at the bottom with $a + b \in 2\mathbb{Z}_{\geq 0}$. In between there is a finite number of *Morse layers* consisting of either of the two crossings \times , \times , a cap \cap or a cup \cup accompanied with an appropriate number of vertical bars $|$ to match the connectivities. An oriented tangle diagram and our conventions for positive and negative crossings can be seen in Figure 4.

To proceed efficiently, we will introduce a symbolic way of encoding summands of $[[T]]$ and $\Psi[[T]]$, where T is a Morse presentation of a tangle. For $[[T]]$, the Morse layers from bottom to top are written from left to right with symbols 0 and 1 denoting smoothings of crossings and \bullet placed whenever the Morse layer is a cap or a cup. A matrix element $d_{b,a}$ of $[[T]]$ changes 0-symbol of a to 1-symbol of b at some index $1 \leq i \leq n$. The sign s of $d_{b,a}$ is defined as $(-1)^k$ where k is the number of symbols 1 in a with indices $j < i$.

For $\Psi[[T]]$ the colors of loops need to be stored as well: given a loop l in a cell a of $\Psi[[T]]$, we denote the highest Morse layer which contains a piece of l , by $\max(l)$. The color of the loop l is engraved to symbol of a at index $\max(l)$. Thus for an n -layered Morse presentation of a tangle T , the summands of $[[T]]$ and $\Psi[[T]]$ are *symbolically encoded* with words of $\{0, 1, \bullet\}^n$ and $\{0, \text{blue}, \text{red}, 1, \text{blue}, \text{red}, \bullet, \text{blue}, \text{red}\}^n$ respectively, see Figure 4 for examples. Due to technical reasons, we allow for degenerate tangles with zero Morse layers and n degenerate vertical lines. For a degenerate tangle T the unique summand of $[[T]]$ and $\Psi[[T]]$ is denoted with e .

3 Algorithmic matchings for Khovanov complexes

In this section, we will define a greedy matching on Khovanov complexes of tangles with fixed Morse presentations. In it, the following two maps play a crucial role:

$$\begin{aligned} i: \{\text{matrix elements of } \Psi[[T]]\} &\rightarrow \mathbb{Z}_{>0} \\ u: \{\text{isomorphism matrix elements of } \Psi[[T]]\} &\rightarrow \mathbb{Z}_{>0}. \end{aligned}$$

For a matrix element $a \rightarrow b$ of $\Psi[[T]]$ we define $i(a \rightarrow b)$ to be the index of the Morse layer for which a character 0, blue or red of a changes to a character 1, blue or red of b . Denote $L_{a \rightarrow b}$ to be the set of red loops in a merged by $a \rightarrow b$ and blue loops in b split out by $a \rightarrow b$. Notice that by Lemma 2.2 we have $L_{a \rightarrow b} \neq \emptyset$ if and only if $a \rightarrow b$ is an isomorphism. Hence we can define $u(a \rightarrow b) = \min\{\max(l) \mid l \in L_{a \rightarrow b}\}$ and one should note that $i(a \rightarrow b) \leq u(a \rightarrow b)$ always holds. Given a (candidate) Morse matching

Isomorphisms:	
i)	ii)
iii)	iv)
v)	vi)
Non-trivial morphisms:	
vii)	viii)
ix)	

Figure 5: A local dictionary for matrix elements of $\Psi[[T]]$. The pictures i)-vi) represent identity cobordisms. The pictures vii) and viii) correspond to adding a dot to the black component whereas ix) is a saddle.

Merge-type	Split-type

Figure 6: Using green as a placeholder color for red, blue or black, we can divide the isomorphisms of Figure 5 into two classes. Types i), ii) and v) amount to the merge-type, whereas iii), iv) and vi) make up the split-type.

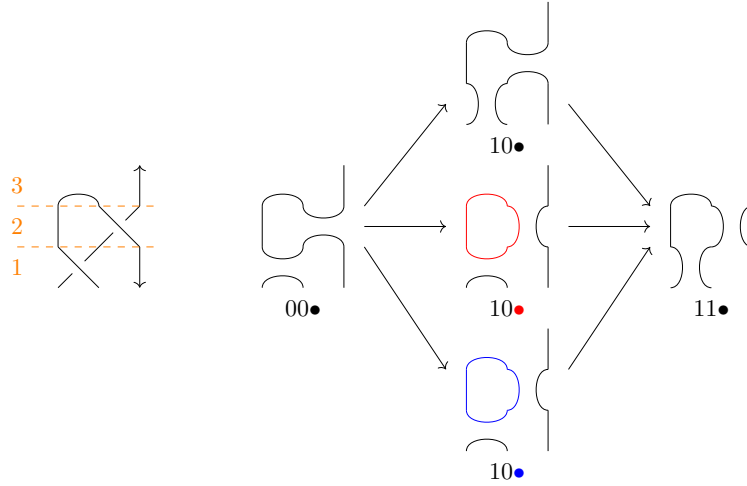


Figure 7: A Morse presentation of a tangle T (left) and its delooped hypercube complex $\Psi[[T]]$ (right). The complex has two isomorphisms, $f: 00\bullet \rightarrow 10\bullet$ and $g: 10\bullet \rightarrow 11\bullet$ which satisfy $i(f) = 2$, $i(g) = 1$ and $u(f) = u(g) = 3$. Both isomorphism get matched in M_{gr} and hence $M_{\text{gr}}\Psi[[T]]$ consists of only the picture $10\bullet$ which in turn proves invariance of Khovanov homology under Reidemeister 2 move.

M and an edge $(a \rightarrow b) \in G(\Psi[T], M)$ we are often somewhat loose with the orientations and write $i(a \rightarrow b)$ and $u(a \rightarrow b)$ regardless of whether $a \rightarrow b$ or $b \rightarrow a$ actually represents a matrix element of $\Psi[T]$.

For a fixed tangle T and $j, k \in \mathbb{Z}_{>0}$ we define $A_{j,k} = i^{-1}\{j\} \cap u^{-1}\{k\}$. Furthermore, we set $N_1 = M_{1,1} = A_{1,1}$ and recursively assign for any $j \in \mathbb{Z}_{>0}$

$$N_j = \{(a \rightarrow b) \in A_{j,j} \mid a, b \text{ are not matched in any } N_l \text{ with } l < j\}$$

and for any pair $j, k \in \mathbb{Z}_{>0}$

$$M_{j,k} = \left\{ (a \rightarrow b) \in A_{j,k} \left| \begin{array}{l} a, b \text{ are not matched in any } M_{l,m} \\ \text{with } m < k \\ \text{or with } m = k \text{ and } j > l \end{array} \right. \right\}.$$

Finally we define *the lexicographic matching* to be $M_{\text{lex}} = \bigsqcup_j N_j$ and *the greedy matching*² to be $M_{\text{gr}} = \bigsqcup_{j,k} M_{j,k}$.

It is immediate that both M_{lex} and M_{gr} satisfy Conditions 1-3 of being a Morse matching. In Proposition 3.4 we prove that $G(\Psi[T], M_{\text{lex}})$ is always acyclic and thus M_{lex} a Morse matching for all tangle diagrams. Curiously, the matching M_{gr} is not always acyclic, although it often appears to be; in Section 7 we find that in a test set of 2977 braid diagrams for exactly one B the graph $G(\Psi[B], M_{\text{gr}})$ contains directed cycles.

Although, M_{gr} has the obvious aforementioned caveat that it does not always work, for concrete homology calculations it seems to be a more useful tool than M_{lex} . In previous work of the author [Kel24], explicit Morse matchings were imposed on 2- and 3-strand torus braids. These ad hoc matchings can now be seen as instances of M_{gr} and hence their acyclicity proofs (Lemmas 3.2 and 4.1 from [Kel24]) show that graphs $G(\Psi[\sigma_1^n], M_{\text{gr}})$ and $G(\Psi[(\sigma_1\sigma_2)^n], M_{\text{gr}})$ contain no directed cycles. For 4-strand torus braids, M_{gr} also gives an acyclic matching which is proven in Proposition 3.6. This leads to the following conjecture:

Conjecture 3.1. *The greedy matching is a Morse matching for all torus braids, that is, the graphs $G(\Psi[(\sigma_1 \dots \sigma_{m-1})^n], M_{\text{gr}})$ contain no directed cycles for all n, m .*

Both M_{lex} and M_{gr} are defined on the whole graph $G(\Psi[T])$, but in practice one can ignore large portions of $G(\Psi[T])$ when evaluating M_{lex} and M_{gr} . In this sense they bear resemblance to Bar-Natan's scanning algorithm [Bar06], where small "local" cancellations end up massively reducing the large "global" complex. To efficiently³ construct $M_{\text{lex}}\Psi[T]$ and $M_{\text{gr}}\Psi[T]$, two questions need to answered:

$$\text{Given a tangle diagram } T, \text{ what are the unmatched cells of } M_{\text{lex/gr}}\Psi[T]? \quad (2)$$

$$\text{Given unmatched cells } a \text{ and } b, \text{ what are all paths from } a \text{ to } b \text{ in } G(\Psi[T], M_{\text{lex/gr}})? \quad (3)$$

The cells of $\Psi[T]$ can be represented as formal words of symbols which is why we can also manipulate them as such. To do so, we denote \mathcal{S} as the free monoid generated by symbols $0, \mathbf{0}, \mathbf{1}, \mathbf{1}, \bullet, \bullet, \bullet$, that is, as a set

$$\mathcal{S} = \bigcup_{n=0}^{\infty} \{0, \mathbf{0}, \mathbf{1}, \mathbf{1}, \bullet, \bullet, \bullet\}^n.$$

The multiplication in \mathcal{S} is the concatenation of words and marked with $[\cdot]$, e.g. $0\mathbf{1}\bullet\mathbf{1} = 0\mathbf{1}\bullet\mathbf{1}$ and the neutral element is denoted with e . The number of characters in a word w is denoted with $|w|$.

²The matching M_{lex} is named *lexicographic*, as it seems to move $\mathbf{0}$ and $\mathbf{1}$ characters to the lower Morse layers in an orderly fashion. The matching M_{gr} is labeled greedy, since it is a maximal partial matching on $G(\Psi[T])$ that is, there does not exist any strictly larger partial matching of isomorphisms containing M_{gr} .

³In terms of *computational efficiency*, Bar-Natan's algorithm seems to greatly outperform our use of discrete Morse theory. Hence we aim towards *mathematical efficiency*, by which we mean that we hope to construct an easy-to-use theory and prove theorems using it.

Given a tangle diagram T , we define $\text{cut}_m(T)$ as the tangle consisting of the first m Morse layers of T . For a formal set of words $W \subset \text{cells}(\text{cut}_m(T)) \subset \mathcal{S}$ we denote $\text{expand}(W)$ as the set of all sensible continuations of W under T , that is,

$$\text{expand}(W) = \{w.s \in \text{cells}(\text{cut}_{m+1}(T)) \mid w \in W, s \in \{0, \mathbf{0}, \mathbf{0}, 1, \mathbf{1}, \mathbf{1}, \bullet, \bullet, \bullet\}\}.$$

It is easy to see that for any tangle diagram T , we have $\text{cells}(\Psi[T]) = \text{expand} \circ \dots \circ \text{expand}(\{e\})$. We can now algorithmically answer Question 2 for M_{lex} and for M_{gr} .

Algorithm 1 Obtaining unmatched cells of $M_{\text{lex}}\Psi[T]$ and answering Question 2, case M_{lex} .

Input T , a Morse presentation of a tangle diagram.

Output U , the set of unmatched cells of $M_{\text{lex}}\Psi[T]$.

- 1: $U \leftarrow \{e\}$
 - 2: **for** $k=1, \dots, \#\text{Morse layers of } T$ **do**
 - 3: $U \leftarrow \text{expand}(U)$
 - 4: Remove all pairs of cells (a, b) from U with $i(a \rightarrow b) = u(a \rightarrow b) = k$
 - 5: **return** U
-

Algorithm 2 Obtaining unmatched cells of $M_{\text{gr}}\Psi[T]$ and answering Question 2, case M_{gr} .

Input T , a Morse presentation of a tangle diagram.

Output U , the set of unmatched cells of $M_{\text{gr}}\Psi[T]$.

- 1: $U \leftarrow \{e\}$
 - 2: **for** $k=1, \dots, \#\text{Morse layers of } T$ **do**
 - 3: $U \leftarrow \text{expand}(U)$
 - 4: **for** $j=k, \dots, 1$ **do**
 - 5: Remove all pairs of cells (a, b) from U with $i(a \rightarrow b) = j$ and $u(a \rightarrow b) = k$
 - 6: **return** U
-

In a directed acyclic graph, the set of all paths from a to b can be obtained by using an exhaustive depth-first search. For a cell v in the graph $G(\Psi[T])$, the set of edges arriving to v or departing from v can easily be attained, but it is not obvious which ones are contained in $M_{\text{lex/gr}}$, that is, which edges are reversed. Naturally, this information is crucial in constructing the set of all paths from a to b . It follows that we can use an exhaustive search to answer Question 3 assuming that we first give an answer to the following question:

Given $a \in \text{cells}(\Psi[T])$, what is the cell a is matched to in $M_{\text{lex/gr}}$ or is a is left unmatched? (4)

In addition to existence, the properties of a single edge f in $G(\Psi[T])$ are also not hard to investigate; Lemma 2.2 tells us whether f is an isomorphism and $i(f), u(f)$ are easy to compute. Combining these one can straightforwardly decide whether in $G(\Psi[T])$ there exists an isomorphism edge f to, or from, a with specific values $i(f)$ and $u(f)$. This is to say that given a cell a and integers j, k one can evaluate the function:

$$\text{isopair}(a, j, k) = \begin{cases} b, & \text{if } \exists f: a \rightarrow b, f \text{ isomorphism edge of } G(\Psi[T]), i(f) = j, u(f) = k \\ b, & \text{if } \exists g: b \rightarrow a, g \text{ isomorphism edge of } G(\Psi[T]), i(g) = j, u(g) = k \\ \star, & \text{otherwise} \end{cases}$$

Using this, we can answer Question 4 for M_{lex} , where the algorithm is simple, and for M_{gr} , where a possibly branching recursion is needed.

Lemma 3.2. *Let x, y be cells of $\Psi[T_1]$ and $\Psi[T_2]$ respectively. Assume that first m Morse layers of T_1 and T_2 agree and the first m characters on the symbolic encodings of x and y also coincide.*

Algorithm 3 Matching a vertex in $M_{\text{lex}}\Psi[[T]]$ and answering Question 4, case M_{lex} .

Input $a \in \text{cells}(\Psi[[T]])$, tangle diagram T is implicit

Output a is unmatched or a is matched to $b \in \text{cells}[[T]]$ in M_{lex}

```

1: for  $k=1, \dots, \# \text{Morse layers of } T$  do
2:    $b \leftarrow \text{isopair}(a, k, k)$ 
3:   if  $b \neq \star$  then
4:     return  $a$  matched to  $b$ 
5: return  $a$  unmatched

```

Algorithm 4 Matching a vertex in $M_{\text{gr}}\Psi[[T]]$ and answering Question 4, case M_{gr} .

Input $a \in \text{cells} \Psi[[T]]$, tangle diagram T is implicit

Output a is unmatched or a is matched to $b \in \text{cells}[[T]]$ in M_{gr}

```

1: function MATCHESBACK( $x, y$ )
2:   if  $x = \star$  then
3:     return False
4:   for  $k=1, \dots, \# \text{Morse layers of } T$  do
5:     for  $j=k, \dots, 1$  do
6:        $z \leftarrow \text{isopair}(x, j, k)$ 
7:       if  $z=y$  then
8:         return True
9:       else if MATCHESBACK( $z, x$ ) then
10:        return False
11:
12: for  $k=1, \dots, \# \text{Morse layers of } T$  do
13:   for  $j=k, \dots, 1$  do
14:      $b \leftarrow \text{isopair}(a, j, k)$ 
15:     if MATCHESBACK( $b, a$ ) then
16:       return  $a$  matched to  $b$ 
17: return  $a$  unmatched

```

The following equivalences hold:

$$\exists a_1: (a_1 \rightarrow x) \in M_{\text{lex}}, u(a_1 \rightarrow x) \leq m \iff \exists a_2: (a_2 \rightarrow y) \in M_{\text{lex}}, u(a_2 \rightarrow y) \leq m \quad (5)$$

$$\exists b_1: (x \rightarrow b_1) \in M_{\text{lex}}, u(x \rightarrow b_1) \leq m \iff \exists b_2: (x \rightarrow b_2) \in M_{\text{lex}}, u(x \rightarrow b_2) \leq m \quad (6)$$

$$\exists c_1: (c_1 \rightarrow x) \in M_{\text{gr}}, u(c_1 \rightarrow x) \leq m \iff \exists c_2: (c_2 \rightarrow y) \in M_{\text{gr}}, u(c_2 \rightarrow y) \leq m \quad (7)$$

$$\exists d_1: (x \rightarrow d_1) \in M_{\text{gr}}, u(x \rightarrow d_1) \leq m \iff \exists d_2: (x \rightarrow d_2) \in M_{\text{gr}}, u(x \rightarrow d_2) \leq m. \quad (8)$$

Proof. We first claim the following auxiliary result: For cells $w.r_1$ of $\Psi[[T_1]]$, $w.r_2$ of $\Psi[[T_2]]$ and $j, k \leq |w|$, we have $\text{isopair}((w.r_1), j, k) \in \{\star\} \cup \{v.r_1 \mid v \in \mathcal{S}\}$ and

$$\begin{aligned} \text{isopair}((w.r_1), j, k) = \star &\implies \text{isopair}((w.r_2), j, k) = \star \\ \text{isopair}((w.r_1), j, k) = v.r_1, \quad |v| = |w| &\implies \text{isopair}((w.r_2), j, k) = v.r_2. \end{aligned}$$

The auxiliary result holds due to the fact that a loop in the vertex $w.r_1$, which realizes the value of u , has to be completely contained in Morse layers $1, \dots, |w|$ and remains unaffected when swapping r_1 with r_2 .

In the lemma, the existence of a_1, a_2, b_1 and b_2 can be obtained by running Algorithm 3 for (x, T_1) and (y, T_2) and stopping when $k = m + 1$. Similarly, the existence of c_1, c_2, d_1 and d_2 is attained from Algorithm 4. The statement of the lemma follows now from analyzing the algorithms separately with the auxiliary result: for both inputs x and y the same number of orders is executed and line-by-line their action can be controlled with the auxiliary result. \square

Lemma 3.3. *Let $a \rightarrow b \rightarrow c$ be a path in $G(\Psi[[T]], M_{\text{lex/gr}})$ with $(b \rightarrow a) \in M_{\text{lex/gr}}$ and $(c \rightarrow d) \notin M_{\text{lex/gr}}$ for all d . Then $i(b \rightarrow c) \leq u(a \rightarrow b)$. Dually, let $e \rightarrow f \rightarrow g$ be a path in $G(\Psi[[T]], M_{\text{lex/gr}})$ with $(g \rightarrow f) \in M_{\text{lex/gr}}$ and $(h \rightarrow e) \notin M_{\text{lex/gr}}$ for all h . Then $i(e \rightarrow f) \leq u(f \rightarrow g)$.*

Notice that if $a \rightarrow b \rightarrow c$ or $e \rightarrow f \rightarrow g$ are subpaths of either a cycle or a path contributing towards the differential ∂ of $M_{\text{lex/gr}} \Psi[[T]]$, then the conditions $(c \rightarrow d), (h \rightarrow e) \notin M_{\text{lex/gr}}$ automatically hold. This follows from Condition 2 of Morse matching which $M_{\text{lex/gr}}$ satisfy by construction.

Proof. If $i(b \rightarrow c) > u(a \rightarrow b)$, then b and c agree on the first $u(a \rightarrow b)$ characters. Hence by Lemma 3.2 there has to exist $(c \rightarrow d) \in M_{\text{lex/gr}}$ contradicting our assumptions. The case $e \rightarrow f \rightarrow g$ is analogous. \square

Proposition 3.4. *For any tangle diagram T , the lexicographic matching M_{lex} is a Morse matching on $\Psi[[T]]$.*

Proof. Assume towards contradiction that there exists a directed cycle L in $G(\Psi[[T]], M_{\text{lex}})$. Let $a \rightarrow b \rightarrow c \rightarrow d$ be a subpath of L such that $(c \rightarrow b) \in M_{\text{lex}}$ and $i(b \rightarrow c) \leq i(f)$ for all edges f of L . Denote the $i(b \rightarrow c)$:th Morse layer of T with F .

Case I: $F = |\dots| \times |\dots|$. Since $(c \rightarrow b) \in M_{\text{lex}}$ we have $i(b \rightarrow c) = u(b \rightarrow c)$. The 1-smoothing of F in b must be $|\dots| \textcolor{red}{\rangle} \textcolor{red}{\langle} |\dots|$ and $(c \rightarrow b) \in G(\Psi[[T]])$ is merge-type, see Figure 6. Lemma 3.3 and the i -minimality of $b \rightarrow c$ yield

$$i(b \rightarrow c) \leq i(c \rightarrow d) \leq u(b \rightarrow c) = i(b \rightarrow c)$$

giving $i(c \rightarrow d) = i(b \rightarrow c)$. Now each possible type i), ii) or v) of $c \rightarrow b$, yields $b = d$ which implies a contradiction: $(b \rightarrow c) \notin M_{\text{lex}}$ and $(b \rightarrow c) \in M_{\text{lex}}$.

Case II: $F = |\dots| \times |\dots|$. Now 0-smoothing of F in c must be $|\dots| \textcolor{red}{\rangle} \textcolor{red}{\langle} |\dots|$ and hence $(c \rightarrow b) \in G(\Psi[[T]])$ is split-type. As in Case I, one can here that $a = c$ yielding a contradiction.

Case III: $F = |\dots| \frown |\dots|$ or $F = |\dots| \smile |\dots|$. This is impossible; the function i can only take values in the indices of the Morse layers which contain crossings in them. \square

A Morse presentation of a tangle diagram is called a *negative braid word*, if its every Morse layer is of the form $|\dots| \times |\dots|$ and the strands are oriented from bottom to top. The canonical

generators σ_i of the braid groups correspond to the crossings of the tangle diagram in a standard way, so that



represents the negative braid word of the 4-strand torus braid $(\sigma_1\sigma_2\sigma_3)^n$.

Lemma 3.5. *Let B be a negative braid word and let $a \rightarrow b$ be a merge-type isomorphism in the graph $G(\Psi[B], M_{\text{gr}})$.*

1. *If $i(a \rightarrow b) = u(a \rightarrow b)$, then $(a \rightarrow b) \in M_{\text{gr}}$ or a, b are both otherwise matched in M_{gr} .*
2. *If $i(a \rightarrow b) < u(a \rightarrow b)$, then $(a \rightarrow b) \notin M_{\text{gr}}$ since a is otherwise matched in M_{gr} .*
3. *Unmatched cells of $G(\Psi[B], M_{\text{gr}})$ contain only characters $0, \mathbf{0}, 1$.*

Proof. Suppose $i(a \rightarrow b) = u(a \rightarrow b)$. Then a and b agree on the first $i(a \rightarrow b) - 1$ characters and thus by Lemma 3.2 either both a and b or neither of them is matched with arrows whose u value is at most $i(a \rightarrow b) - 1$. In case neither is, it follows from Algorithm 4 that $(a \rightarrow b) \in M_{\text{gr}}$.

Now suppose $i(a \rightarrow b) < u(a \rightarrow b)$. Consider the highest point of the red circle in a from which u is measured. This Morse layer must be 0-smoothed as $|\cdots| \smile |\cdots|$. By the paragraph above, a is matched to a cell whose same Morse layer is $|\cdots| \smile |\cdots|$ or a is matched to some other vertex which is not b .

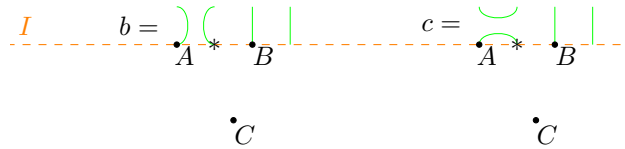
Let c be an unmatched cell of $\Psi[B] \subset \{0, \mathbf{0}, 1, \mathbf{1}, \bullet, \circ, \bullet, \circ\}^n$. Since B is a braid, all of its Morse layers are crossings and thus the characters \bullet, \circ, \bullet cannot appear in c . The highest points of loops are contained in 0-smoothed Morse layers $|\cdots| \smile |\cdots|$ and hence characters $\mathbf{1}, \mathbf{1}$ are excluded. By Claim 1, every cell containing a red loop is matched and thus $\mathbf{0}$ cannot be contained in c . From what remains, we conclude that $c \in \{0, \mathbf{0}, 1\}^n$. \square

Proposition 3.6. *For $n \in \mathbb{Z}_{\geq 0}$, the greedy matching M_{gr} is a Morse matching on $\Psi[(\sigma_1\sigma_2\sigma_3)^n]$.*

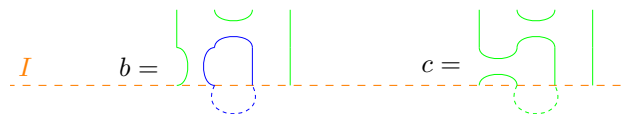
Proof. Again, we assume towards contradiction that there exists a directed cycle L in the graph $G(\Psi[(\sigma_1\sigma_2\sigma_3)^n], M_{\text{gr}})$. Let $z \rightarrow a \rightarrow b \rightarrow c \rightarrow d$ be a subpath of L such that $(a \rightarrow b), (c \rightarrow d) \in M_{\text{gr}}$ and $i(b \rightarrow c) \leq i(f)$ for all edges f of L . We denote $I = i(b \rightarrow c)$.

If $c \rightarrow b$ is a merge-type isomorphism, it follows from Lemma 3.5 that $I = u(b \rightarrow c)$. From this one can reach a contradiction $b = d$ similar to Case I of the proof of Proposition 3.4. We can thus assume that $c \rightarrow b$ is split-type isomorphism and divide into cases with I .

Case I: $I \in 3\mathbb{Z} + 1$. The I :th Morse layer is 1-smoothed in b and 0-smoothed in c . In the Morse layers $1, \dots, I - 1$ of b and c the $*$ -marked component is connected to either to A , to B or in the bottom boundary to C :



The only way $b \rightarrow c$ is a split-type isomorphism is if $*$ is connected to B . In $(\sigma_1\sigma_2\sigma_3)^n$ the $I + 1$:th Morse layer is $|\smile|$ and by Lemma 3.5 it has to be smoothed in b as $|\smile|$ and so b and c are of the form:

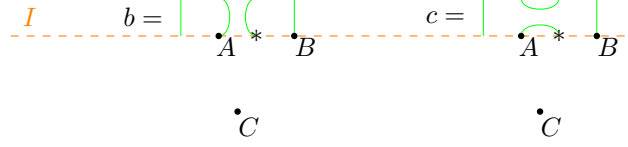


Hence $u(b \rightarrow c) = I + 1$ and by i minimality if $b \rightarrow c$ and Lemma 3.3 we get

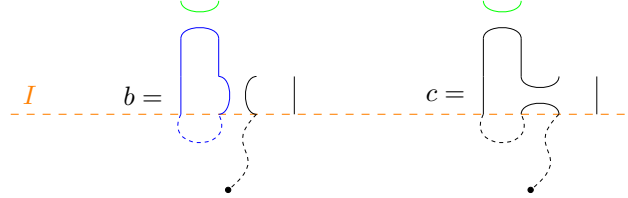
$$I \leq i(a \rightarrow b) \leq u(b \rightarrow c) = I + 1.$$

The $I+1$:th Morse layer of b is 0-smoothed rendering $i(a \rightarrow b) = I+1$ impossible. Thus $i(a \rightarrow b) = I$ but since $b \rightarrow c$ is split type, we get that $a = c$ which is a contradiction.

Case II: $I \in 3\mathbb{Z} + 2$. We similarly divide into cases based on connectivity of $*$ in the Morse layers $1, \dots, I-1$ of b and c :

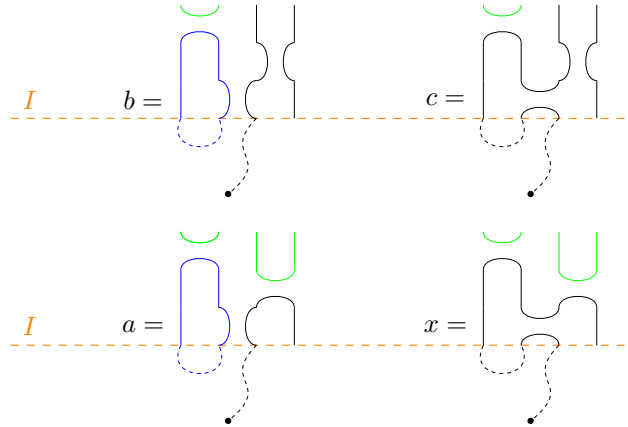


The connection $*$ to B is almost identical with the similar connectivity in the case $I \in 3\mathbb{Z} + 1$. The only difference in arguments can be handled by moving the left-most line to the right-most position in all of the pictures. Since $c \rightarrow b$ is split-type, $*$ cannot be connected to A and we can proceed by assuming that $*$ is connected to the bottom boundary C . In order for b to be matched to c , they have to be of the form:



Hence $u(b \rightarrow c) = I + 2$ and it follows that either $i(a \rightarrow b) \in \{I, I + 1, I + 2\}$. From these, $i(a \rightarrow b) = I + 2$ is impossible, since $I + 2$:th Morse layer of b is 0-smoothed. The value $i(a \rightarrow b) = I$ yields a contradiction with $a = c$, so we proceed with $i(a \rightarrow b) = I + 1$.

We denote $x = \text{isopair}(a, I, I + 2)$, so the cells at our disposal are pictorially:



Since $(c \rightarrow b) \in M_{\text{gr}}$, we aim to show that $(x \rightarrow a) \in M_{\text{gr}}$ as well. This will be a contradiction, as $(a \rightarrow z) \in M_{\text{gr}}$ and M_{gr} is a matching. Now $(x \rightarrow a) \in A_{I, I+2}$, so in order for $(x \rightarrow a) \notin M_{I, I+2}$ either a or x has to be matched in $M_{I+1, I+2}$, $M_{I+2, I+2}$ or in $M_{J, K}$ for some $J, K \leq I + 1$. We can exclude these possibilities one-by-one.

- By staring at the diagrams of a and x , one can conclude that $\text{isopair}(y, j, k) = *$, whenever

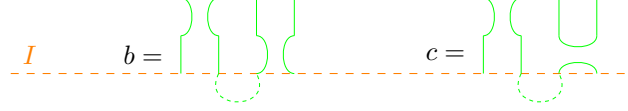
$$(y, j, k) \in \{(a, I + 1, I + 2), (a, I + 2, I + 2), (a, I, I + 1), (a, I + 1, I + 1), \\ (a, I, I), (x, I + 1, I + 2), (x, I + 2, I + 2)\} \cup \{(x, J, I + 1) \mid J \leq I + 1\}.$$

Hence a and x cannot be matched in the corresponding $M_{j, k}$ sets.

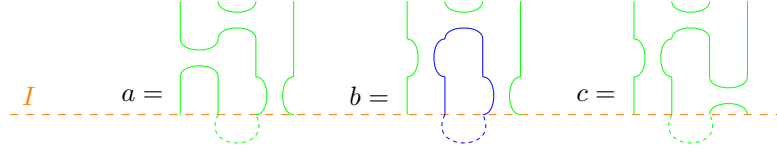
- Since $(c \rightarrow b) \in M_{\text{gr}}$ and $u(c \rightarrow b) = I + 2$, the cell c cannot be matched in $M_{J,K}$ for $K \leq I$. The first I characters of c and x coincide, so by Lemma 3.2, x is not matched in any $M_{J,K}$ for $J, K \leq I$ either.
- We know that $i(a \rightarrow z) \geq I$ and $(a \rightarrow z) \in M_{\text{gr}}$ which is why a cannot be matched in any $M_{J,K}$ with $J < I$.

The three arguments above eliminate all opportunities for a and x to be matched before $M_{I,I+2}$. Thus $(x \rightarrow a) \in M_{I,I+2} \subset M_{\text{gr}}$ and we have reached a contradiction.

Case III: $I \in 3\mathbb{Z}$. In order for $c \rightarrow b$ to be a split-type isomorphism, the connectivity below I :th Morse layer and the smoothing at $I + 1$:th Morse layer have to be look like



Now it can be argued with Lemma 3.5 that $I + 2$:th Morse layer of b has to be $| \text{ } \smile \text{ } |$. Hence $u(b \rightarrow c) = I + 2$ and with the help of 3.3 we can conclude that $i(a \rightarrow b) = I + 1$ so that diagrammatically we acquire:



Since $i(c \rightarrow b) \in M_{\text{gr}}$ instead of $(a \rightarrow c) \in M_{\text{gr}}$ the arrow $a \rightarrow z$ was prioritized in M_{gr} over the arrow $a \rightarrow c$, that is,

$$(a \rightarrow z) \in M_{I+2,I+2} \cup M_{I,I+1} \cup M_{I+1,I+1} \cup M_{I,I} \cup \bigcup_{J < I} M_{J,K}.$$

The first four cases can be deemed impossible as $(a \rightarrow z) \notin A_{j,k}$ for the relevant j, k whereas last case is eliminated by $i(a \rightarrow z) \geq I$. Again, we have reached a contradiction and thus proven that M_{gr} is a Morse matching on $\Psi[(\sigma_1\sigma_2\sigma_3)^n]$. \square

4 Torus braids with 4 strands

In this section, we derive the main results from properties of the Morse complexes $M_{\text{gr}}\Psi[(\sigma_1\sigma_2\sigma_3)^n]$ whose proofs are postponed to Sections 5 and 6.

4.1 Upper bounds on the homological dimensions

For brevity, throughout Sections 4, 5 and 6 we will write $C_n = M_{\text{gr}}\Psi[(\sigma_1\sigma_2\sigma_3)^n]$ and U_n for the unmatched cells of $G(\Psi[(\sigma_1\sigma_2\sigma_3)^n], M_{\text{gr}})$, so that U_n forms a basis for C_n . For a cell w we denote $h(w)$ and $q(w)$ for its the homological and quantum degrees respectively. Let X denote the set of all matched and unmatched cells, $X = \bigcup_{n=0}^{\infty} \text{cells}(\Psi[(\sigma_1\sigma_2\sigma_3)^n])$ and define functions

$$\begin{aligned} t_{\mathcal{A}}: X &\rightarrow \mathbb{R}, & t_{\mathcal{A}}(w) &= -\frac{1}{2}n(w) + \frac{1}{2}h(w) - \frac{1}{4}q(w) - 1 \\ t_{\mathcal{B}}: X &\rightarrow \mathbb{R}, & t_{\mathcal{B}}(w) &= 3n(w) - \frac{3}{2}h(w) + q(w) - \frac{5}{2} \\ t_{\mathcal{C}}: X &\rightarrow \mathbb{R}, & t_{\mathcal{C}}(w) &= -\frac{9}{4}n(w) + h(w) - \frac{3}{4}q(w) - \frac{1}{4}. \end{aligned}$$

where $n(w)$ denotes the unique index n for which $w \in \text{cells}(\Psi[(\sigma_1\sigma_2\sigma_3)^n])$. In order to compare the complexes C_n for different n , grading shifts are required: For an individual cell w and or a whole complex A we write $w[a]\{b\}$ or $A[a]\{b\}$ to shift the homological degree by a and the quantum degree by b .

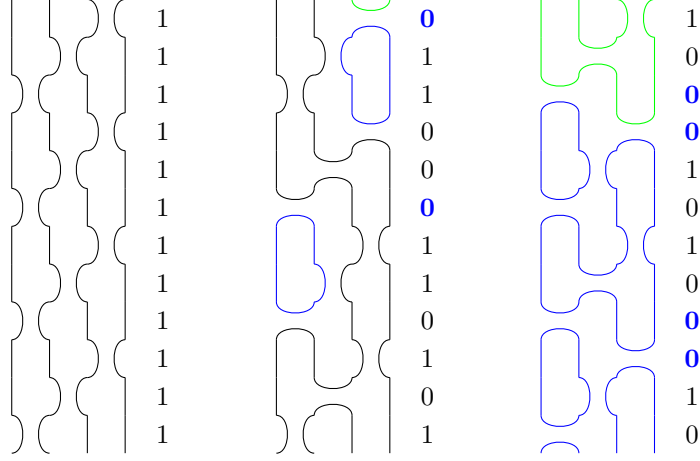


Figure 8: The three periodic building blocks \mathcal{A} , \mathcal{B} and \mathcal{C} of unmatched cells of $G(\Psi[(\sigma_1\sigma_2\sigma_3)^n], M_{\text{gr}})$. The maps \mathbf{a}_n , \mathbf{b}_n and \mathbf{c}_n from Proposition 4.1 take a diagram w of U_n which contains at least one of the periodic building blocks \mathcal{A} , \mathcal{B} and \mathcal{C} and duplicates the first instance of this block, making the tangle diagram 12 Morse layers taller and an unmatched cell in U_{n+4} .

Proposition 4.1. *For all $n \geq 0$ there are bijections*

$$\begin{aligned} \mathbf{a}_n &: \{w \in U_n \mid t_{\mathcal{A}}(w) \geq 1\} \rightarrow \{w \in U_{n+4} \mid t_{\mathcal{A}}(w) \geq 2\} \\ \mathbf{b}_n &: \{w \in U_n \mid t_{\mathcal{B}}(w) \geq 1\} \rightarrow \{w \in U_{n+4} \mid t_{\mathcal{B}}(w) \geq 2\} \\ \mathbf{c}_n &: \{w \in U_n \mid t_{\mathcal{C}}(w) \geq 1\} \rightarrow \{w \in U_{n+4} \mid t_{\mathcal{C}}(w) \geq 2\}. \end{aligned}$$

The bijections shift the homological and quantum degrees and maintain the connectivity of the underlying Temperley-Lieb diagrams, so that

$$w_1 = (\mathbf{a}_n(w_1))\{12\}, \quad w_2 = (\mathbf{b}_n(w_2))[6]\{20\}, \quad w_3 = (\mathbf{c}_n(w_3))[8]\{24\}$$

as objects in the category $\text{Mat}(\text{Cob}_{\bullet}^3(8))$.

Diagrammatically the correspondences \mathbf{a}_n , \mathbf{b}_n and \mathbf{c}_n are described in Figure 8 and a more formal description will be given in Section 5.

The i th chain space of a complex A over $\text{Mat}(\text{Cob}_{\bullet}^3(2m))$ is denoted by A^i . To further split A^i to quantum gradings, denote the direct sum of those Temperley-Lieb diagrams with $\{j\}$ quantum grading shift by $A^{i,j}$, so that $\bigoplus_{j \in \mathbb{Z}} A^{i,j} = A^i$. To measure the size an object $B \in \text{Cob}(2m)$, we define $\dim_{\text{Cob}}(B) \in \mathbb{Z}_{\geq 0}$ to be the number of loopless Temperley-Lieb diagrams in $\Psi(B)$. Similarly we define size of the whole chain complex with

$$\dim_{\text{Kom}}(A) = \sum_{i \in \mathbb{Z}} \dim_{\text{Cob}}(A^i).$$

Corollary 4.2. *The dimensions of $C_n^{i,j}$ and C_n admit constant and quadratic bounds respectively:*

$$\max\{\dim_{\text{Cob}}(C_n^{i,j}) \mid i, j \in \mathbb{Z}, n \geq 0\} < \infty \quad (9)$$

$$\dim_{\text{Kom}}(C_n) = O(n^2). \quad (10)$$

Proof. With Lean's linarith tactic, one can show that over \mathbb{Q} the system of inequalities

$$\begin{aligned} 2 &> -\frac{1}{2}n + \frac{1}{2}h - \frac{1}{4}q - 1 \\ 2 &> 3n - \frac{3}{2}h + q - \frac{5}{2} \\ 2 &> -\frac{9}{4}n + h - \frac{3}{4}q - \frac{1}{4} \end{aligned}$$

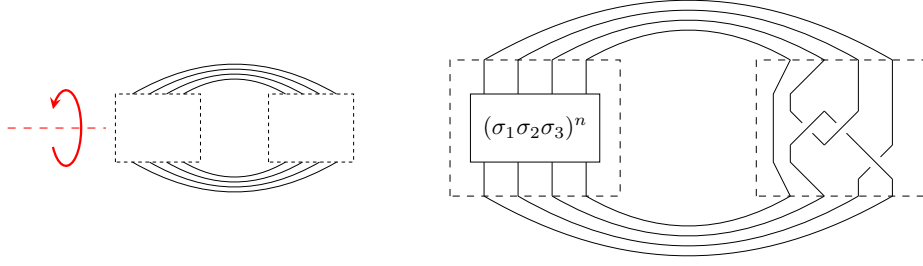


Figure 9: Our convention for composing 8-ended tangles (left) and an example link $(\sigma_1\sigma_2\sigma_3)^n \otimes_{\text{Link}} T$ (right), for which Theorem 4.3 applies. The red rotation axis is applied in the proof of Theorem 4.3.

implies $n < 39$. Hence, either $t_{\mathcal{A}}(w) \geq 2$, or $t_{\mathcal{B}}(w) \geq 2$ or $t_{\mathcal{C}}(w) \geq 2$ holds for any $w \in U$ with $n(w) \geq 39$. It follows from Proposition 4.1 that

$$\max\{\dim_{\text{Cob}}(C_n^{i,j}) \mid i, j \in \mathbb{Z}, 0 \leq n\} = \max\{\dim_{\text{Cob}}(C_n^{i,j}) \mid i, j \in \mathbb{Z}, 0 \leq n \leq 38\} < \infty.$$

Morse complex C_n consists of unmatched cells of the complex $\Psi[(\sigma_1\sigma_2\sigma_3)^n]$ which yields

$$\dim_{\text{Cob}}(C_n^{i,j}) \leq \dim_{\text{Cob}}((\Psi[(\sigma_1\sigma_2\sigma_3)^n])^{i,j}).$$

On the other hand the complex $\Psi[(\sigma_1\sigma_2\sigma_3)^n]$ is supported in bigradings $[-3n, 0] \times [-9n, -3n]$, hence

$$\dim_{\text{Kom}}(C_n) \leq 18n^2 \cdot \max\{\dim_{\text{Cob}}(C_n^{i,j}) \mid i, j \in \mathbb{Z}, n \geq 0\} = O(n^2).$$

□

Given two 8-ended tangles T_1 and T_2 we define an unoriented link $T_1 \otimes_{\text{Link}} T_2$ by connecting the strands together as in Figure 9. Choosing an orientation o on $T_1 \otimes_{\text{Link}} T_2$ yields an oriented link which is denoted with $T_1 \otimes_{\text{Link}, o} T_2$. From the wonderful work of Bar-Natan, we know that not only tangles can be composed with this planar algebra operation, but also two objects O_1, O_2 of $\text{Cob}(8)$ can be fused as an object $O_1 \otimes_{\text{Cob}} O_2$ in $\text{Cob}(0)$ (join the pictures and add up their grading shifts). Even complexes $A, B \in \text{Mat}(\text{Cob}_{\bullet}^3(8))$ can be merged as a complex $A \otimes_{\text{Kom}} B$ where

$$(A \otimes_{\text{Kom}} B)^{i,j} = \bigoplus_{a+c=i, b+d=j} A^{a,b} \otimes_{\text{Cob}} B^{c,d}.$$

Assuming that orientations agree throughout, the Bar-Natan bracket complex commutes with the composition of tangles:

$$[[T_1 \otimes_{\text{Link}, o} T_2]] \simeq [[T_1]] \otimes_{\text{Kom}} [[T_2]].$$

The standard Khovanov TQFT is an additive functor F from $\text{Cob}_{\bullet}^3(0)$ to graded \mathbb{Z} -modules which maps a diagram with k loops to $(\mathbb{Z}\{-1\} \oplus \mathbb{Z}\{1\})^{\otimes k}$. Naturally, F can be applied to a whole chain complex A over $\text{Mat}(\text{Cob}_{\bullet}^3(0))$ to obtain a bigraded complex $F(A)$ and to access the (i, j) -graded \mathbb{Z} -module of $F(A)$, we write $F^{i,j}(A)$. For a bigraded complex of \mathbb{Z} -modules B , we write $H(B)$ for the bigraded homology module and $H^{i,j}(B)$ for the individual homology groups. Finally, for an oriented link diagram L the even Khovanov homology $\text{Kh}^{i,j}(L) = H^{i,j}(F[[L]])$ is the (co)homology obtained from

$$F^{i-1,j}[[L]] \rightarrow F^{i,j}[[L]] \rightarrow F^{i+1,j}[[L]]. \quad (11)$$

One can add a basepoint to a link diagram L , and from there to the diagrams of $\text{Cob}_{\bullet}^3(0)$ that generate the complex $[[L]]$. With the basepoints in hand, F gets replaced by the reduced version \bar{F} where a diagram D of k loops and one basepoint gets mapped $(\mathbb{Z}\{-1\} \oplus \mathbb{Z}\{1\})^{\otimes k-1}$. This yields the reduced Khovanov homology $\bar{\text{Kh}}(L) = H(\bar{F}[[L]])$. The even Khovanov homology also has a strange cousin, odd Khovanov homology $\text{Kh}_{\text{odd}}^{i,j}(L)$, which is also obtained from (11) although with different

sign convention on the maps [ORS13]. The odd theory also has a reduced version, $\overline{\text{Kh}}_{\text{odd}}$, which satisfies

$$\text{Kh}_{\text{odd}}^{i,j}(L) \cong \overline{\text{Kh}}_{\text{odd}}^{i,j-1}(L) \oplus \overline{\text{Kh}}_{\text{odd}}^{i,j+1}(L). \quad (12)$$

The corresponding relation does not hold for the even theory. The unreduced even and odd Khovanov homologies with coefficients $\text{Kh}_{\text{odd/even}}^{i,j}(L; \mathbb{F})$ are taken from (11) by first tensoring with \mathbb{F} before taking the homology.

Theorem 4.3. *Let T be any 8-ended tangle. The dimensions of even and odd Khovanov homologies of links $(\sigma_1\sigma_2\sigma_3)^n \otimes_{\text{Link},o} T$ admit constant and quadratic bounds:*

$$\max_{i,j,n,o,\mathbb{F},\mathcal{H}} \left\{ \dim_{\mathbb{F}} \left(\mathcal{H}^{i,j}((\sigma_1\sigma_2\sigma_3)^n \otimes_{\text{Link},o} T; \mathbb{F}) \right) \right\} < \infty \quad (13)$$

$$\max_{o,\mathbb{F},\mathcal{H}} \left\{ \dim_{\mathbb{F}} \left(\bigoplus_{i,j \in \mathbb{Z}} \mathcal{H}^{i,j}((\sigma_1\sigma_2\sigma_3)^n \otimes_{\text{Link},o} T; \mathbb{F}) \right) \right\} = O(n^2). \quad (14)$$

In (13) the maximum is taken over all integers i, j, n , all orientations o , all fields \mathbb{F} and all theories: $\mathcal{H} \in \{\text{Kh}, \overline{\text{Kh}}, \text{Kh}_{\text{odd}}, \overline{\text{Kh}}_{\text{odd}}\}$ with every choice of basepoint. In (14) the maximum is taken similarly over all $o, \mathbb{F}, \mathcal{H}$ and the left-hand side is to be interpreted as a function of n .

In particular, Theorem 4.3 yields constant and quadratic bounds on $\text{Kh}(T(4, n))$ by choosing T to be the trivial tangle with 4 vertical lines.

Proof. Let us first look at the even unreduced Khovanov homology and $n \geq 0$. Fixing n , a diagram T and an orientation o , we have

$$\llbracket (\sigma_1\sigma_2\sigma_3)^n \otimes_{\text{Link},o} T \rrbracket \simeq C_n \otimes_{\text{Kom}} D$$

where $D = \Psi[T][s_1]\{s_2\}$ and shifts $s_1, s_2 \in \mathbb{Z}$ depend on o . It follows that

$$\dim_{\mathbb{F}} \text{Kh}^{i,j}((\sigma_1\sigma_2\sigma_3)^n \otimes_{\text{Link},o} T; \mathbb{F}) \leq \text{rank } F^{i,j}(C_n \otimes_{\text{Kom}} D).$$

By opening up the definition of tensor product and using additivity of $F^{i,j}$ we get

$$F^{i,j}(C_n \otimes_{\text{Kom}} D) = \bigoplus_{a,b,c,d \in \mathbb{Z}} F^{i,j}(C_n^{a,b} \otimes_{\text{Cob}} D^{c,d}).$$

The complex D consists of finitely many loopless Temperley-Lieb diagrams with 8 boundary points. Hence there exist x_1, x_2, y_1, y_2 such that D is supported in degrees $[x_1, x_2] \times [y_1, y_2]$ and $\max_{i,j} \{\dim_{\text{Cob}} D^{i,j}\}$ is finite. Any pair of loopless diagrams A, B can in total produce at most 4 loops in $A \otimes_{\text{Cob}} B$ which is why

$$F^{i,j}(C_n^{a,b} \otimes_{\text{Cob}} D^{c,d}) \not\equiv 0$$

implies that

$$i = a + c \quad (15)$$

$$j \in [b + d - 4, b + d + 4] \quad (16)$$

$$c \in [x_1, x_2] \quad (17)$$

$$d \in [y_1, y_2]. \quad (18)$$

Denote K as the set of 4-tuples (a, b, c, d) satisfying (15)-(18). It is easy to see that

$$\#K = 9(x_2 - x_1 + 1)(y_2 - y_1 + 1)$$

and that $\#K$ does not depend on i, j, n, o, \mathbb{F} . Combining the above and Corollary 4.2 yields

$$\begin{aligned} \dim_{\mathbb{F}} \text{Kh}^{i,j}((\sigma_1\sigma_2\sigma_3)^n \otimes_{\text{Link},o} T; \mathbb{F}) &\leq \text{rank} \left(\bigoplus_{(a,b,c,d) \in K} F^{i,j}(C_n^{a,b} \otimes_{\text{Cob}} D^{c,d}) \right) \\ &\leq 16 \cdot \#K \cdot \max_{n,k,l} \{\dim_{\text{Cob}} C_n^{k,l}\} \cdot \max_{k,l} \{\dim_{\text{Cob}} D^{k,l}\} < \infty \end{aligned}$$

proving (13) for $n \geq 0$ and unreduced even Khovanov homology. Replacing F with \bar{F} in the proof above, yields the constant bound (13) for $n \geq 0$ for the reduced even Khovanov homology with any choice of basepoint.

As previously mentioned, odd Khovanov homology is defined similarly to even Khovanov homology, but with different sign conventions. The reduction of discrete Morse theory only cares whether the morphisms are zero, nonzero or isomorphisms — properties which are not affected by signs. Let A denote the odd unreduced Khovanov complex of \mathbb{Z} -modules

$$\rightarrow F^{i-1,*}[(\sigma_1\sigma_2\sigma_3)^n \otimes_{\text{Link},o} T] \rightarrow F^{i,*}[(\sigma_1\sigma_2\sigma_3)^n \otimes_{\text{Link},o} T] \rightarrow F^{i+1,*}[(\sigma_1\sigma_2\sigma_3)^n \otimes_{\text{Link},o} T] \rightarrow$$

with the odd differentials. We can use discrete Morse theory on A and reverse all the edges which correspond to edges reversed in $G((\sigma_1\sigma_2\sigma_3)^n, M_{\text{gr}})$ and call the resulting Morse complex MA . This matching is acyclic since the corresponding graph is a Cartesian product of two acyclic graphs. By observing carefully, one can see that there are isomorphisms of chain spaces

$$(MA)^{i,*} \cong F^{i,*}(C_n \otimes_{\text{Kom}} D).$$

It follows that the constant bound (13) holds for unreduced odd Khovanov homology, $n \geq 0$. The reduced odd Khovanov homology case follows from (12).

In case $n < 0$, we can rotate the link around the red axis displayed in Figure 9 and take the mirror image. This gives out a new link diagram for which $n > 0$. Rotation does not affect the invariants and mirroring a link dualizes the homology: $\mathcal{H}^{i,j}(L, \mathbb{F}) \cong \mathcal{H}^{-i,-j}(L^!, \mathbb{F})$ (See [Kho00] for even and [PL16] for odd Khovanov homology). Hence (13) holds for negative n as well.

For all n and all theories, the quadratic bound (14) can be deduced from the constant bound (13) by finding a quadratic bound on the support of the whole complex. \square

4.2 Homology results: recursions and vanishing of $\text{Kh}(T(4, -n))$

The following powerful proposition states that \mathbf{a}_n and \mathbf{c}_n commute with the differentials and are thus in some sense chain maps in their respective degrees. If similar commutation would hold for \mathbf{b}_n , one could use it to obtain all Khovanov homology of $T(4, n)$. While we do expect \mathbf{b}_n to follow along, rigorously proving this would likely require some new ideas compared to our brute force approach in Section 6.

Proposition 4.4. *Given $t_{\mathbf{A}}(w), t_{\mathbf{A}}(u) \geq 1$, the matrix elements of C_n and C_{n+4} are equal:*

$$\partial_{u,w} = \partial_{\mathbf{a}_n(u), \mathbf{a}_n(w)}.$$

Given $t_{\mathbf{C}}(x) \geq 6$ and $t_{\mathbf{C}}(y) \geq 1$, the matrix elements of C_n and C_{n+4} are equal:

$$\partial_{y,x} = \partial_{\mathbf{c}_n(y), \mathbf{c}_n(x)}.$$

Let us now restate and prove Theorem 1.1 from the introduction.

Theorem 1.1. *The unreduced and reduced Khovanov homology groups of negative 4-strand torus links admit recursions:*

$$\text{Kh}^{i,j}(T(4, -n)) \cong \text{Kh}^{i,j-12}(T(4, -n-4)), \quad \overline{\text{Kh}}^{i,j}(T(4, -n)) \cong \overline{\text{Kh}}^{i,j-12}(T(4, -n-4))$$

for all $n, i, j \in \mathbb{Z}$ such that $n \geq 0$ and $-2n + 2i - j \geq 14$. They also admit recursions:

$$\text{Kh}^{i,j}(T(4, -n)) \cong \text{Kh}^{i-8,j-24}(T(4, -n-4)), \quad \overline{\text{Kh}}^{i,j}(T(4, -n)) \cong \overline{\text{Kh}}^{i-8,j-24}(T(4, -n-4))$$

for all $n, i, j \in \mathbb{Z}$ such that $n \geq 0$ and $-9n + 4i - 3j \geq 41$.

If necessary, Theorem 1.1 could be extended to account for all possible tangle compositions $(\sigma_1\sigma_2\sigma_3)^n \otimes_{\text{Link},o} T$ as Theorem 4.3 did. For the sake of simplicity we only consider the trivial decompositions: 4-strand torus links.

Proof. Let I be the trivial 8-ended tangle diagram with 4 vertical lines and 0 crossings and let o be the orientation so that

$$T(4, -n) = (\sigma_1 \sigma_2 \sigma_3)^n \otimes_{\text{Link}, o} I$$

as links. There is a homotopy equivalence

$$[[T(4, -n)]] \simeq C_n \otimes_{\text{Kom}} I'$$

where I' is the complex with one object I in the homological degree 0 and quantum shift 0. It follows that $\text{Kh}^{i,j}(T(4, -n))$ can be computed from the sequence

$$\bigoplus_{a,b \in \mathbb{Z}} F^{i-1,j}(C_n^{a,b} \otimes_{\text{Cob}} I) \rightarrow \bigoplus_{a,b \in \mathbb{Z}} F^{i,j}(C_n^{a,b} \otimes_{\text{Cob}} I) \rightarrow \bigoplus_{a,b \in \mathbb{Z}} F^{i+1,j}(C_n^{a,b} \otimes_{\text{Cob}} I)$$

which is equivalent to the sequence

$$\bigoplus_{b=j-4}^{j+4} F^{i-1,j}(C_n^{i-1,b} \otimes_{\text{Cob}} I) \rightarrow \bigoplus_{b=j-4}^{j+4} F^{i,j}(C_n^{i,b} \otimes_{\text{Cob}} I) \rightarrow \bigoplus_{b=j-4}^{j+4} F^{i+1,j}(C_n^{i+1,b} \otimes_{\text{Cob}} I). \quad (19)$$

Now, let $n, i, j \in \mathbb{Z}$ such that $n \geq 0$ and $-2n + 2i - j \geq 14$. It follows that $t_{\mathcal{A}}(w) \geq 1$ for all $w \in U_n$ with $(h(w), q(w)) \in [i-1, i+1] \times [j-4, j+4]$. Thus, by Proposition 4.4 there is a commutative diagram in the category $\text{Mat}(\text{Cob}_{\bullet}^3(8))$:

$$\begin{array}{ccccc} \bigoplus_{b=j-4}^{j+4} C_n^{i-1,b} & \longrightarrow & \bigoplus_{b=j-4}^{j+4} C_n^{i,b} & \longrightarrow & \bigoplus_{b=j-4}^{j+4} C_n^{i+1,b} \\ \downarrow & & \downarrow & & \downarrow \\ \bigoplus_{b=j-4}^{j+4} C_{n+4}^{i-1,b} \{12\} & \longrightarrow & \bigoplus_{b=j-4}^{j+4} C_{n+4}^{i,b} \{12\} & \longrightarrow & \bigoplus_{b=j-4}^{j+4} C_{n+4}^{i+1,b} \{12\} \end{array} \quad (20)$$

where the vertical arrows are isomorphisms induced by \mathbf{a}_n . Applying $F(- \otimes_{\text{Cob}} I)$ to (20) yields commuting isomorphisms between (19) and

$$\bigoplus_{b=j-4}^{j+4} F^{i-1,j}(C_{n+4}^{i-1,b} \{12\} \otimes_{\text{Cob}} I) \rightarrow \bigoplus_{b=j-4}^{j+4} F^{i,j}(C_{n+4}^{i,b} \{12\} \otimes_{\text{Cob}} I) \rightarrow \bigoplus_{b=j-4}^{j+4} F^{i+1,j}(C_{n+4}^{i+1,b} \{12\} \otimes_{\text{Cob}} I).$$

This sequence gives out the homology group $H^{i,j}(F(C_{n+4}\{12\} \otimes_{\text{Kom}} I'))$ which can be seen isomorphic to $\text{Kh}^{i,j-12}(T(4, -n-4))$. Hence $\text{Kh}^{i,j}(T(4, -n)) \cong \text{Kh}^{i,j-12}(T(4, -n-4))$. The same proof works for the reduced Khovanov homology: simply replace F with \overline{F} and Kh with $\overline{\text{Kh}}$.

The second recursion is deduced from Proposition 4.4 analogously. \square

To prove a vanishing result for $T(4, -n)$, we need a quick lemma whose proof is postponed to Section 5.

Lemma 4.5. *For all $w \in U$ it holds that $t_{\mathcal{A}}(w), t_{\mathcal{C}}(w) \geq -\frac{3}{2}$.*

Proposition 4.6. *The Khovanov homology groups of 4-strand torus link vanishes at (i, j) -bidegree:*

$$\text{Kh}^{i,j}(T(4, -n)) \cong 0, \quad \overline{\text{Kh}}^{i,j}(T(4, -n)) \cong 0$$

whenever $n \geq 0$ and either $-2n + 2i - j < -6$ or $-9n + 4i - 3j < -17$.

Proof. Let $n \geq 0$ and take the contraposition that $\text{Kh}^{i,j}(T(4, -n)) \not\cong 0$. By the proof of Theorem 1.1 this homology group is computed from Sequence 19 and hence

$$\bigoplus_{b=j-4}^{j+4} F^{i,j}(C_n^{i,b} \otimes_{\text{Cob}} I) \not\cong 0.$$

One of the $C_n^{i,j}$ must be non-zero and so there exist $w \in U_n$ with $h(w) = i$ and $q(w) \in [j-4, j+4]$. Lemma 4.5 now yields:

$$\begin{aligned} -\frac{3}{2} &\leq t_{\mathcal{A}}(w) \leq -\frac{1}{2}n + \frac{1}{2}i - \frac{1}{4}j \\ -\frac{3}{2} &\leq t_{\mathcal{C}}(w) \leq -\frac{9}{4}n + i - \frac{3}{4}j + \frac{11}{4} \end{aligned}$$

which can be massaged to $-2n + 2i - j \geq -6$ and $-9n + 4i - 3j \geq -17$ proving the claim. The reduced case is proven analogously. \square

Theorem 1.2, which states that Figures 1, 16 and 17 describe $\text{Kh}^{i,j}(T(4, -n))$, can now be obtained as a corollary of Theorem 1.1, Proposition 4.6 and some computer data.

Proof of Theorem 1.2. Given $n \geq 83$, at least one of the recursions of Theorem 1.1 or one of the vanishing results of Proposition 4.6 applies for every n, i, j for which Figures 1, 16 and 17 claim $\text{Kh}^{i,j}(T(4, -n))$. This can be verified with the help of `Lean`'s `linarith` tactic, by proving case-by-case that the inequalities of the figures imply the inequalities of Theorem 1.1 and Proposition 4.6. Hence, it is straightforward to see that if the figures are accurate for $n = 28, \dots, 82$, then by induction they are accurate for $n \geq 83$. Luckily, Khovanov homology of small links is computable: we use Lewark's program `Khoca` [LL16] to compute $\text{Kh}(T(4, -28)), \dots, \text{Kh}(T(4, -82))$ and check (with simple `Python` scripts) that the results match with Figures 1, 16 and 17. \square

4.3 Comparison with GOR-conjecture

In order to match our conventions to the Gorsky-Oblomkov-Rasmussen conjecture and to the rational Gordian bounds in [LMZ24] we will consider positive torus links in this subsection and the following one.

The stable Khovanov homology of n -strand torus links (not to be confused with the stable Khovanov homotopy type [LS14]) is defined as

$$\text{Kh}(T(n, \infty)) = \lim_{m \rightarrow \infty} (\text{Kh}(T(n, m))\{-(n-1)(m-1)+1\}).$$

Stošić showed that this is a well-defined limit as for every bigrading (i, j) the shifted homology groups are eventually isomorphic [Sto07].

Conjecture 4.7 ([GOR13]). *The stable Khovanov homology $\text{Kh}(T(n, \infty))$ is the dual to the homology of the Koszul complex from the sequence $s_0, \dots, s_{n-1} \in \mathbb{Z}[x_0, \dots, x_{n-1}]$ where*

$$s_k = \sum_{i=0}^k x_i x_{k-i}.$$

The monomials x_i are bigraded with $h(x_i) = 2i$ and $q(x_i) = 2i+2$ and the Koszul differential respects the quantum grading and lowers the homological grading by 1.

Following [GOR13], we denote the dual Koszul homology as $\text{Kh}_{\text{alg}}(T(n, \infty))$. The next two propositions verify that our computations for $\text{Kh}(T(4, \infty))$ coincide with $\text{Kh}_{\text{alg}}(T(4, \infty))$ as conjectured.

Proposition 4.8. *Both $\text{Kh}(T(4, \infty))$ and $\text{Kh}_{\text{alg}}(T(4, \infty))$ have 4-torsion at bidegrees $(9+4k, 14+6k)$ for $k \geq 0$.*

Proof. Let $m \geq 2$ and consider the monomials $x_0 x_2^m$ in $\text{Kh}_{\text{alg}}(T(4, \infty))$ at Koszul degree 0. The homology at Koszul degree 0 is defined as

$$\mathbb{Z}[x_0, x_1, x_2, x_3] / (x_0^2, 2x_0 x_1, x_1^2 + 2x_0 x_2, 2x_0 x_3 + 2x_1 x_2).$$

Therefore in order to prove that $x_0x_2^m$ represents 4-torsion, it suffices to show that for all $z \in \mathbb{Z}$, there exist $p_0, p_1, p_2, p_3 \in \mathbb{Z}[x_0, x_1, x_2, x_3]$ such that

$$zx_0x_2^m = p_0x_0^2 + p_12x_0x_1 + p_2(x_1^2 + 2x_0x_2) + p_3(2x_0x_3 + 2x_1x_2). \quad (21)$$

if and only if $z \in 4\mathbb{Z}$. Let $z \in \mathbb{Z}$ and suppose that p_0, p_1, p_2, p_3 satisfy Equation 21. On the right hand side of Equation 21, the only way to generate a $zx_0x_2^m$ monomial is to ensure that p_2 contains a $\frac{z}{2}x_2^{m-1}$ monomial. As a byproduct a $\frac{z}{2}x_1^2x_2^{m-1}$ term is also generated and to offset it, p_3 needs to have a $-\frac{z}{4}x_1x_2^{m-2}$ monomial. Now $\frac{z}{4}$ has to make sense as an integer, so we obtain that $z \in 4\mathbb{Z}$. On the other hand, given $z \in 4\mathbb{Z}$, a solution for Equation 21 is easy to generate:

$$zx_0x_2^m = 0 \cdot x_0^2 + \left(\frac{z}{4}x_2^{m-2}x_3\right)2x_0x_1 + \frac{z}{2}x_2^{m-1}(x_1^2 + 2x_0x_2) - \frac{z}{4}x_1x_2^{m-2}(2x_0x_3 + 2x_1x_2).$$

The monomial $x_0x_2^m$ has bidegree $(4m, 2 + 6m)$ so when dualizing the homological degree of the torsion groups increases by 1 yielding the result for $\text{Kh}_{\text{alg}}(T(n, \infty))$. Observing Figures 1 and 17, mirroring both degrees $(i, j) \mapsto (-i, -j)$, dualizing and then renormalizing with the quantum degrees one can see that every $\text{Kh}^{9+4k, 14+6k}(T(4, \infty))$ also contains a $\mathbb{Z}/4\mathbb{Z}$ summand for $k \geq 0$. \square

Proposition 4.9. *Over \mathbb{F}_2 , our stable Khovanov homology computations in Figure 1 agree with $\text{Kh}_{\text{alg}}(T(4, \infty))$. More precisely, as \mathbb{F}_2 vector spaces*

$$\text{Kh}^{i,j}(T(4, \infty); \mathbb{F}_2) \cong \text{Kh}_{\text{alg}}^{i,j}(T(4, \infty); \mathbb{F}_2)$$

whenever $i \geq 42$ and $j \geq \frac{3}{2}i - 1$.

Proof. By Theorem 1.5 of [GOR13], $\text{Kh}_{\text{alg}}(T(n, \infty); \mathbb{F}_2)$ has the following Poincaré series

$$P_n(t, q; \mathbb{F}_2) = \prod_{i=0}^{n-1} \frac{1 + t^{2i+1}q^{2i+4}}{1 - t^{2i}q^{2i+2}} \prod_{i=0}^{\lfloor \frac{n-1}{2} \rfloor} \frac{1 - t^{4i}q^{4i+4}}{1 + t^{4i+1}q^{4i+4}}$$

where t represents the homological gradings and q the quantum gradings. In the case of $n = 4$ this can be simplified and expanded as a power series at $(0, 0)$, so that

$$P_4(t, q; \mathbb{F}_2) = \frac{(1 + q^2)(1 + t^2q^4)(1 + t^3q^6)(1 + t^7q^{10})}{(1 - t^4q^6)(1 - t^6q^8)} = \sum_{a, b \geq 0} c_{a,b} t^a q^b$$

for some $c_{a,b} \geq 0$. Consider another power series $P'(t, q)$, where the expansion of $(1 - t^6q^8)^{-1}$ is truncated:

$$P'(t, q) = \frac{(1 + q^2)(1 + t^2q^4)(1 + t^3q^6)(1 + t^7q^{10})}{1 - t^4q^6} \prod_{i=0}^6 (t^6q^8)^i = \sum_{a, b \geq 0} d_{a,b} t^a q^b.$$

Straightforward calculations show that $b - \frac{3}{2}a \geq -1$ implies $c_{a,b} = d_{a,b}$ and that $c_{a,b} = d_{a,b} = 0$ whenever $b - \frac{3}{2}a \geq 5$. Any monomial contributing to $d_{a,b}$ with $a \geq 49$ must involve a $(t^4q^6)^k$ term with $k \geq 1$ from the expansion of $(1 - t^4q^6)^{-1}$. Hence $d_{a,b} = d_{a+4, b+6}$ whenever $a \geq 45$.

Denote $C(a, b) = \dim_{\mathbb{F}_2} \text{Kh}^{a,b}(T(4, \infty); \mathbb{F}_2)$. Observing Figure 1 and Figure 17 for the homological degree -41 , using the universal coefficient theorem and then mirroring the degrees we obtain that for $k \geq 11$:

$$\begin{aligned} C(4k - 2, 6k - 4) &= 8, & C(4k - 2, 6k - 2) &= 7, & C(4k - 2, 6k) &= 3, \\ C(4k - 1, 6k - 2) &= 8, & C(4k - 1, 6k) &= 6, & C(4k - 1, 6k + 2) &= 2, \\ C(4k, 6k) &= 8, & C(4k, 6k + 2) &= 5, & C(4k, 6k + 4) &= 1, \\ C(4k + 1, 6k + 2) &= 7, & C(4k + 1, 6k + 4) &= 4, & C(4k + 1, 6k + 6) &= 1, \end{aligned}$$

and $C(a, b) = 0$ whenever $b \geq \frac{3}{2}a + 5$. We verify that $c_{a,b} = C(a, b)$ for all $42 \leq a \leq 49$ and $-1 \leq b - \frac{3}{2}a < 5$ by computing the coefficients $c_{a,b}$ from the rational function $P_4(t, q; \mathbb{F}_2)$ with **Mathematica**. The claim follows from induction. \square

4.4 Rational replacements and $\mathbb{Z}[G]$ -complexes

A unified way of incorporating several versions of Khovanov homology was introduced by Naot as $\mathbb{Z}[G]$ -complexes [Nao06], where G is a formal variable (not a group). Given a knot diagram K , one assigns to it $\text{BN}(K)$ which is the reduced Khovanov complex associated to the Frobenius algebra $\mathbb{Z}[G][X]/(X^2 + GX)$ over $\mathbb{Z}[G]$. For us, the key properties are:

1. The chain homotopy type of $\text{BN}(K)$ is a knot invariant.
2. Setting $G = 0$ on $\text{BN}(K)$ and taking the homology recovers the reduced Khovanov homology:

$$H(\text{BN}(K) \otimes_{\mathbb{Z}[G]} \mathbb{Z}[G]/G) \cong_{\mathbb{Z} \text{ Mod}} \overline{\text{Kh}}(K).$$

(In spectral sequence lingua, this is the fact that the reduced Lee spectral sequence starts at the the reduced Khovanov homology.)

3. Setting $G = 1$ collapses the homology, except for one copy of \mathbb{Z} in homological degree 0:

$$H(\text{BN}(K) \otimes_{\mathbb{Z}[G]} \mathbb{Z}[G]/(G - 1)) \cong_{\mathbb{Z} \text{ Mod}} \mathbb{Z}.$$

(The reduced Lee spectral sequence abuts to the trivial Lee homology.)

4. The G -torsion order on $H(\text{BN}(K))$ gives an lower bound on the rational Gordian distance.

A diagrammatic introduction to $\mathbb{Z}[G]$ -complexes and proofs to 1-3 can be found in [ILM21] and 4 will be expanded upon after the following algebraic result. Since in $\mathbb{Z}[G]$ -modules the brackets $[\cdot]$ are used for the formal variable, we will denote the homological and quantum gradings with superscripts of i and j respectively.

Proposition 4.10. *For any $n \geq 2$ there is a split of $\mathbb{Z}[G]$ -complexes $\text{BN}(T(4, 2n + 1)) \simeq \mathcal{D}_n \oplus \mathcal{E}_n$ where \mathcal{D}_n is supported in homological gradings $[0, 4n]$. The four term complex \mathcal{E}_n is*

$$\begin{array}{ccccc} & & i^{4n+1}j^{12n+4}\mathbb{Z}[G] & & \\ & \nearrow^{G^2} & & \searrow^2 & \\ i^{4n}j^{12n}\mathbb{Z}[G] & & \oplus & & i^{4n+2}j^{12n+4}\mathbb{Z}[G] \\ & \searrow_{2G} & & \nearrow_{-G} & \\ & & i^{4n+1}j^{12n+2}\mathbb{Z}[G] & & \end{array}$$

Proof. For any $n \geq 4$, the reduced Khovanov homology $\overline{\text{Kh}}(T(4, 2n + 1))$ in homological degrees $[4n, 4n + 2]$ is given by:

$j \backslash i$	$4n$	$4n + 1$	$4n + 2$
$12n + 4$			\mathbb{Z}_2
$12n + 2$	\mathbb{Z}	\mathbb{Z}	
$12n$	$\mathbb{Z} \oplus \mathbb{Z}_2$		

and $\overline{\text{Kh}}^{i,*}(T(4, 2n + 1))$ vanishes for $i \geq 4n + 3$. By duality of Khovanov homology, this can be obtained from $\overline{\text{Kh}}^{i,*}(T(4, -2n - 1))$ for $i \leq -4n + 1$. In these degrees, the reduced Khovanov homology of negative torus knots can be obtained from Theorem 1.1, Proposition 4.6 and computer data analogously to the proof of Theorem 1.2.

By using Gaussian elimination and Smith normal form for the zero degree morphisms of $\text{BN}(T(4, 2n + 1))$ one can obtain a $\mathbb{Z}[G]$ chain complex (A, ∂) which is chain homotopic $\text{BN}(T(4, 2n + 1)) \simeq A$. Moreover chain spaces and zero degree morphisms of A are of the form

$$\begin{array}{ccccccc} & & 0 \rightarrow & i^{4n}j^{12n+2}\mathbb{Z}[G] & & & \\ & & & \oplus & & & \\ & & & \searrow_0 & & i^{4n+1}j^{12n+4}\mathbb{Z}[G] & \xrightarrow{2} i^{4n+2}j^{12n+4}\mathbb{Z}[G] \\ & 0 \rightarrow & i^{4n}j^{12n}\mathbb{Z}[G] & & \oplus & & \\ & & & \oplus & & & \\ & & & \searrow_0 & & i^{4n+1}j^{12n+2}\mathbb{Z}[G] & \\ & & 2 \rightarrow & i^{4n}j^{12n}\mathbb{Z}[G] & & & \end{array}$$

Additionally the differentials ∂^{4n} and ∂^{4n+1} carry higher powers of G which are determined by the differences in quantum degree, that is,

$$\partial^{4n} = \begin{bmatrix} a_1 G & a_2 G^2 & a_3 G^2 \\ 0 & a_4 G & a_5 G \end{bmatrix}, \quad \partial^{4n+1} = \begin{bmatrix} 2 & bG \end{bmatrix}$$

for some $a_1, \dots, a_5, b \in \mathbb{Z}$. From $\partial^{4n+1}\partial^{4n} = 0$ one can deduce that $a_1 = 0$. Subsequently $\partial^{4n}\partial^{4n-1} = 0$ yields $a_3 = a_5 = 0$.

Since setting $G = 1$ collapses the homology in these degrees, b has to be odd and furthermore a_2 and a_4 have to be non-zero. Hence $A = \mathcal{D}_n \oplus \mathcal{E}'_n$ where \mathcal{E}'_n is

$$\begin{array}{ccccc} & & i^{4n+1}j^{12n+4}\mathbb{Z}[G] & \xrightarrow{2} & i^{4n+2}j^{12n+4}\mathbb{Z}[G] \\ & \nearrow^{a_2 G^2} & \oplus & \nwarrow_{bG} & \\ i^{4n}j^{12n}\mathbb{Z}[G] & \xrightarrow{a_4 G} & i^{4n+1}j^{12n+2}\mathbb{Z}[G] & \xrightarrow{bG} & \end{array}$$

Since $2a_2 = -a_4b$ and b is odd, $a_4 = 2c$ for some $c \in \mathbb{Z}$. Now $(-bG, 2)$ is cycle in homological degree $4n+1$ and it is non-trivial if $c \neq \pm 1$. Moreover, if $c \neq \pm 1$ the element $(-bG, 2)$ would continue to represent a nontrivial cycle after setting $G = 1$. Hence c has to be ± 1 and \mathcal{E}'_n is of the form

$$\begin{array}{ccccc} & & i^{4n+1}j^{12n+4}\mathbb{Z}[G] & \xrightarrow{2} & i^{4n+2}j^{12n+4}\mathbb{Z}[G] \\ & \nearrow^{\mp bG^2} & \oplus & \nwarrow_{bG} & \\ i^{4n}j^{12n}\mathbb{Z}[G] & \xrightarrow{\pm 2G} & i^{4n+1}j^{12n+2}\mathbb{Z}[G] & \xrightarrow{bG} & \end{array}$$

which is isomorphic to the complex \mathcal{E}_n we were aiming for.

The Khovanov homologies $\overline{\text{Kh}}^{i_1,*}(T(4,5))$ and $\overline{\text{Kh}}^{i_2,*}(T(4,7))$ for homological degrees $i_1 \geq 8$ and $i_2 \geq 12$ are given by

$j \backslash i_1$	8	9	10
28			\mathbb{Z}_2
26		\mathbb{Z}	
24	\mathbb{Z}		

$j \backslash i_2$	12	13	14
40			\mathbb{Z}_2
38	\mathbb{Z}	\mathbb{Z}	
36	\mathbb{Z}		

respectively. Hence cases $n = 2$ and $n = 3$ can be proven similarly as $n \geq 4$ but with one or two fewer initial steps needed. \square

Let R be a ring and A an $R[G]$ module. For $a \in A$ we denote $\text{ord}_G(a) = \infty$ if $G^n a \neq 0$ for all $n \geq 0$ and $\text{ord}_G(a) = \min\{n \geq 0 \mid G^n a = 0\}$ otherwise. Furthermore for a knot K and $i \in \mathbb{Z}$ we denote

$$u_i(K; R) = \max\{\text{ord}_G(a) \mid a \in H^{i,*}(\text{BN}(K) \otimes_{\mathbb{Z}[G]} R[G]), \text{ord}_G(a) < \infty\}.$$

A 4-ended tangle T is called *rational*, if (B^3, T) is homeomorphic as a pair to $(D^2 \times [0, 1], \{(-\frac{1}{2}, 0) \cup (\frac{1}{2}, 0)\} \times [0, 1])$, see Figure 10. Two knots K_1, K_2 are said to be related by a *rational tangle replacement* if an isotopy representative of K_1 can be turned into an isotopy representative of K_2 by replacing one rational tangle with another inside a small B^3 . The rational tangle replacement is said to be *proper*, if both rational tangles share the same connectivity. The *rational Gordian distance* between knots K_1 and K_2 is the minimal number of proper rational tangle replacements needed to transform K_1 into K_2 . This defines a metric on knots and its values $u_q(K_1, K_2)$ are non-negative integers.

Theorem 4.11 ([LMZ24], Theorem 1.2, Proposition 3.31). *For any knots K_1, K_2 and ring R*

$$\max_{i \in \mathbb{Z}} |u_i(K_1; R) - u_i(K_2; R)| \leq u_q(K_1, K_2).$$

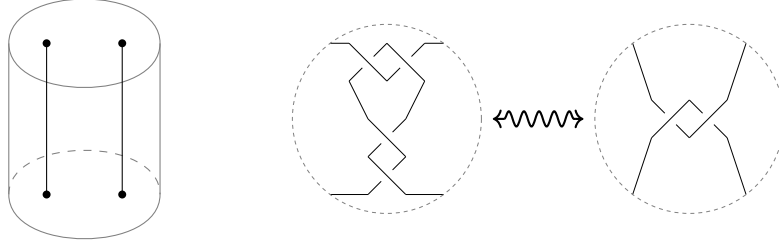


Figure 10: On the left, the pair $(D^2 \times [0, 1], \{(-\frac{1}{2}, 0) \cup (\frac{1}{2}, 0)\} \times [0, 1])$ which is our model for rational tangles. In the center and on the right we see two rational tangles. Switching one with the other in some region of a knot is a proper rational tangle replacement, since both rational tangles share the same connectivity.

Let us now restate Proposition 1.3 from the introduction and prove it using Proposition 4.10 and Theorem 4.11.

Proposition 1.3. *Suppose K is a knot which admits a diagram with c_+ positive crossings. If $n \geq 2$ and $c_+ \leq 4n$ then $u_q(T(4, 2n+1), K) \geq 2$. Distinct 4-strand torus knots are at least 2 rational replacements from each other: $u_q(T(4, n), T(4, m)) \geq 2$ whenever $n, m \in 2\mathbb{Z}+1$, $n \neq m$ and $|n|, |m| \geq 5$.*

Proof. Let K be a knot admitting a diagram with $c_+ \leq 4n$ positive crossings. Thus chain homotopy class of $\text{BN}(K)$ has a representative which vanishes at homological degree $4n+1$ and in particular $u_{4n+1}(K; \mathbb{F}_2) = 0$. On the other hand Proposition 4.10 yields $u_{4n+1}(T(4, 2n+1); \mathbb{F}_2) = 2$ which combined with Theorem 4.11 proves $u_q(T(4, 2n+1), K) \geq 2$.

The second claim similarly follows from Proposition 4.10 and Theorem 4.11. Without loss of generality, one of the following cases applies:

- If $n > m > 0$, then $u_{4n+1}(T(4, n); \mathbb{F}_2) = 2$ and $u_{4n+1}(T(4, m); \mathbb{F}_2) = 0$ which suffices for $u_q(T(4, n), T(4, m)) \geq 2$.
- If $n > 0 > m$, then $T(4, m)$ has a diagram with 0 positive crossings and the first claim can be applied.
- The set of rational tangles is closed under taking mirror images so by reversing the orientations throughout, the first case also yields $u_q(T(4, n), T(4, m)) \geq 2$ whenever $0 > m > n$.

□

5 Proof of Proposition 4.1

In this section, we will prove Proposition 4.1 which introduces the correspondences $\mathbf{a}_n, \mathbf{b}_n, \mathbf{c}_n$. The first order of business is to introduce a purely combinatorial set of formal words

$$W \subset \mathcal{S} = \bigcup_{n=0}^{\infty} \{0, \mathbf{0}, \mathbf{0}, 1, \mathbf{1}, \bullet, \bullet, \bullet\}^n$$

and prove that $W = U$ where $U = \bigcup_n U_n$ and U_n is the set of unmatched cells of $G(\Psi[(\sigma_1 \sigma_2 \sigma_3)^n], M_{\text{gr}})$. After this, the functions $\mathbf{a}_n, \mathbf{b}_n, \mathbf{c}_n$ are easy to define formally on W and recursive properties of W will allow us to inductively verify that these functions generate one-to-one correspondences in the designated gradings.

We establish functions $g_1, \dots, g_6, I_{\mathcal{A}}, I_{\mathcal{B}}, I_{\mathcal{C}}$ whose domain and codomain are the power set $\mathcal{P}(\mathcal{S})$ and which are defined by

$$\begin{aligned}
I_{\mathcal{A}}(A) &= \{a.(111)^k \mid a \in A, k \geq 0\} \\
I_{\mathcal{B}}(A) &= \{a.(101011\mathbf{000110})^k \mid a \in A, k \geq 0\} \\
I_{\mathcal{C}}(A) &= \{a.(01\mathbf{0001})^k \mid a \in A, k \geq 0\} \\
g_1(A) &= \{a.000, a.001, a.010, a.011 \mid a \in A\} \\
g_2(A) &= \{a, a.100, a.110, a.00011\mathbf{0} \mid a \in A\} \\
g_3(A) &= \{a.100001, a.110001, a.00011\mathbf{0001} \mid a \in A\} \\
g_4(A) &= \{a, a.101, a.101010, a.101011.c \mid a \in A, c \in \{e, \mathbf{000}, \mathbf{001}, \mathbf{010}, \mathbf{011}\}\} \\
g_5(A) &= \{a.101010\mathbf{001}, a.101011\mathbf{000110001} \mid a \in A\} \\
g_6(A) &= \{a, a.01\mathbf{0} \mid a \in A\}.
\end{aligned}$$

Furthermore, we assign

$$\begin{aligned}
W &= (g_1 \circ I_{\mathcal{A}})(\{e\}) \cup (g_4 \circ I_{\mathcal{B}} \circ g_2 \circ I_{\mathcal{A}})(\{e\}) \\
&\quad \cup (g_6 \circ I_{\mathcal{C}} \circ g_5 \circ I_{\mathcal{B}} \circ g_2 \circ I_{\mathcal{A}})(\{e\}) \cup (g_6 \circ I_{\mathcal{C}} \circ g_3 \circ I_{\mathcal{A}})(\{e\}) \quad (22)
\end{aligned}$$

where e denoted the length 0 word of \mathcal{S} . The compositions of Equation 22 can be viewed as the maximal paths in the schematic:

$$\begin{array}{ccccccc}
& & & N_3 & & & N_7 \\
& & g_1 \nearrow & & g_4 \nearrow & & \\
N_1 & \xrightarrow{I_{\mathcal{A}}} & N_2 & \xrightarrow{g_2} & N_4 & \xrightarrow{I_{\mathcal{B}}} & N_6 & \xrightarrow{g_5} & N_8 \\
& & g_3 \searrow & & & & & \downarrow I_{\mathcal{C}} \\
& & & N_5 & \xrightarrow{I_{\mathcal{C}}} & N_9 & \xrightarrow{g_6} & N_{10}
\end{array} \quad (23)$$

where $N_1, \dots, N_{10} = \mathcal{P}(K)$ and $\{e\}$ is plugged in from N_1 .

Lemma 5.1. *The set of unmatched cells U coincides with the formal set of words W , that is, $W = U$.*

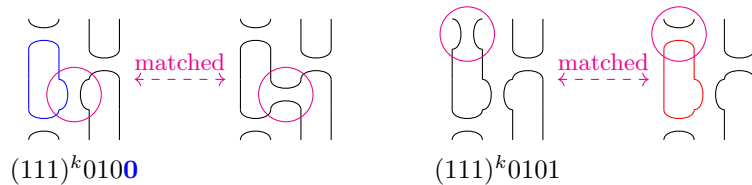
Proof. Let us begin by denoting $W_n = \{w \in W : |w| = 3n\}$ which turns our goal into showing that $W_n = U_n$ for each n . The base case of the induction is immediate: $W_0 = \{e\} = U_0$. Now assume $W_n = U_n$. From Algorithm 2 and Lemma 3.5 one can see

$$U_{n+1} = \left\{ ac_1c_2c_3 \left| \begin{array}{l} a \in W_n, c_1, c_2, c_3 \in \{0, \mathbf{0}, 1\} \\ ac_1 \in \text{cells}(\Psi[(\sigma_1\sigma_2\sigma_3)^n\sigma_1]), ac_1 \text{ is not matched in } M_{*,3n+1} \\ ac_1c_2 \in \text{cells}(\Psi[(\sigma_1\sigma_2\sigma_3)^n\sigma_1\sigma_2]), ac_1c_2 \text{ is not matched in } M_{*,3n+2} \\ ac_1c_2c_3 \in \text{cells}(\Psi[(\sigma_1\sigma_2\sigma_3)^{n+1}]), ac_1c_2c_3 \text{ is not matched in } M_{*,3n+3} \end{array} \right. \right\}.$$

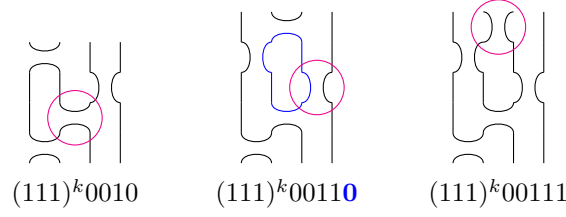
Hence our goal is to verify that for all $a \in W_n$ and $c_1, c_2, c_3 \in \{0, \mathbf{0}, 1\}$:

$$\begin{aligned}
&ac_1c_2c_3 \in \text{cells}(\Psi[(\sigma_1\sigma_2\sigma_3)^{n+1}]), \text{ and } ac_1, ac_1c_2 \text{ and } ac_1c_2c_3 \\
&\text{are not matched with Algorithm 4 in the last 3 Morse layers} \iff ac_1c_2c_3 \in W_{n+1}. \quad (24)
\end{aligned}$$

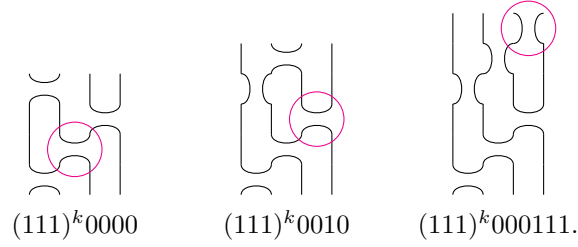
We begin with the case $a \in (g_1 \circ I_{\mathcal{A}})(\{e\})$ and consider the possible continuations $ac_1c_2c_3$ by first splitting to cases based on c_1 , then on c_2 and finally on c_3 . If $a = (111)^k010$, then both possible c_1 continuations $a.\mathbf{0}$ and $a.1$ will be matched



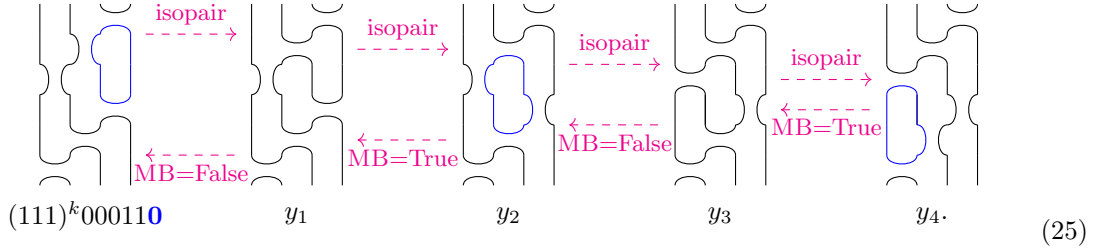
and the same argument shows that all continuations of $a = (111)^k 011$ will be matched. Similarly all possible continuations of $a = (111)^k 001$ are matched:



where the magenta circles indicate the i values of the matching arrows. For $a = (111)^k 000$ the continuations $a.0$, $a.10$, $a.111$ are matched:

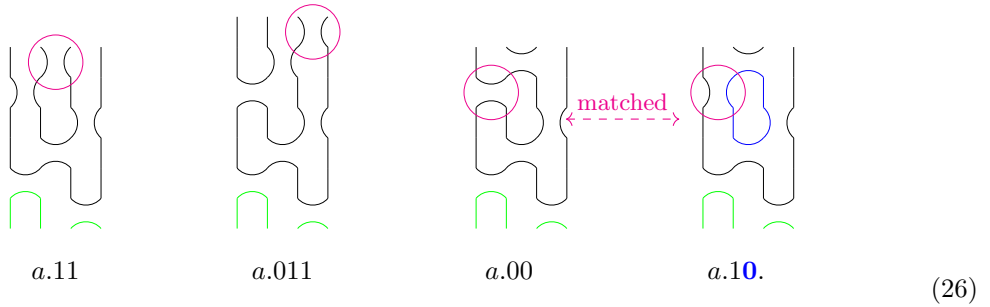


By running Algorithm 4 on the cell $(111)^k 000110$ we can see that the continuation 110 ends up being unmatched:

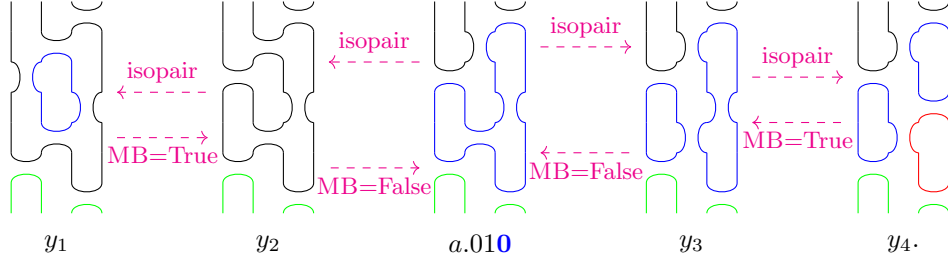


Let us elaborate on (25): The isopair arrows are executing lines 6 and 14 whereas the MB=True/False arrows execute lines 9 and 15 and state whether MATCHESBACK returns True or False. From this we can see that $(y_3 \rightarrow y_4), (y_1 \rightarrow y_2) \in M_{\text{gr}}$ and thus $(111)^k 000110 \in U_{n+1}$. Clearly, $(111)^k 000110 \in W_{n+1}$ as well and W_{n+1} contains those precisely those continuations which are in U_{n+1} . In other words we have proven Equivalence 24 in the case of $a \in (g_1 \circ I_{\mathcal{A}})(\{e\})$.

Next assume that $a \in (g_6 \circ I_{\mathcal{C}} \circ g_5 \circ I_{\mathcal{B}} \circ g_2 \circ I_{\mathcal{A}})(\{e\}) \cup (g_6 \circ I_{\mathcal{C}} \circ g_3 \circ I_{\mathcal{A}})(\{e\})$, so $a = \dots 0001$ or $a = \dots 0001010$ where each 0 is individually a placeholder for either 0 or 10 . Let us first investigate $a = \dots 0001$ first: The continuations 11 and 011 get matched via merge-type isomorphisms whereas 00 and 10 get matched with each other:

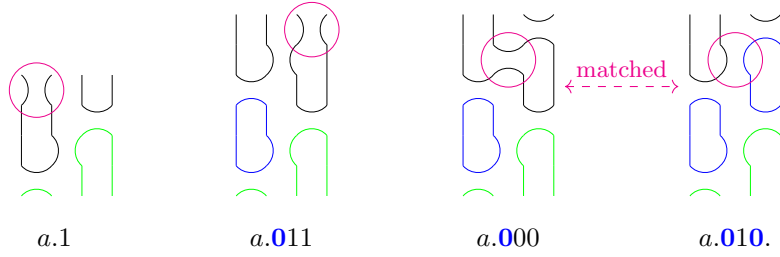


Again, running Algorithm 4 we can see that the cell $a.01\mathbf{0}$ remains unmatched:



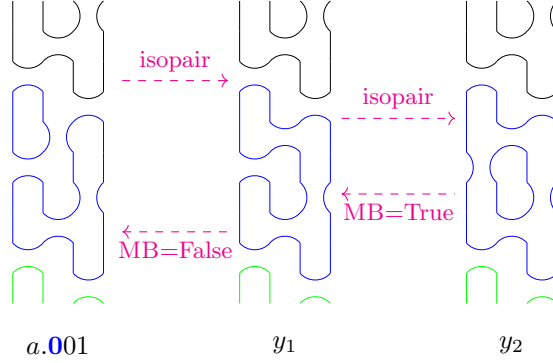
as the arrows $(y_2 \rightarrow y_1), (y_4 \rightarrow y_3)$ are contained in M_{gr} .

Next, case $a = \dots \mathbf{0001010}$: Continuations 1 and $\mathbf{011}$ get similarly matched with merge-type arrows whereas $\mathbf{010}$ get pairs up with $\mathbf{000}$:



(27)

The continuation $\mathbf{001}$ remains unmatched



since $(y_1 \rightarrow y_2) \in M_{\text{gr}}$. By comparing these unmatched continuations with the definition of W , we can see that Equivalence 24 holds also in the case $a \in (g_6 \circ I_{\mathcal{C}} \circ g_5 \circ I_{\mathcal{B}} \circ g_2 \circ I_{\mathcal{A}})(\{e\}) \cup (g_6 \circ I_{\mathcal{C}} \circ g_3 \circ I_{\mathcal{A}})(\{e\})$. We omit the details of the last case: showing that Equivalence 24 holds for $a \in (g_4 \circ I_{\mathcal{B}} \circ g_2 \circ I_{\mathcal{A}})(\{e\})$. \square

To additionally ensure that no mistakes were made in the vast amount of cases of the previous proof, $U_n = W_n$ is verified with `braidalgo.py` for $n = 0, \dots, 50$.

In order to manage the recursions of W , we define the formal words of length 12

$$\mathcal{A} = 1^{12}, \quad \mathcal{B} = 101011\mathbf{000110}, \quad \mathcal{C} = (01\mathbf{0001})^2$$

and for every $* \in \{\mathcal{A}, \mathcal{B}, \mathcal{C}\}$ and $r \in \mathbb{Z}_{\geq 0}$ set

$$\mathcal{W}_{*,r} = \{a \in W \mid a \text{ contains at least } r \text{ disjoint instances of } * \text{ as a subword}\}.$$

We also define bijections $\gamma_*: \mathcal{W}_{*,1} \rightarrow \mathcal{W}_{*,2}$, where the value $\gamma_*(w)$ is obtained by replacing the first occurrence of subword $*$ in the word w by the subword $*^2$. Let us establish two lemmas which allow us to connect the formal recursions γ_* on W with quantum and homological gradings in C_n .

Lemma 5.2. For $n \geq 24$ it holds that

$$U_n \subset \bigcup_{* \in \{\mathcal{A}, \mathcal{B}, \mathcal{C}\}} \mathcal{W}_{*,2} = \bigcup_{* \in \{\mathcal{A}, \mathcal{B}, \mathcal{C}\}} \text{im } \gamma_*.$$

Proof. By staring at the definition of W one can confirm that the longest word in W which does not contain $\mathcal{A}^2, \mathcal{B}^2$ or \mathcal{C}^2 has length $3 \cdot 23$ and longer words must contain one of these patterns. \square

Lemma 5.3. Suppose $w \in U$ and $*, *' \in \{\mathcal{A}, \mathcal{B}, \mathcal{C}\}$. If $w \in \mathcal{W}_{*,n}$ we have

$$t_{*'}(w) + \delta_{*,*'} = t_{*'}(\gamma_*(w)) \quad (28)$$

where δ is the Kronecker delta ($\delta_{*,*'} = 1$, if $* = *'$ and $\delta_{*,*'} = 0$ otherwise). The inequality $t_*(w) \geq m$ implies $w \in \mathcal{W}_{*,m}$.

Proof. The first claim amounts to a simple degree computation and for the second claim proceed with an induction on n . For words $w \in U_n$ with $n \leq 23$ the implication is verified with `basecases.py`. Suppose now that it holds for all $w \in U_{n-4}$ with $n \geq 24$ and let $w \in U_n$ with $t_*(w) \geq m$. By Lemma 5.2 we have $w = \gamma_{*'}(v)$ for some v and $*'$. Applying Equation 28 to this yields $t_*(v) \geq m - \delta_{*,*}'$. Hence by the induction assumption $v \in \mathcal{W}_{*,k}$ where $k = m - \delta_{*,*}'$. Thus $w = \gamma_{*'}(v) \in \mathcal{W}_{*,m}$. \square

We can now prove Lemma 4.5 with an analogous induction.

Proof of Lemma 4.5. With `basecases.py` we verify that $t_{\mathcal{A}}(w), t_{\mathcal{C}}(w) \geq -\frac{3}{2}$ for all $w \in U_n$ with $n \leq 23$. Now, let $w \in U_n$ and assume that $t_{\mathcal{A}}(v), t_{\mathcal{C}}(v) \geq -\frac{3}{2}$ for all $v \in U_{n-4}$. By Lemma 5.2 and Equation 28 we have

$$t_{\mathcal{A}}(w) = t_{\mathcal{A}}(\gamma_*(v)) \geq t_{\mathcal{A}}(v) + \delta_{*,\mathcal{A}} \geq -\frac{3}{2}$$

using some $v \in U_{n-4}$ and $* \in \{\mathcal{A}, \mathcal{B}, \mathcal{C}\}$. Similarly $t_{\mathcal{C}}(w) \geq -\frac{3}{2}$. \square

We will now define the functions \mathbf{a}_n , \mathbf{b}_n and \mathbf{c}_n as restrictions and corestrictions:

$$\begin{aligned} \mathbf{a}_n &: \{w \in U_n \mid t_{\mathcal{A}}(w) \geq 1\} \rightarrow \{w \in U_{n+4} \mid t_{\mathcal{A}}(w) \geq 2\}, \quad \mathbf{a}_n(w) = \gamma_{\mathcal{A}}(w) \\ \mathbf{b}_n &: \{w \in U_n \mid t_{\mathcal{B}}(w) \geq 1\} \rightarrow \{w \in U_{n+4} \mid t_{\mathcal{B}}(w) \geq 2\}, \quad \mathbf{b}_n(w) = \gamma_{\mathcal{B}}(w) \\ \mathbf{c}_n &: \{w \in U_n \mid t_{\mathcal{C}}(w) \geq 1\} \rightarrow \{w \in U_{n+4} \mid t_{\mathcal{C}}(w) \geq 2\}, \quad \mathbf{c}_n(w) = \gamma_{\mathcal{C}}(w). \end{aligned}$$

Thus proving Proposition 4.1 amounts to verifying that \mathbf{a}_n , \mathbf{b}_n and \mathbf{c}_n are well-defined bijections which respect the connectivities and shift the gradings in the assigned way.

Proof of Proposition 4.1. Let $* \in \{\mathcal{A}, \mathcal{B}, \mathcal{C}\}$ and $w \in U_n$ with $t_*(w) \geq 1$. Then by Lemma 5.3 $w \in \mathcal{W}_{*,1}$ and we can apply γ_* to w . The Equation 28 yields $t_*(\gamma_*(w)) \geq 2$ and hence \mathbf{a}_n , \mathbf{b}_n and \mathbf{c}_n are well defined. The proof of surjectivity works similarly through Lemma 5.3 and Equation 28. The functions \mathbf{a}_n , \mathbf{b}_n and \mathbf{c}_n are also injections, since $\gamma_{\mathcal{A}}$, $\gamma_{\mathcal{B}}$ and $\gamma_{\mathcal{C}}$ are.

A simple grading computation shows that for all $a \in \mathcal{W}_{a,1}$, $b \in \mathcal{W}_{b,1}$, $c \in \mathcal{W}_{c,1}$

$$\begin{aligned} (h(a), q(a)) &= (h(\gamma_{\mathcal{A}}(a)), q(\gamma_{\mathcal{A}}(a))) + (0, 12) \\ (h(b), q(b)) &= (h(\gamma_{\mathcal{B}}(b)), q(\gamma_{\mathcal{B}}(b))) + (6, 20) \\ (h(c), q(c)) &= (h(\gamma_{\mathcal{C}}(c)), q(\gamma_{\mathcal{C}}(c))) + (8, 24). \end{aligned}$$

It is also easy to see from Figure 8 that connectivities of the underlying Temperley-Lieb diagrams remain unchanged. \square

6 Proof of Proposition 4.4

In this section we prove Proposition 4.4 separately for cases \mathbf{a}_n and \mathbf{c}_n .

6.1 Case \mathfrak{a}_n

The proof for \mathfrak{a}_n is more or less straightforward, as the equalities of matrix elements are induced by a correspondences of paths which in turn are given by a graph embedding. The proof comes as a consequence of the following slightly more general lemma.

Lemma 6.1. *Let B be a negative braid word on n strands, $1 \leq i \leq n-1$ and assume M_{gr} is a Morse matching on $G(\Psi[\sigma_i B])$. Then M_{gr} is a Morse matching on $G(\Psi[B])$ and the injective map*

$$\varphi: \text{cells}(\Psi[B]) \rightarrow \text{cells}(\Psi[\sigma_i B]\{1\}), \quad \varphi(w) = (1.w)\{1\}$$

sends any matrix element of $M_{\text{gr}}\Psi[B]$ to its additive inverse: $d_{b,a} = -\partial_{\varphi(b),\varphi(a)}$.

Proof. It is easy to see that φ preserves the degrees and the connectivity of diagrams. Additionally, φ defines a graph homomorphism

$$\varphi: G(\Psi[B]) \rightarrow G(\Psi[\sigma_i B]\{1\})$$

which is a graph isomorphism into the induced subgraph of its image. We want to show that φ also gives a graph isomorphism with the arrows of M_{gr} reversed on both graphs. In other words, we want to show that

$$\rho: G(\Psi[B], M_{\text{gr}}) \rightarrow G(\Psi[\sigma_i B]\{1\}, M_{\text{gr}}), \quad \rho(x) = \varphi(x)$$

is a graph isomorphism into the induced subgraph of its image. This amounts to showing that an edge $a \rightarrow b$ is contained in the greedy matching of $\Psi[B]$ if and only if the edge $\varphi(a) \rightarrow \varphi(b)$ is contained in the greedy matching of $\Psi[\sigma_i B]$. Morally, this follows from the fact that 1-smoothing of the first crossing does not change the geometry of the pictures and from Lemma 3.5.

A rigorous argument proving this falls back on Algorithm 4. We write isopair_B , $\text{isopair}_{\sigma_i B}$, MATCHESBACK_B and $\text{MATCHESBACK}_{\sigma_i B}$ to distinguish the implicit underlying tangle diagram in Algorithm 4. By additionally writing $\varphi(\star) = \star$, we get that for all $j, k \geq 0$, $w \in \text{cells}(\Psi[B])$

$$\varphi(\text{isopair}_B(w, j, k)) = \text{isopair}_{\sigma_i B}(\varphi(w), j+1, k+1).$$

By doing an induction on the sequence

$$(j, k) = (1, 1), (2, 2), (1, 2), (3, 3), (2, 3), (1, 3), (4, 4), \dots$$

and utilizing Lemma 3.5 one can show that for all a, b, j, k it holds that

$$\varphi(\text{MATCHESBACK}_B(\text{isopair}_B(a, j, k), b)) = \text{MATCHESBACK}_{\sigma_i B}(\text{isopair}_{\sigma_i B}(\varphi(a), j+1, k+1), \varphi(b)).$$

Thus $(a \rightarrow b) \in M_{\text{gr}} \iff \varphi(a) \rightarrow \varphi(b)$ and ρ is a graph isomorphism to the induced subgraph of its image. It follows that, the acyclicity of $G(\Psi[\sigma_i B])$ can be pulled back to $G(\Psi[B])$ making M_{gr} a Morse matching on the latter graph.

The graph embedding ρ gives rise to injective maps

$$\rho_{y,x}: \{\text{paths from } x \text{ to } y\} \rightarrow \{\text{paths from } \rho(x) \text{ to } \rho(y)\}$$

by

$$\rho_{y,x}(x \rightarrow a_1 \rightarrow \dots \rightarrow a_n \rightarrow y) = (\rho(x) \rightarrow \rho(a_1) \rightarrow \dots \rightarrow \rho(a_n) \rightarrow \rho(y)).$$

Moreover, the maps $\rho_{y,x}$ are surjective, since Lemma 3.5 obstructs the existence of an arrow $(a \rightarrow b) \in G(\Psi[\sigma_i B], M_{\text{gr}})$ with $a \in \text{im } \rho$ and $b \notin \text{im } \rho$.

Recall that the differentials d of $M_{\text{gr}}\Psi[B]$ and ∂ of $M_{\text{gr}}\Psi[\sigma_i B]$ are defined as sums:

$$d_{b,a} = \sum_{p \in \{\text{paths: } a \rightarrow b\}} R_B(p), \quad \partial_{\varphi(b),\varphi(a)} = \sum_{p' \in \{\text{paths: } \rho(a) \rightarrow \rho(b)\}} R_{\sigma_i B}(p')$$

where the paths are evaluated by the remembering functors:

$$\begin{aligned} R_B &: G(\Psi[B], M_{\text{gr}}) \rightarrow \text{Mat}(\text{Cob}_{\bullet}^3(8)) \\ R_{\sigma_i B} &: G(\Psi[\sigma_i B], M_{\text{gr}}) \rightarrow \text{Mat}(\text{Cob}_{\bullet}^3(8)). \end{aligned}$$

Under the two remembering functors, a single edge $x \rightarrow y$ gets mapped to equal cobordisms but with opposite signs:

$$R_B(x \rightarrow y) = -R_{\sigma_i B}(\varphi(x) \rightarrow \varphi(y)).$$

Every path contributing to $d_{b,a}$ and to $\partial_{\varphi(b), \varphi(a)}$ zig-zags between two homological layers and thus has an odd number of edges. Hence the sign swaps for every path and we can use bijectivity of $\rho_{y,x}$ to get $d_{b,a} = -\partial_{\varphi(b), \varphi(a)}$. \square

Proof of Proposition 4.4, case \mathbf{a}_n . Proposition 3.6 shows that M_{gr} is a Morse matching on the graph $G(\Psi[(\sigma_1\sigma_2\sigma_3)^n])$, for all n . From Lemma 6.1, it follows that M_{gr} is a Morse matching on graphs $G(\Psi[\sigma_3(\sigma_1\sigma_2\sigma_3)^n])$ and $G(\Psi[\sigma_2\sigma_3(\sigma_1\sigma_2\sigma_3)^n])$ as well. Now, let $w, u \in U_n$ with $t_{\mathbf{A}}(w), t_{\mathbf{A}}(u) \geq 1$ and assume that $\partial_{u,w}$ is a matrix element of $C_n = M_{\text{gr}}(\Psi[(\sigma_1\sigma_2\sigma_3)^n])$. Applying φ from Lemma 6.1 twelve times coincides with the function \mathbf{a}_n from Proposition 4.1, that is,

$$(\varphi \circ \varphi \circ \dots \circ \varphi)(x) = \mathbf{a}_n(x)$$

for any unmatched cell x . Thus

$$\partial_{u,w} = (-1)^{12} \partial_{(\varphi \circ \dots \circ \varphi)(u), (\varphi \circ \dots \circ \varphi)(w)} = \partial_{\mathbf{a}_n(u), \mathbf{a}_n(w)}.$$

\square

6.2 Case \mathbf{c}_n

Unfortunately, in the proof of Proposition 4.4, case \mathbf{c}_n , we do not manage to generate a simple graph isomorphism which would automatically yield a correspondence of paths. Nevertheless, the basic idea remains the same: a correspondence of paths Φ_n will give out an equality of matrix elements. This time, constructing the map Φ_n will require some amount of manual labor and showing that Φ_n works in the case of \mathbf{c}_n is also more demanding.

With directed graphs we have respected to the usual convention that paths follow the orientation of edges. To contrast these usual *orientation preserving paths* we say that a sequence of vertices a_1, \dots, a_k is an *orientation neglecting path* if for every i there exists either an edge $a_i \rightarrow a_{i+1}$ or an edge $a_{i+1} \rightarrow a_i$ in the underlying directed graph. Given $a, b \in U_n$ we define $\text{ZZ}(a, b)$ to be the set of orientation preserving zig-zag paths from a to b and $Z_n = \{p \in \text{ZZ}(a, b) \mid a, b \in U_n, t_{\mathbf{C}}(a) \geq 6, t_{\mathbf{C}}(b) \geq 1\}$.

The proof of Proposition 4.4, case \mathbf{c}_n is broken down into the following three tasks:

1. Define a set $A_n \subset Z_n$. For each orientation preserving path $(p: a \rightarrow b) \in A_n$ define an orientation neglecting path $\Phi_n(p): \mathbf{c}_n(a) \rightarrow \mathbf{c}_n(b)$.
2. Show that $\Phi_n(p)$ is in fact always orientation preserving and hence $\Phi_n: A_n \rightarrow Z_{n+4}$ is a well-defined and injective map. Prove that $R(p) = R(\Phi_n(p))$ as morphisms in $\text{Mat}(\text{Cob}_{\bullet}^3(8))$ for all $p \in A_n$.
3. Prove that for all $a, b \in U_n$ with $t_{\mathbf{C}}(a) \geq 6, t_{\mathbf{C}}(b) \geq 1$ we have

$$\sum_{p \in \text{ZZ}(a, b)} R(p) = \sum_{p \in \text{ZZ}(a, b) \cap A_n} R(p) \tag{29}$$

$$\sum_{p' \in \text{ZZ}(\mathbf{c}_n(a), \mathbf{c}_n(b))} R(p') = \sum_{p' \in \text{ZZ}(\mathbf{c}_n(a), \mathbf{c}_n(b)) \cap \text{im } \Phi_n} R(p'). \tag{30}$$

Once the three tasks are completed, one can calculate

$$\begin{aligned}\partial_{b,a} &= \sum_{p \in \text{ZZ}(a,b)} R(p) = \sum_{p \in \text{ZZ}(a,b) \cap A_n} R(p) = \\ &= \sum_{p' \in \text{ZZ}(\epsilon_n(a), \epsilon_n(b)) \cap \text{im } \Phi_n} R(p') = \sum_{p' \in \text{ZZ}(\epsilon_n(a), \epsilon_n(b))} R(p') = \partial_{\epsilon_n(b), \epsilon_n(a)}\end{aligned}$$

for any $a, b \in U_n$ with $t_{\mathcal{C}}(a) \geq 6$ and $t_{\mathcal{C}}(b) \geq 1$ concluding the proof.

6.2.1 Task 1: setting up Φ_n

Informally, the definition of Φ_n will consist of *local subpaths* $B_m(p)$ which are transformed into different *global environments* $s, r \in \mathcal{R}$ with *surgey maps* $\Lambda_{s,t}$ and then appended on both sides with *local moves* such as \diamond_m and ∇_m . Let us dive into the specifics.

Let $p = (p_1 \rightarrow \dots \rightarrow p_{2k}) \in Z_n$ be a zig-zag path. For $m \leq n$ and $j < k$ we define the index

$$\beta_m(p, 2j+1) = \min\{l > j \mid l = k \text{ or } i(p_{2l} \rightarrow p_{2l+1}) > 3m\}.$$

We further define $B_m(p)$ to be the first subpath of p satisfying the following conditions:

1. $B_m(p) = (p_{2a+1} \rightarrow \dots \rightarrow p_{2b})$
2. $a = 0$ or $i(p_{2a} \rightarrow p_{2a+1}) > 3m$
3. $b = k$ or $i(p_{2b} \rightarrow p_{2b+1}) > 3m$
4. $i(p_{2j} \rightarrow p_{2j+1}) \leq 3m$ for all $a < j < b$
5. $i(p_{2a+1} \rightarrow p_{2a+2}) \leq 3m$.

Such subpath need not to exist which is why one needs to be slightly careful when using the notation.

The set of global environments \mathcal{R} consists of upper-halves dissected cells of $\Psi[(\sigma_1\sigma_2\sigma_3)^n]$ for varying n , that is,

$$\mathcal{R} = \{r \in \mathcal{S} \mid vr \in \text{cells } \Psi[(\sigma_1\sigma_2\sigma_3)^n], n \in \mathbb{Z}_{\geq 0}, |r| \in 3\mathbb{Z}\}.$$

Recall that a cell of $\Psi[(\sigma_1\sigma_2\sigma_3)^n]$ contains a choice of smoothing, 0 or 1, for each crossing as well as a choice of color, red or blue, for each loop. This data is also present in every $r \in \mathcal{R}$ but additionally there is extra information on the colors (red, blue or black) of the arcs whose boundary is at the bottom of r . This extra data determines whether the arcs in r were boundary arcs in vr (color black) or whether the arcs in r were part of complete loops in vr with either color red or blue.

For words $r, s \in \mathcal{R}$ we denote $r \sim s$, if the connectivity of the underlying Temperley-Lieb diagrams of r and s are the same. This defines an equivalence relation on \mathcal{R} and we denote the equivalence classes by $[r]_{\sim}$. Given $r \in \mathcal{R}$ we define a function $\text{col}_r: [r]_{\sim} \rightarrow [r]_{\sim}$ where $\text{col}_r(s)$ is the element in \mathcal{R} which is obtained from s by changing the colors of the bottom boundary arcs of s to match those of r , see Figure 11. A stronger equivalence relation \approx on \mathcal{R} is also needed: $r \approx s$, if $r \sim s$ and $\text{col}_r(s) = r$, that is, r and s almost exactly the same; they may differ only by the coloring of their bottom components.

Given a global environment $s \in \mathcal{R}$ and $n \in \mathbb{Z}_{\geq 0}$ we define

$$V_{s,n} = \{vr \in \text{cells } \Psi[(\sigma_1\sigma_2\sigma_3)^n] \mid r \approx s, t_{\mathcal{C}}(v) \geq 1\}$$

and for any $t \in [s]_{\sim}$ we have the surgey map

$$\Lambda_{s,t,n}: V_{s,n} \rightarrow V_{t,n}, \Lambda_{s,t,n}(vr) = v \text{col}_r(t).$$

where $m = n + \frac{1}{3}(|t| - |w|)$. Suppose that $a, b \in V_{s,n}$ and there is an edge $(a \rightarrow b) \in G(\Psi[(\sigma_1\sigma_2\sigma_3)^n], M_{\text{gr}})$. It follows that there will also exist an edge $\Lambda_{s,t,n}(a) \rightarrow \Lambda_{s,t,n}(b)$ or an edge $\Lambda_{s,t,n}(b) \rightarrow \Lambda_{s,t,n}(a)$ in

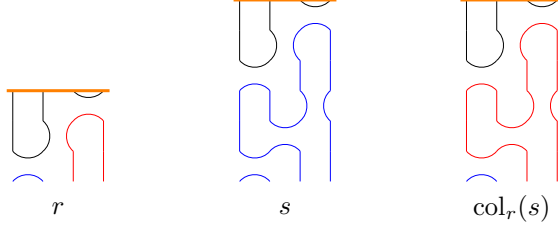


Figure 11: Two global environments $r, s \in \mathcal{R}$. Since $r \sim s$ we can apply col_r to s , and the stronger relation applies: $s \approx \text{col}_r(s)$.

the codomain $G(\Psi[(\sigma_1\sigma_2\sigma_3)^m], M_{\text{gr}})$. The orientation of $a \rightarrow b$ might change under $\Lambda_{s,t,m}$, as a priori it cannot be guaranteed that both or neither of the edges are contained in their respective greedy matchings. Hence $\Lambda_{s,t,m}$ will map an orientation preserving path p to an orientation neglecting path $\Lambda_{s,t,m}(p)$, and it is not immediately clear whether $\Lambda_{s,t,m}(p)$ is an honest orientation preserving path in the directed graph $G(\Psi[(\sigma_1\sigma_2\sigma_3)^m], M_{\text{gr}})$.

As previously stated, Φ_n cannot be built only by using graph isomorphisms, e.g. suitable maps Λ . To patch this lack of bijectivity, Figures 12 and 13 present additional local moves $\Diamond_m \nabla_m \llbracket_m \Diamond_m^{-1}, \nabla_m^{-1}, \overline{\nabla}, \overline{\nabla}^{-1}, \overline{\llbracket}$ which are employed to describe Φ_n , whenever it fails to map vertices of paths in a one-to-one correspondence. The local moves are chained together to stretch the paths and make them longer. For example by stating that a path $p = (p_1 \rightarrow \dots \rightarrow p_{2k}) \in Z_n$ satisfies equation

$$p = \overline{\nabla} \llbracket_{n-3} B_{n-3}(p) \overline{\nabla}^{-1}$$

we mean that $p_1 \rightarrow p_2 \rightarrow p_3$ follows $\overline{\nabla}$, then $p_3 \rightarrow p_7$ follows \llbracket_{n-3} , then $p_7 \rightarrow p_{2k-2}$ follows $B_{n-3}(p)$ and finally $p_{2k-2} \rightarrow p_{2k}$ follows $\overline{\nabla}^{-1}$. More specifically, Morse layers $3n-11$ to $3n-3$ of p_3 are as in picture $\overline{\nabla}(iii)$ and Morse layers $3(n-3)$ to $3(n-1)$ of the same vertex p_3 are as in picture $\llbracket_{n-3}(i)$.

Finally we can define Φ_n and A_n . Assuming that $p \in Z_n$ is a path for which $B_{n-2}(p)$ exists we assign

$$p = B_{n-2}(p) \implies \Phi_n(p) = \Lambda(B_{n-2}(p)) \quad (31)$$

$$p = \llbracket_{n-2} B_{n-2}(p) \implies \Phi_n(p) = \llbracket_{n+2} \Diamond_n \llbracket_{n-2} \Lambda(B_{n-2}(p)) \Diamond_n^{-1} \quad (32)$$

$$p = \Diamond_{n-2} B_{n-2}(p) \Diamond_{n-2}^{-1} \implies \Phi_n(p) = \Diamond_{n+2} \llbracket_n \Diamond_{n-2} \Lambda(B_{n-2}(p)) \Diamond_{n-2}^{-1} \Diamond_{n+2}^{-1} \quad (33)$$

$$p = \nabla_{n-2} B_{n-2}(p) \nabla_{n-2}^{-1} \implies \Phi_n(p) = \nabla_{n+2} \nabla_n \nabla_{n-2} \Lambda(B_{n-2}(p)) \nabla_{n-1}^{-1} \nabla_{n+1}^{-1} \overline{\nabla}^{-1} \quad (34)$$

and assuming that $B_{n-3}(p)$ exists we assign

$$p = \overline{\nabla} \nabla_{n-3} B_{n-3}(p) \nabla_{n-2}^{-1} \implies \Phi_n(p) = \overline{\nabla} \nabla_{n+1} \nabla_{n-1} \nabla_{n-3} \Lambda(B_{n-3}(p)) \nabla_{n-2}^{-1} \nabla_n^{-1} \nabla_{n+2}^{-1} \quad (35)$$

$$p = \overline{\nabla} \llbracket_{n-3} B_{n-3}(p) \overline{\nabla}^{-1} \implies \Phi_n(p) = \overline{\nabla} \llbracket_{n+1} \Diamond_{n-1} \llbracket_{n-3} \Lambda(B_{n-3}(p)) \Diamond_{n-1}^{-1} \overline{\nabla}^{-1} \quad (36)$$

$$p = \overline{\llbracket} \Diamond_{n-3} B_{n-3}(p) \Diamond_{n-3}^{-1} \implies \Phi_n(p) = \overline{\llbracket} \Diamond_{n+1} \llbracket_{n-1} \Diamond_{n-3} \Lambda(B_{n-3}(p)) \Diamond_{n-3}^{-1} \Diamond_{n+1}^{-1} \quad (37)$$

$$p = \llbracket_{n-3} B_{n-3}(p) \implies \Phi_n(p) = \llbracket_{n+1} \Diamond_{n-1} \llbracket_{n-3} \Lambda(B_{n-3}(p)) \Diamond_{n-1}^{-1}. \quad (38)$$

Denote A_n as the subset of Z_n for which we have defined Φ_n in Implications 31-38. The subscripts of Λ are omitted and they are to be understood from the context: for example in Implication 32 we mean $\Lambda = \Lambda_{s,t,n}$ where vs is the 5th vertex of p , wt is 13th vertex of $\Phi_n(p)$ and $|v| = |w| = 3(n-2)$. This concludes the definitions of Φ_n and A_n and we have therefore completed Task 1.

6.2.2 Task 2: Φ_n is well defined and invariant under R

We will now begin to make use of the assumption $t_{\mathcal{C}}(a) \geq 6$. Recall that by Lemma 5.3 and the classification of unmatched cells the inequality $t_{\mathcal{C}}(a) \geq 6$ implies that

$$a = v(01\mathbf{0001})^{12} \quad \text{or} \quad a = v(01\mathbf{0001})^{12}01\mathbf{0}$$

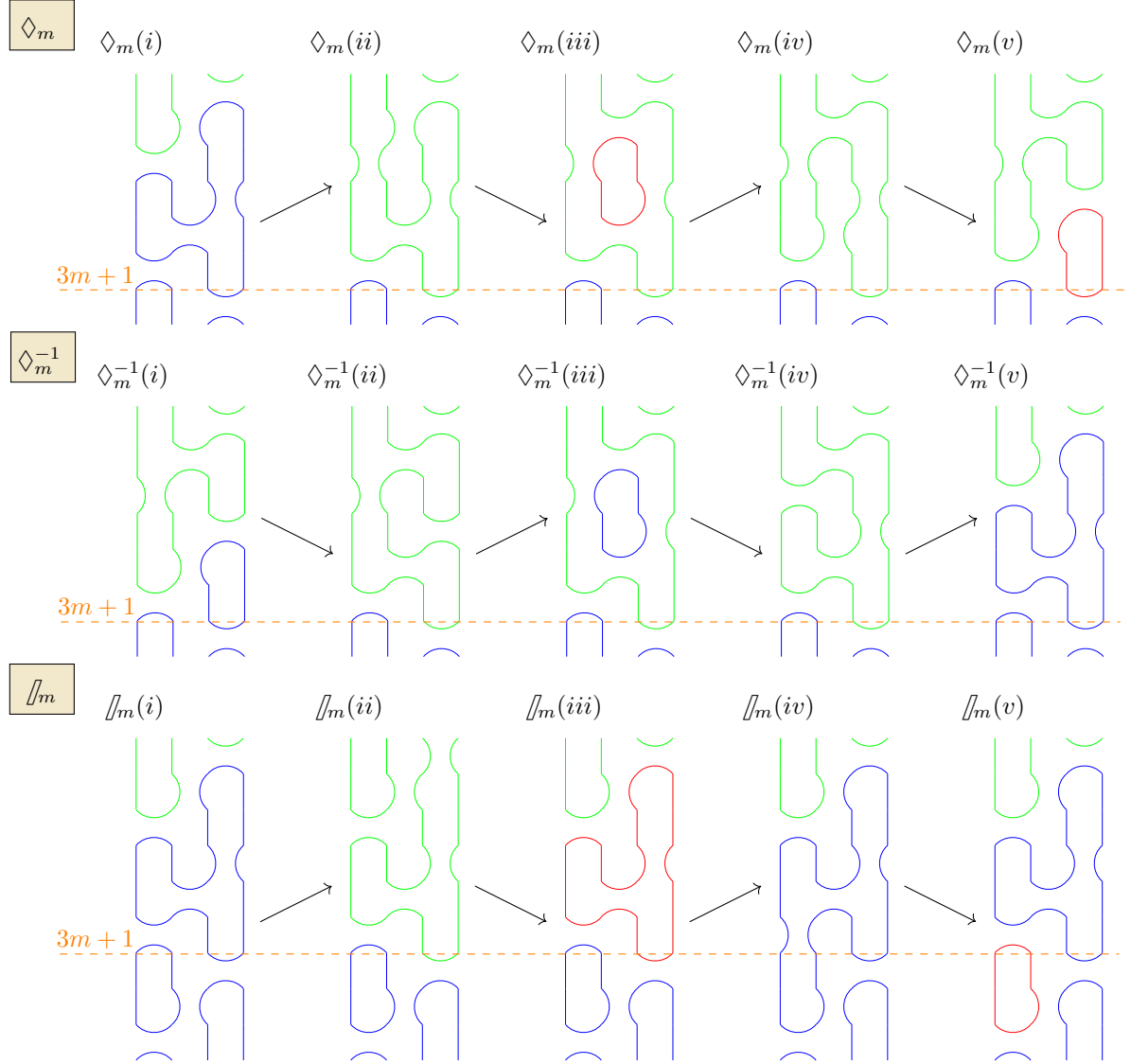


Figure 12: Local moves part I. The typographic naming of the moves tries to mimic their patterns visually: the move \Diamond_m consists of 4 edges which change the smoothings at 4 different crossings forming a diamond. In the move \P_m there are two changes of smoothings in the top right and two in the bottom left and the move ∇_m is a half of \Diamond_m . The superscripts in \Diamond_m^{-1} , ∇_m^{-1} , $\overline{\nabla}^{-1}$ suggest that these inverses of the moves \Diamond_m , ∇_m , $\overline{\nabla}$ in an informal sense. The subscript m determines the Morse layer, where the local move is applied. The slope on the arrows indicate whether they are going upwards or downwards in the homological degree. In the Morse complexes, all paths that contribute towards the differentials have to zig-zag between homological layer and hence all the local moves are also always zig-zagging.

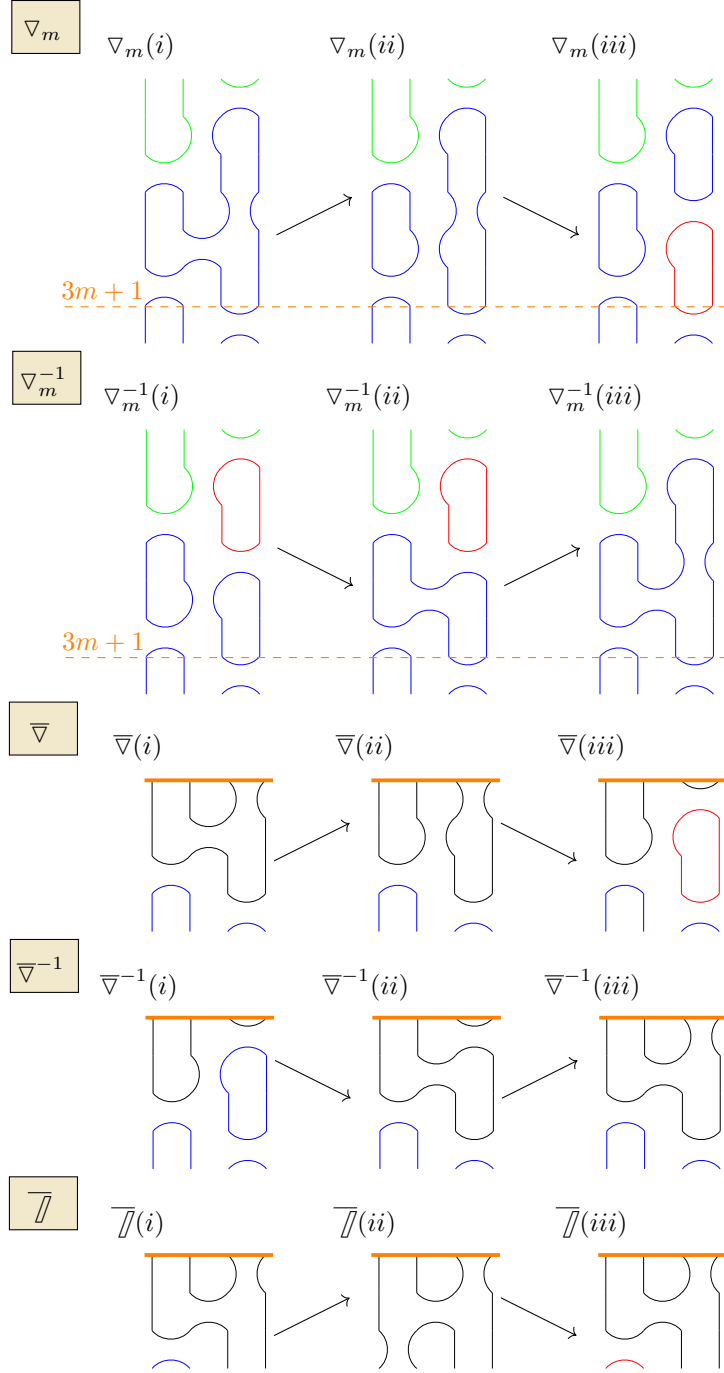


Figure 13: Local moves part II. The moves ∇ , ∇^{-1} , $\overline{\nabla}$ are always located at the very top of the braid which is drawn with an orange line in the pictures.

for some $v \in \mathcal{S}$. Inside this repeating region, it will be easier for us to control how edges and paths behave. The next combinatorial lemma confines the quantum degree of the relevant zig-zag paths.

Lemma 6.2. *Let a, b be unmatched cells of U_n with $\text{hdeg}(a) + 1 = \text{hdeg}(b)$. Assume that there exists a path from a to b in $G(\Psi[(\sigma_1\sigma_2\sigma_3)^n], M_{\text{gr}})$. Then $\text{qdeg}(b) \leq \text{qdeg}(a) + 3$.*

Proof. Denote $o(w)$ as the number of characters 1 at the start of the word w for any vertex w in $G(\Psi[(\sigma_1\sigma_2\sigma_3)^n], M_{\text{gr}})$. It follows from Lemma 3.5 that o is increasing along edges and paths. Hence it suffices to show that for all $n \geq 0$ and unmatched cells a, b of U_n the following implication holds:

$$h(a) + 1 = h(b), \quad o(a) \leq o(b) \implies q(b) \leq q(a) + 3. \quad (39)$$

The differences of h, o, q do not vary under γ_* recursions, that is, for all $* \in \{\mathcal{A}, \mathcal{B}, \mathcal{C}\}$ and unmatched cells a, b we have:

$$\begin{aligned} h(\gamma_*(a)) - h(\gamma_*(b)) &= h(a) - h(b) \\ o(\gamma_*(a)) - o(\gamma_*(b)) &= o(a) - o(b) \\ q(\gamma_*(a)) - q(\gamma_*(b)) &= q(a) - q(b). \end{aligned}$$

Thus if Implication 39 holds for a pair a, b , then for all $* \in \{\mathcal{A}, \mathcal{B}, \mathcal{C}\}$, it will hold for the pair $\gamma_*(a), \gamma_*(b)$ too.

We start out by verifying Implication 39 for all $n = 0, \dots, 82$ with `basecases.py`. Next we assume that Implication 39 holds for $n - 4$ where $n \geq 83$ and take a, b to be unmatched cells of U_n with $h(a) + 1 = h(b)$ and $o(a) \leq o(b)$.

Case: $t_{\mathcal{A}}(a) \geq 2$. From Lemma 5.3 it follows that $a = \gamma_{\mathcal{A}}(x)$ for some unmatched cell x of C_{n-4} . Since $o(a) \leq o(b)$, it is easy to see that $b = \gamma_{\mathcal{A}}(y)$ for some y also. Since Implication 39 holds for x, y by the induction assumption, we get $q(b) \leq q(a) + 3$.

Case: $t_{\mathcal{A}}(a) < 2, t_{\mathcal{C}}(b) < 2$. From our assumptions and Lemma 4.5 we get the following set of equalities and inequalities:

$$-\frac{3}{2} \leq t_{\mathcal{A}}(a) < 2, \quad -\frac{3}{2} \leq t_{\mathcal{C}}(a), \quad -\frac{3}{2} \leq t_{\mathcal{A}}(b), \quad -\frac{3}{2} \leq t_{\mathcal{C}}(b) < 2, \quad h(a) + 1 = h(b), \quad n \geq 83.$$

By using `Lean`'s `linarith` tactic, these can be seen to imply $t_{\mathcal{B}}(a) \geq 2$ and $t_{\mathcal{B}}(b) \geq 2$. It follows that there exists x, y with $b = \gamma_{\mathcal{B}}(x)$, $a = \gamma_{\mathcal{B}}(y)$ and hence $q(b) \leq q(a) + 3$ holds by the induction assumption.

Case: $t_{\mathcal{C}}(b) \geq 2, t_{\mathcal{C}}(a) \geq 2$. As in the previous case, this immediately suffices.

Case: $t_{\mathcal{C}}(b) \geq 2, t_{\mathcal{C}}(a) < 2$. Opening up the definition of $t_{\mathcal{C}}$ gives

$$-\frac{9}{4}n + h(a) - \frac{3}{4}q(a) - \frac{1}{4} < 2 \leq -\frac{9}{4}n + h(a) + 1 - \frac{3}{4}q(b) - \frac{1}{4}$$

which directly implies $q(a) + \frac{4}{3} > q(b)$. □

In order to prove that the maps Λ induce graph isomorphisms between graphs G , we need to partially classify the edges of M_{gr} in $G(\Psi[(\sigma_1\sigma_2\sigma_3)^n])$.

Lemma 6.3. *Let $(a \rightarrow b) \in M_{\text{gr}}$ for the graph $G(\Psi[(\sigma_1\sigma_2\sigma_3)^n])$. Suppose that $u(a \rightarrow b) > 3m$ and write $a = c_1 \dots c_{3n}$, $b = d_1 \dots d_{3n}$ as strings of characters. Assume that $t_{\mathcal{C}}(c_1 \dots c_{3m}) \geq 1$. Then $(c_1 \dots c_{3m}) = (d_1 \dots d_{3m}) \in U$ and $a \rightarrow b$ is of one of the following the types in Figure 14 for some $k \geq 1$. In particular $i(a \rightarrow b) > 3m$.*

Proof. Since $t_{\mathcal{C}}(c_1 \dots c_{3m}) \geq 1$, it follows from Lemma 5.3 that $c_1 \dots c_{3m}$ contains at least one instance of the subword $\mathcal{C} = (01\mathbf{000}1)^2$. By comparing this with the definition of W one can see that $c_{3m-6} \dots c_{3m} = 000101\mathbf{0}$ or $c_{3m-9} \dots c_{3m} = 000101\mathbf{000}1$. In the proof of Lemma 5.1, we ran Algorithm 4 for such cells to classify the unmatched cells U . As a by-product we obtained all of the relevant matched arrows in Pictures 26 and 27. Those six arrows are exactly the ones depicted in Figure 14. □

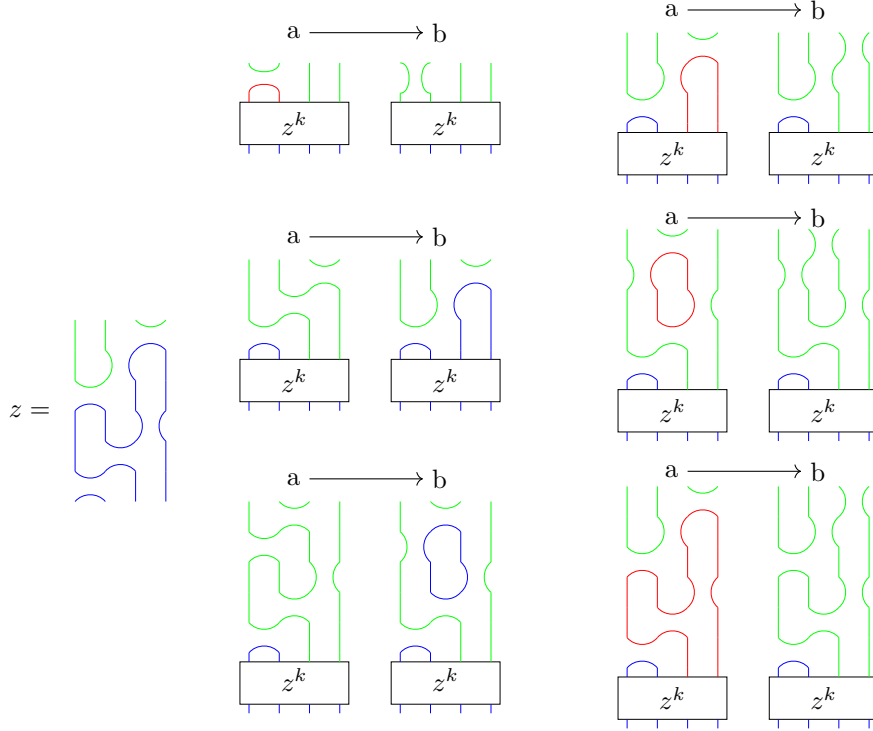


Figure 14: Classification of reversed arrow with u evaluated in the repeating region. The first Morse layer of the pictured subword $z^k = (\mathbf{001010})^k$ is $3m - 5$ or $3m - 8$ in all of the diagrams.

Notice that all of the arrow types of Figure 14 are represented in the local moves, Figures 12 and 13. However, in the graph $G(\Psi[(\sigma_1\sigma_2\sigma_3)^n], M_{\text{gr}})$ these arrows are reversed so the downward arrows from Figures 12 and 13 have opposite direction compared to the ones pictured in Figure 14.

We define a function τ on \mathcal{R} so that computing $t_{\mathcal{C}}$ can be done in parts:

$$t_{\mathcal{C}}(v) + \tau(u) = t_{\mathcal{C}}(vu). \quad (40)$$

Concretely, this is obtained by assigning

$$\tau: \mathcal{R} \rightarrow \mathbb{Q}, \quad \tau(r) = -\frac{1}{4}|r| + \frac{1}{4}(\#1 \text{ in } r) + \frac{3}{4}(\#\mathbf{0} \text{ in } r) - \frac{3}{4}(\#\mathbf{0} \text{ in } r).$$

In order to control the $t_{\mathcal{C}}(v)$ while having a handle on the a whole word $w = vr$ and the global environment $r \in \mathcal{R}$, we set

$$\mathcal{T}: X \times \mathcal{Q} \rightarrow \mathbb{R}, \quad \mathcal{T}(w, r) = t_{\mathcal{C}}(w) - \max\{\tau(s) \mid s \approx r\} - \frac{9}{4}$$

where $X = \bigcup_{n=0}^{\infty} \text{cells}(\Psi[(\sigma_1\sigma_2\sigma_3)^n])$. Recall that given $s \in \mathcal{R}$ and $n \in \mathbb{Z}_{\geq 0}$ we wrote

$$V_{s,n} = \{vr \in \text{cells}(\Psi[(\sigma_1\sigma_2\sigma_3)^n]) \mid r \approx s, t_{\mathcal{C}}(v) \geq 1\}.$$

This set of vertices accompanied with a restricted set of edges

$$E_{s,n} = \{(a \rightarrow b) \in G(\Psi[(\sigma_1\sigma_2\sigma_3)^n], M_{\text{gr}}) \mid a, b \in V_{s,n}, i(a \rightarrow b) \leq 3n - |s|\}.$$

together make up a useful subgraph $G_{s,n} = (V_{s,n}, E_{s,n})$ of the graph $G(\Psi[(\sigma_1\sigma_2\sigma_3)^n], M_{\text{gr}})$. From these subgraph, the paths can be copied with the graph isomorphisms Λ . The next lemma gives us a computable condition which ensures that certain subpaths are contained in $G_{s,n}$.

Lemma 6.4. *Let $p = (p_1 \rightarrow \cdots \rightarrow p_{2k}) \in Z_n$ be a zig-zag path and for each j write $p_j = v_j r_j$ for some $v_j \in \text{cells}(\Psi[(\sigma_1 \sigma_2 \sigma_3)^m])$ and $r_j \in \mathcal{R}$. Suppose $i(p_{2l+1} \rightarrow p_{2l+2}) \leq 3m$ and $\mathcal{T}(p_1, r_{2l+1}) \geq 1$ and denote $b = \beta_m(p, 2j+1)$. Then*

1. $p_{2l+1} \rightarrow \cdots \rightarrow p_{2b}$ is a path in $G_{r,n}$ where $r = r_{2l+1}$
2. $r_{2l+1} \approx r_{2b}$
3. v_{2b} is either of the form $c_1 \dots c_{3m-6} \mathbf{001010}$ or $c_1 \dots c_{3m-9} \mathbf{001010010}$ for some characters $c_i \in \{0, \mathbf{0}, 1\}$.
4. If $p_{2b} \notin U$, then $i(p_{2b} \rightarrow p_{2b+1}) > 3m$ and $p_{2b} \rightarrow p_{2b+1}$ is one of the arrows in Figure 14.

Proof. Claim 1 is proven with an induction on the subpath $p_{2l+1} \rightarrow \cdots \rightarrow p_{2b}$ and it is not difficult to see that Claims 2-4 follow from it. From Lemma 6.2 we get that for all j ,

$$(h(p_j), q(p_j)) \in (h(p_1), q(p_1)) + ([0, 1] \times [0, 3])$$

and hence $t_{\mathcal{C}}(p_j) \in t_{\mathcal{C}}(p_1) + [-\frac{9}{4}, 1]$. Using it, we can compute

$$t_{\mathcal{C}}(v_{2l+1}) = t_{\mathcal{C}}(p_{2l+1}) - \tau(r_{2l+1}) \geq t_{\mathcal{C}}(p_1) - \frac{9}{4} - \max\{\tau(s) \mid s \approx r\} \geq \mathcal{T}(p_1, r_{2l+1}) \geq 1 \quad (41)$$

which means $p_{2l+1} \in G_{r,n}$. Since $i(p_{2l+1} \rightarrow p_{2l+2}) \leq 3m$ we get $r_{2l+1} \approx r_{2l+2}$ and thus the lower bound 41 can be applied for v_{2l+2} as well, yielding $(p_{2l+1} \rightarrow p_{2l+2}) \in G_{r,n}$.

Assume next that $(p_{2l+1} \rightarrow \cdots \rightarrow p_{2t}) \in G_{r,n}$ for some $t > l$ and that $i(p_{2t} \rightarrow p_{2t+1}) \leq 3m$. Then by Lemma 6.3 $u(p_{2t} \rightarrow p_{2t+1}) \leq 3m$ and hence we can get from Lemma 3.3 that $i(p_{2t+1} \rightarrow p_{2t+2}) \leq 3m$. It follows that $r_{2t} \cong r_{2t+1} \cong r_{2t+2}$ and so $(p_{2l+1} \rightarrow \cdots \rightarrow p_{2t+2}) \in G_{r,n}$ which proves Claim 1 by induction. \square

We can now proceed in showing that in certain cases the maps Λ are graph isomorphisms.

Lemma 6.5. *Let $n \in \mathbb{Z}_{\geq 0}$ and $s, t \in \mathcal{R}$ with $s \sim t$. Then $\Lambda_{s,t,n}: V_{s,n} \rightarrow V_{t,m}$ induces a graph isomorphism from $G_{s,n} \rightarrow G_{t,m}$ where $m = n + \frac{1}{3}(|t| - |s|)$. Thus any path p in $G_{s,n}$ will be mapped to an orientation preserving path $\Lambda_{s,t,n}(p)$ and in addition $R(p) = R(\Lambda_{s,t,n}(p))$.*

Proof. It is immediate that $\Lambda = \Lambda_{s,t,n}$ is a bijection and that, both edge sets are the same if one disregards the direction of the arrows. Therefore to show that Λ is a graph isomorphism, it suffices to show that

$$(a \rightarrow b) \in M_{\text{gr}} \iff (\Lambda(a) \rightarrow \Lambda(b)) \in M_{\text{gr}}. \quad (42)$$

for all edges $(a \rightarrow b) \in M_{\text{gr}}$. In case $a \rightarrow b$ is not an isomorphism, it is immediate that Equivalence 42 holds since neither $a \rightarrow b$ nor $\Lambda(a) \rightarrow \Lambda(b)$ are contained in their respective greedy matchings.

Thus we can assume that $a \rightarrow b$ is an isomorphism and writing $u(a \rightarrow b)$ makes sense. If $u(a \rightarrow b) \leq 3n - |s|$ then Equivalence 42 holds by Lemma 3.2. On the other hand $u(a \rightarrow b) > 3n - |s| \geq i(a \rightarrow b)$ is impossible by Lemma 6.3. \square

Proof for Task 2. A straightforward evaluation of \mathcal{T} (albeit tedious due to the number of cases) shows that for all paths $p \in A_n$ and $p \in \text{im } \Phi_n$ we have

$$\mathcal{T}(p_1, r_{2l+1}) \geq 1$$

where p_1 is the first vertex of p and $v_{2l+1}r_{2l+1}$ is the first vertex of the either subpath $B_{n-2}(p)$ or $B_{n-3}(p)$ and $\text{length}(r_{2l+1})$ is 6 or 9 respectively. Thus, it follows from Lemma 6.4 that the subpaths are contained in their respective graphs $G_{s,n}$. Hence, we can use Lemma 6.5 to see that $\Lambda(B_{n-2}(p))$ and $\Lambda(B_{n-3}(p))$ are orientation preserving subpaths and that $R(B_{n-2}(p)) = R(\Lambda(B_{n-2}(p)))$ and $R(B_{n-3}(p)) = R(\Lambda(B_{n-3}(p)))$ as morphisms in $\text{Mat}(\text{Cob}_{\bullet}^3(8))$. Since the local moves are always orientation preserving subpaths, it follows that $\Phi_n(p)$ is an orientation preserving path for all $p \in A_n$.

In order to wrap up the proof, we still need to show that the first and last steps of p and $\Phi_n(p)$ agree under R . This in turn is straightforward evaluation of the functor R . More concretely, say in the case of Implication 33, given

$$(p_1 \rightarrow \cdots \rightarrow p_{2k}) = p = \diamond_{n-2} B_{n-2}(p) \diamond_{n-2}^{-1}, \quad \text{and} \quad (q_1 \rightarrow \cdots \rightarrow q_{2m}) = \Phi_n(p)$$

one can see that $R(p_1 \rightarrow p_5)$ and $R(q_1 \rightarrow q_{13})$ are equal as cobordisms (including signs!) and that similarly $R(p_{2k-4} \rightarrow p_{2k}) = R(q_{2m-8} \rightarrow q_{2m})$. Analogous statements can be verified for Implications 32 and 34-38. \square

6.2.3 Task 3: (co)restrictions to Φ_n coincide with the differentials

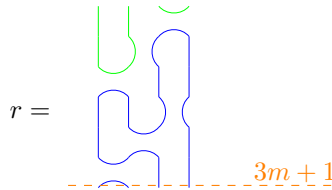
The remaining task in order to prove Proposition 4.4, case \mathbf{c}_n , is to show that under the functor R the set of all zig-zag paths Z_n and Z_{n+4} behave similarly to the sets of paths A_n and $\text{im } \Phi_n$. This is the most laborious part, since it consists of classifying all of the paths of Z_n and Z_{n+4} to an extent. At first, we will work at the minuscule edge-level scale; then the edges are patched up to medium-sized blocks and finally the large scale classification of paths is completed by sewing together the medium-sized blocks.

In any path zig-zag $(p_1 \rightarrow \cdots \rightarrow p_{2k}) \in Z_n$ a downward edge $p_{2j} \rightarrow p_{2j+1}$ is uniquely determined by the vertex p_{2j} since the reversed edges of M_{gr} form a matching on the graph. In most cases, the upward edges $p_{2j+1} \rightarrow p_{2j+2}$ are determined by the value $i(p_{2j+1} \rightarrow p_{2j+2})$, only in the case of splitting a red circle, isomorphism iv) from Figure 5, an additional choice of color needs to be made. This is useful: in Lemma 3.3 we obtained an upper bound for i and the next lemma grants us lower bounds for it.

Lemma 6.6. *Let $p = (p_1 \rightarrow \cdots \rightarrow p_{2k}) \in Z_n$ be a zig-zag path, write $p_{2j+1} = c_1 \dots c_{3n}$ and assume that $\mathcal{T}(p_1, c_{3m+1} \dots c_{3n}) \geq 1$. If $c_{3m+1}c_{3m+2}c_{3m+3} = \mathbf{000}$ or $c_{3m+1} \dots c_{3m+5} = \mathbf{00110}$, where $\mathbf{0} \in \{0, \mathbf{0}, \mathbf{0}\}$,*



then $i(p_{2j+1} \rightarrow p_{2j+2}) \geq 3m + 1$. Also if in either case $i(p_{2j+1} \rightarrow p_{2j+2}) = 3m + 1$ then it cannot hold that $i(p_{2j+2} \rightarrow p_{2j+3}) = u(p_{2j+2} \rightarrow p_{2j+3}) = 3m + 1$. Alternatively, if $i(p_{2j} \rightarrow p_{2j+1}) > 3m + 6$ and $c_{3m+1} \dots c_{3m+5} = \mathbf{001010}$



then $i(p_{2j+1} \rightarrow p_{2j+2}) \geq 3m + 1$.

Proof. Let us consider the first case $c_{3m+1}c_{3m+2}c_{3m+3} = \mathbf{000}$ and assume towards contradiction that $i(p_{2j+1} \rightarrow p_{2j+2}) \leq 3m$. Let $b = \beta_m(p, 2j + 1)$ and write $p_{2b} = d_1 \dots d_{3n}$. Lemma 6.4 yields that $d_{3m+1} \dots d_{3n} \approx c_{3m+1} \dots c_{3n}$ and that $p_{2b} \rightarrow p_{2b+1}$ is one of the arrows from Figure 14. The only arrows compatible with this data match p_{2b} to a higher homological degree which contradicts the fact that p is a zig-zag path. The case $c_{3m+1} \dots c_{3m+5} = \mathbf{00110}$ is proven identically.

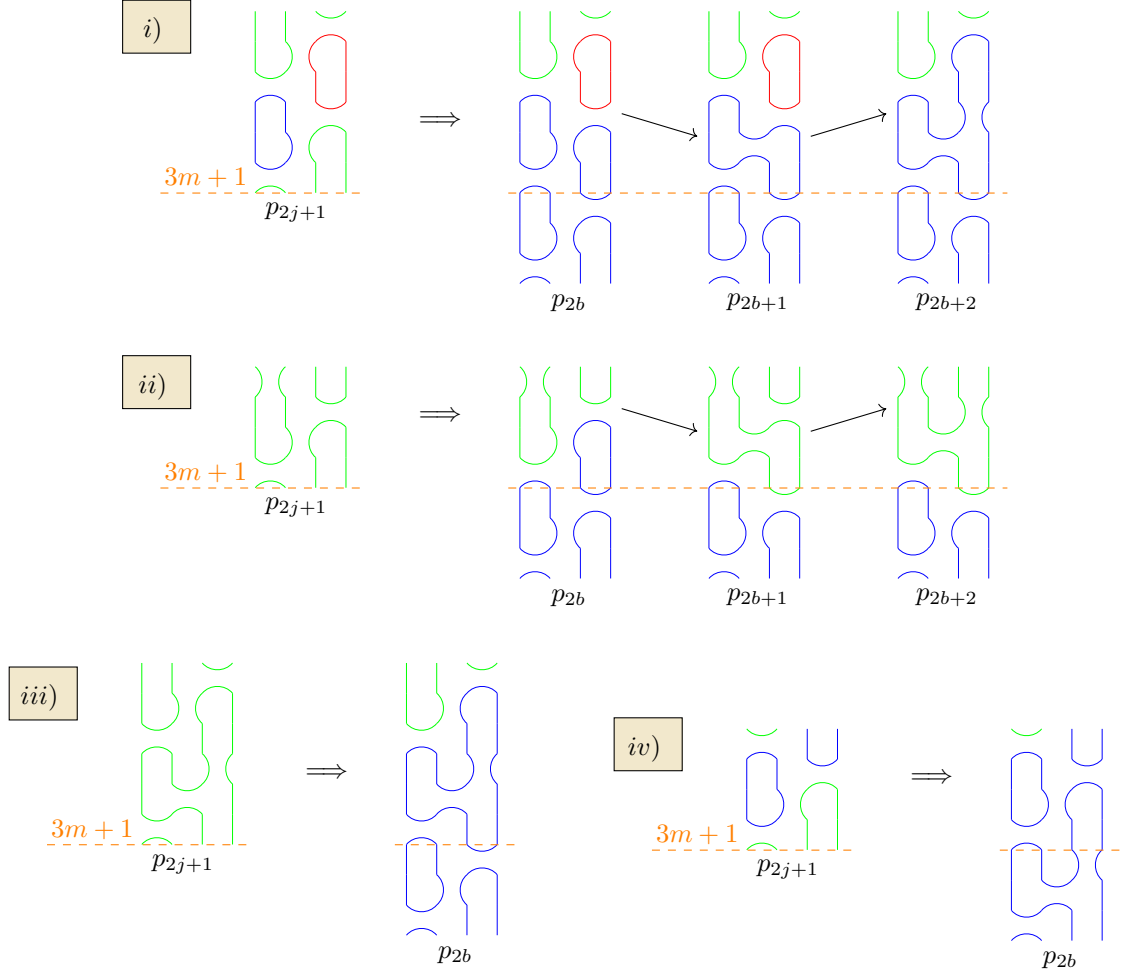
If in either of the cases above, we have $i(p_{2j+1} \rightarrow p_{2j+2}) = 3m + 1$ and $i(p_{2j+2} \rightarrow p_{2j+3}) = u(p_{2j+2} \rightarrow p_{2j+3}) = 3m + 1$, then we can use the claim again to get $3m + 1 \leq i(p_{2j+3} \rightarrow p_{2j+4})$ and

Lemma 3.3 to show that $i(p_{2j+3} \rightarrow p_{2j+4}) \leq 3m + 1$. This is impossible; the arrow $p_{2j+3} \rightarrow p_{2j+4}$ has the wrong direction as we just traversed it from p_{2j+2} to p_{2j+3} .

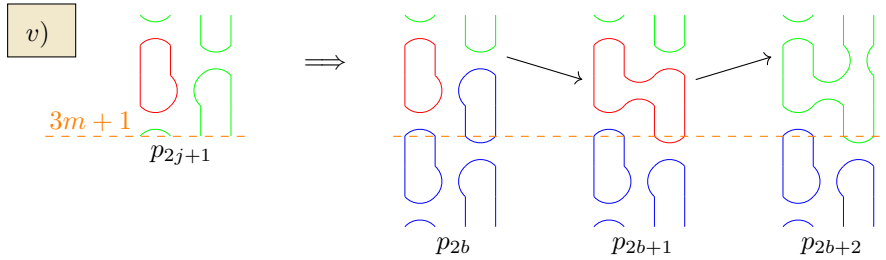
The last case $u(p_{2j} \rightarrow p_{2j+1}) > 3m + 6$ and $c_{3m+1} \dots c_{3m+5} = \mathbf{001010}$ is also similar. If $i(p_{2j+1} \rightarrow p_{2j+2}) < 3m + 1$, assign $b = \beta_m(p, 2j + 1)$ and then $p_{2b} = d_1 \dots d_{3n}$ will be matched up the homological degree due to the classification in Lemma 6.3. \square

Now, we can more concretely pin down implications regarding the next edges after subpaths.

Lemma 6.7. *Let $p = (p_1 \rightarrow \dots \rightarrow p_{2k}) \in Z_n$ be a zig-zag path and write $p_{2j+1} = c_1 \dots c_{3n}$. Assume that $\mathcal{T}(p_1, c_{3m+1} \dots c_{3n}) \geq 1$ and $i(p_{2j+1} \rightarrow p_{2j+2}) \leq 3m$ and denote $b = \beta(p, 2j + 1)$. The following implications determine the Morse layers of p_{2b} based on the Morse layers of p_{2j+1} :*

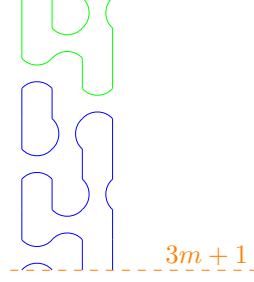


If additionally $\mathcal{T}(p_1, c_{3m+1} \dots c_{3n}) \geq \frac{3}{2}$, then



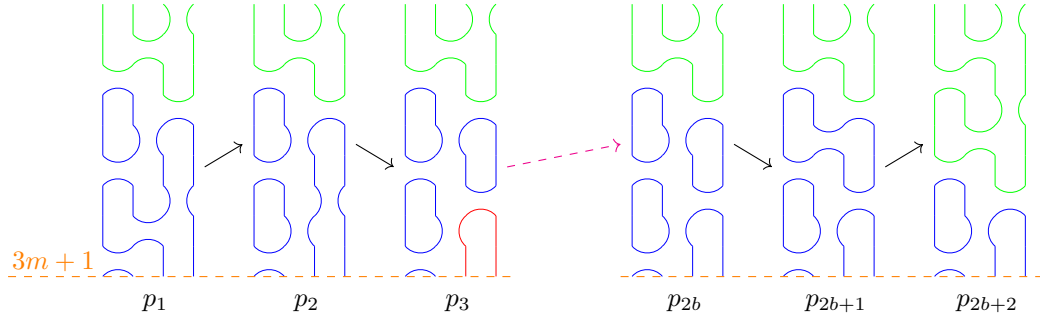
Proof. All of the implications follow from Lemma 6.4: In *i)*, *ii)* and *v)*, $p_{2b} \rightarrow p_{2b+1}$ is the only arrow pictured in Figure 14 which is downward pointing and compatible with $c_{3m+1} \dots c_{3m+4}$ or $c_{3m+1} \dots c_{3m+6}$. In those cases, the second arrow $p_{2b+1} \rightarrow p_{2b+2}$ can be pinned down by excluding other possibilities with Lemmas 3.3 and 6.6. The distinct bound in Implication *v)* follows from the fact that $\mathcal{T}(p_1, d_{3m+1} \dots d_{3n}) + \frac{1}{2} = \mathcal{T}(p_1, c_{3m+1} \dots c_{3n})$ where $d_{3m+1} \dots d_{3n}$ are the last characters of p_{2j+3} . Hence one needs extra cushion in order to guarantee that Lemma 6.6 can be applied. In Implications *iii)* and *iv)*, the depicted p_{2b} is the only configuration which does not get matched up in homological degree. \square

Lemma 6.8. *Let $p = (p_1 \rightarrow \dots \rightarrow p_{2k}) \in Z_n$ be a zig-zag path and write $p_1 = c_1 \dots c_{3n}$. If $c_{3m+1} \dots c_{3m+9} = 001010001$*



and $\mathcal{T}(p_1, c_{3m+1} \dots c_{3n}) \geq \frac{5}{2}$, then $i(p_1 \rightarrow p_2) \neq 3m + 2$.

Proof. Assuming $i(p_1 \rightarrow p_2) = 3m + 2$ leads to



where the $b = \beta_m(p, 3)$. At p_3 , Lemma 3.3 was used to deduce that $i(p_3 \rightarrow p_4) \leq 3m + 3$. There are no arrows with values $i(p_3 \rightarrow p_4) = 3m + 1, 3m + 2, 3m + 3$: at $3m + 1$ two blue circles are merged, $3m + 2$ is already 1-smoothed and at $3m + 3$ the arrow has the wrong direction. By writing $p_3 = d_1 \dots d_{3n}$, we can compute that

$$\frac{5}{2} \leq \mathcal{T}(p_1, c_{3m+1} \dots c_{3n}) = \mathcal{T}(p_1, d_{3m+1} \dots d_{3n}) + \frac{3}{2}$$

and thus Lemma 6.7 iv) can also be applied at p_3 to obtain p_{2b} and p_{2b+1} where $b = \beta_m(p, 3)$. Then at p_{2b+1} we can use Lemmas 3.3 and 6.6 to pin down the i value and acquire the edge $p_{2b+1} \rightarrow p_{2b+2}$. However, the vertex p_{2b+2} is matched upwards and hence p cannot continue as a zig-zag path between the homological levels. This renders the first edge with $i(p_1 \rightarrow p_2) = 3m + 2$ impossible. \square

Lemma 6.9. *Let $p = (p_1 \rightarrow \dots \rightarrow p_{2k}) \in Z_n$ be a zig-zag path. The following implications hold:*

$$(p_{2j-1} \rightarrow p_{2j+1}) = \overline{\mathbb{J}}(i \rightarrow iii) \implies (p_{2j+1} \rightarrow p_{2j+3}) = \diamond_{n-3}(i \rightarrow iii) \quad (43)$$

$$(p_{2j-1} \rightarrow p_{2j+1}) = \overline{\nabla}(i \rightarrow iii) \implies (p_{2j+1} \rightarrow p_{2j+3}) \in \{\nabla_{n-3}(i \rightarrow iii), \mathbb{J}_{n-3}(i \rightarrow iii)\} \quad (44)$$

$$(p_{2j} \rightarrow p_{2j+1}) = \overline{\nabla}^{-1}(i \rightarrow ii) \implies (p_{2j} \rightarrow p_{2j+2}) = \overline{\nabla}^{-1}(i \rightarrow iii) \quad (45)$$

If we further write $p_{2j+1} = c_1 \dots c_{3n}$ and $T = \mathcal{T}(p_1, c_{3m+1} \dots c_{3n})$, then

$$T \geq 1, \quad (p_{2j-1} \rightarrow p_{2j+1}) = \Diamond_m(i \rightarrow iii) \implies (p_{2j-1} \rightarrow p_{2j+3}) = \Diamond_m(i \rightarrow v) \quad (46)$$

$$T \geq 2, \quad (p_{2j-1} \rightarrow p_{2j+1}) = \llcorner_{m+2}(iii \rightarrow v) \implies (p_{2j+1} \rightarrow p_{2j+3}) = \Diamond_m(i \rightarrow iii) \quad (47)$$

$$T \geq \frac{3}{2}, \quad (p_{2j-3} \rightarrow p_{2j+1}) = \Diamond_{m+2}(i \rightarrow v) \implies (p_{2j+1} \rightarrow p_{2j+3}) = \llcorner_m(i \rightarrow iii) \quad (48)$$

$$T \geq 3, \quad (p_{2j-1} \rightarrow p_{2j+1}) = \nabla_{m+2}(i \rightarrow iii) \implies (p_{2j+1} \rightarrow p_{2j+3}) = \nabla_m(i \rightarrow iii) \quad (49)$$

$$T \geq \frac{3}{2}, \quad (p_{2j} \rightarrow p_{2j+1}) = \Diamond_m^{-1}(i \rightarrow ii) \implies (p_{2j} \rightarrow p_{2j+4}) = \Diamond_m^{-1}(i \rightarrow v) \quad (50)$$

$$T \geq 1, \quad (p_{2j} \rightarrow p_{2j+1}) = \nabla_m^{-1}(i \rightarrow ii) \implies (p_{2j} \rightarrow p_{2j+2}) = \nabla_m^{-1}(i \rightarrow iii). \quad (51)$$

Proof. Implication 43: There are 4 meaningful possible values for $i(p_{2j+1} \rightarrow p_{2j+2})$: it is either $3n - 5$, $3n - 3$, $3n - 1$ or $i(p_{2j+1} \rightarrow p_{2j+2}) \leq 3n - 6$. The claim follows from the first option, so we can prove it by excluding the three others. If $i(p_{2j+1} \rightarrow p_{2j+2}) = 3n - 3$, then one can see that the quantum degree increases too much:

$$q(p_1) \leq q(p_{2j+1}) = q(p_{2j}) - 2 = q(p_{2j+2}) - 4 \leq q(p_{2k}) - 4$$

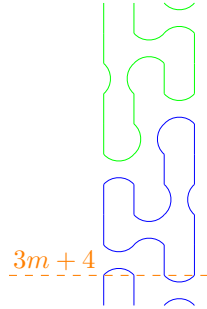
while Lemma 6.2 imposes $q(p_1) \geq q(p_{2k}) - 3$. The value $i(p_{2j+1} \rightarrow p_{2j+2}) = 3n - 1$ is excluded by Lemma 3.3. In the case $i(p_{2j+1} \rightarrow p_{2j+2}) \leq 3n - 6$ we can use Implication ii) of Lemma 6.7 which makes p_{2b+2} be matched upwards, where $b = \beta_{n-2}(p, 2j + 1)$.

Implications 45, 46, 50 and 51 follow by excluding the other possible values of $i(p_{2j+1} \rightarrow p_{2j+2})$ with Lemmas 3.3 and 6.6. For the moment, we postpone the proofs of Implications 44 and 49.

Implication 47: Using Implication v) of Lemma 6.7 at $3m + 3$ excludes $i(p_{2j+1} \rightarrow p_{2j+2}) \leq 3m + 3$ since otherwise p_{2b+2} would be matched upwards, where $b = \beta_{m+1}(p, 2j + 1)$.

Implication 48: There are 4 meaningful possible values for $i(p_{2j+1} \rightarrow p_{2j+2})$: it is either $3m + 6$, $3m + 7$, $i(p_{2j+1} \rightarrow p_{2j+2}) \leq 3m + 3$ or $i(p_{2j+1} \rightarrow p_{2j+2}) \geq 3m + 10$. We deem the case $3m + 7$ impossible by considering the color of the top left green component in the $\Diamond_{m+2}(i)$ diagram. It cannot be blue, since then $p_{2j-3} \rightarrow p_{2j-2}$ would be a merge of two blue circles and thus not a arrow. It cannot be red, since then that component would be blue in the $\Diamond_{m+2}(v)$ which would make $p_{2j+1} \rightarrow p_{2j+2}$ with $i(p_{2j+1} \rightarrow p_{2j+2}) = 3m + 7$ to be a merge of two blue circles. It also cannot be black, as that would increase the quantum degree too much as in the case of Implication 43.

The case $i(p_{2j+1} \rightarrow p_{2j+2}) \geq 3m + 10$ can be ruled out with Lemma 3.3. If $i(p_{2j+1} \rightarrow p_{2j+2}) \leq 3m + 3$, then Implication i) of Lemma 6.7 at $3m + 3$ forces p_{2b+2} to be:



Then $i(p_{2b+2} \rightarrow p_{2b+3}) = 3m + 10$ which causes a contradiction: By Lemma 6.6 at $3m + 10$, $i(p_{2b+3} \rightarrow p_{2b+4}) \geq 3m + 10$ and Lemma 3.3 forces $i(p_{2b+3} \rightarrow p_{2b+4}) \leq 3m + 10$. However, the value $i(p_{2b+3} \rightarrow p_{2b+4}) = 3m + 10$ is impossible, as that arrow is reversed. \square

Given two unmatched cells $a, b \in U_n$, we say that two sets of paths $K, L \subset \mathbb{Z}\mathbb{Z}(a, b)$ are R -equivalent and denote $K \stackrel{R}{\sim} L$, if

$$\sum_{p \in K} R(p) = \sum_{p \in L} R(p).$$

This enables us to rewrite Claim 3 as

$$\text{ZZ}(a, b) \stackrel{R}{\sim} \text{ZZ}(a, b) \cap A_n \quad \text{and} \quad \text{ZZ}(\mathbf{c}_n(a), \mathbf{c}_n(b)) \stackrel{R}{\sim} \text{ZZ}(\mathbf{c}_n(a), \mathbf{c}_n(b)) \cap \text{im } \Phi_n.$$

The following lemma addresses the case where Φ_n does not map all paths of Z_n bijectively to all paths of Z_{n+4} . Instead, the mapping is done up to R -equivalence which suffices for our purposes.

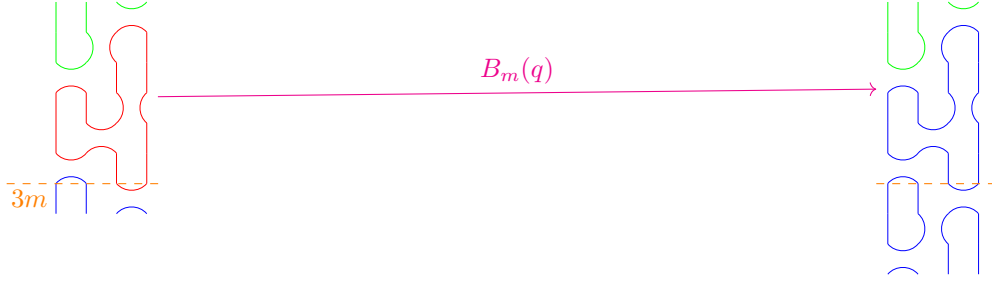
Lemma 6.10. *Let $p_1 \rightarrow \dots \rightarrow p_{2j+1}$ be a zig-zag path in $G(\Psi[(\sigma_1\sigma_2\sigma_3)^n], M_{\text{gr}})$ such that $i(p_l \rightarrow p_{l+1}) > 3m$ for all l . Assume $p_{2j+1} = v.r$ where $r \in \mathcal{S}$, $|v| = 3m$ and $\mathcal{T}(p_1, r) \geq \frac{3}{2}$. Let $y \in U_n$ be an unmatched cell and denote*

$$K = \{(q_1 \rightarrow \dots \rightarrow q_{2k}) \in \text{ZZ}(x, y) \mid q_l = p_l \text{ for } l = 1, \dots, 2j+1, (q_{2j-1} \rightarrow q_{2j+1}) = \text{//}_m(i \rightarrow iii)\}$$

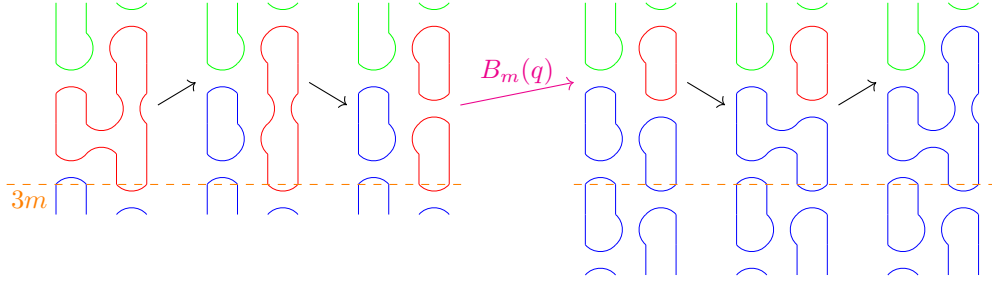
$$L = \{(q_1 \rightarrow \dots \rightarrow q_{2k}) \in \text{ZZ}(x, y) \mid q_l = p_l \text{ for } l = 1, \dots, 2j+1, (q_{2j-1} \rightarrow q_{2j+3}) = \text{//}_m(i \rightarrow v)\}.$$

Then K is R -equivalent to L .

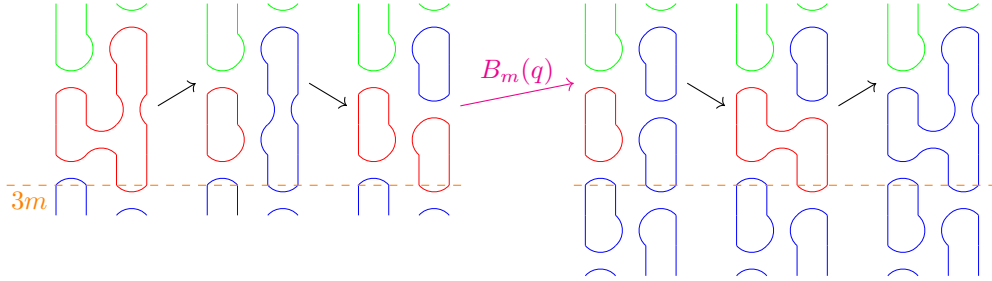
Proof. Throughout this proof, given $q \in K$ we will denote $2b+1$ as the last indices of the subpath $B_{3m}(q)$. In addition to L , we shall define 4 other subsets N_1, \dots, N_4 of K . Let the subset N_1 consist of those zig-zag paths q whose subpath $q_{2j+1} \rightarrow q_{2b+1}$ is of the form



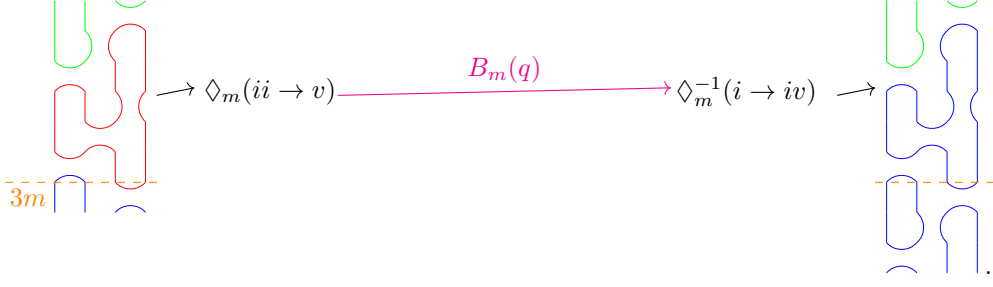
the subset N_2 consist of those zig-zag paths q whose subpath $q_{2j+1} \rightarrow q_{2b+3}$ is of the form



the subset N_3 consist of those zig-zag paths q whose subpath $q_{2j+1} \rightarrow q_{2b+3}$ is of the form



the subset N_4 consist of those zig-zag paths q whose subpath $q_{2j+1} \rightarrow q_{2b+5}$ is of the form



Splitting into cases based on potential values of $i(q_{2j+1} \rightarrow q_{2j+2})$, and further using Lemmas 3.3, 6.6, 6.7 and Implications 46 and 50 from Lemma 6.9 it can be deduced that

$$K = L \sqcup N_1 \sqcup N_2 \sqcup N_3 \sqcup N_4.$$

We can now define a bijection $\Omega_2: N_1 \rightarrow N_2$ which sends $B_m(q)$ to $\Lambda(B_m(q))$, pads it with small subpaths and acts as identity elsewhere. More concretely, if $p = cB_m(q)d \in N_1$, then

$$\Omega_2(q) = c\gamma_2\Lambda(B_m(q))\delta_2d$$

where γ_2 and δ_2 are the 2 edge subpaths from the definition of N_2 . Similarly we define bijections $\Omega_3: N_1 \rightarrow N_3$ and $\Omega_4: N_1 \rightarrow N_4$. It can be verified that Ω_i are well-defined by observing that the subpaths are glued along common vertices. Additionally, the maps Ω_i are bijections, since the maps Λ are graph isomorphisms.

It follows from Lemma 6.5 that $R(B_m(q)) = R(\Lambda(B_m(q)))$ so by computing the value of R on the padding subpaths one can see that

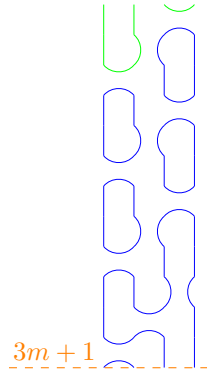
$$R(q) = -R(\Omega_2(q)) = -R(\Omega_3(q)) = R(\Omega_4(q))$$

for all $q \in N_1$. Thus

$$\sum_{q \in K} R(q) = \sum_{q \in L} R(q) + \sum_{q \in N_1} \left(R(q) + R(\Omega_2(q)) + R(\Omega_3(q)) + R(\Omega_4(q)) \right) = \sum_{q \in L} R(q)$$

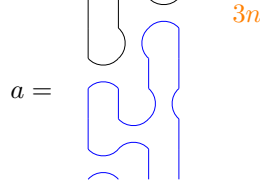
which proves the claim. \square

Proof of Implications 44 and 49 from Lemma 6.9. In Implication 49, there are 4 meaningful possible values for $i(p_{2j+1} \rightarrow p_{2j+2})$: it is either $3m+2$, $3m+6$, or $i(p_{2j+1} \rightarrow p_{2j+2}) \leq 3m+3$ or $i(p_{2j+1} \rightarrow p_{2j+2}) \geq 3m+10$. The two inequalities can be excluded with Lemma 6.6 and 3.3 respectively, so we may assume towards contradiction that $i(p_{2j+1} \rightarrow p_{2j+2}) = 3m+6$. Then $i(p_{2j+2} \rightarrow p_{2j+3}) = 3m+6$, so p_{2j+3} locally coincides with q_{2j+1} from Lemma 6.10. Hence we can use the same classification to deduce that all paths from p_{2j+3} must arrive to a vertex p_{2b} of the form:



and $i(p_{2b} \rightarrow p_{2b+1}) = 3m + 8$. Then a contradiction is reached, since Lemmas 3.3 and 6.6 enforce that $3m + 7 \leq i(p_{2b+1} \rightarrow p_{2b+2}) \leq 3m + 9$, but there are no such arrows in the graph. The candidate arrows are either merges of two blue loops, or a reversed which both make them non-viable. Implication 44 is proven similarly by making use of the classification in the proof of Lemma 6.10. \square

Proof for Task 3. Let $a, b \in U_n$ be unmatched cells with $t_{\mathcal{C}}(a) \geq 6$ and $t_{\mathcal{C}}(b) \geq 1$. Since $t_{\mathcal{C}}(a) \geq 1$, it follows that $a = v.\mathbf{001010}$ or $a = v.\mathbf{001010001}$ for some $v \in U$. Assume first that $a = v.\mathbf{001010}$, that is,



The strategy of proof is to divide $\text{ZZ}(a, b)$ into smaller subsets by the i value of the first edge. To that end, we define

$$I(l) = \{(p_1 \rightarrow \dots \rightarrow p_k) \in \text{ZZ}(x, y) \mid x, y \in C_n, n \in \mathbb{Z}_{\geq 0}, i(p_1 \rightarrow p_2) = l\}.$$

and our goal is to show the subsets $\text{ZZ}(a, b) \cap I(l)$ are R -equivalent with subsets that define A_n resulting in $\text{ZZ}(a, b) \stackrel{R}{\sim} \text{ZZ}(a, b) \cap A_n$.

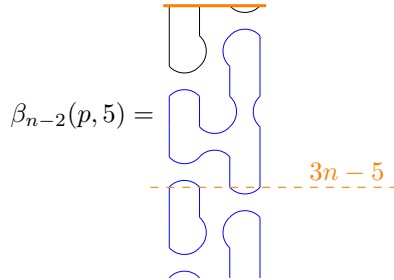
It is immediate that

$$\text{ZZ}(a, b) \cap (I(3n-5) \cup I(3n-3) \cup I(3n-1)) = \emptyset \quad (52)$$

as characters at those indices are either 1:s or correspond to a merge of two blue circles. Next, let $(p_1 \rightarrow \dots \rightarrow p_{2k}) \in \text{ZZ}(a, b) \cap I(3n)$, that is, $i(p_1 \rightarrow p_2) = 3n$. It follows p_2 is matched downwards to p_3 with $i(p_2 \rightarrow p_3) = 3n$ and so $(p_1 \rightarrow p_3) = \llbracket_{n-2}(i \rightarrow iii)$. Hence

$$\begin{aligned} \text{ZZ}(a, b) \cap I(3n) &= \{(p_1 \rightarrow \dots \rightarrow p_{2k}) \in \text{ZZ}(a, b) \mid (p_1 \rightarrow p_3) = \llbracket_{n-2}(i \rightarrow iii)\} \\ &\stackrel{R}{\sim} \{(p_1 \rightarrow \dots \rightarrow p_{2k}) \in \text{ZZ}(a, b) \mid (p_1 \rightarrow p_5) = \llbracket_{n-2}(i \rightarrow v)\} \end{aligned}$$

where Lemma 6.10 is used for the R -equivalence. Supposing now that $p \in \text{ZZ}(a, b)$ and $(p_1 \rightarrow p_5) = \llbracket_{n-2}(i \rightarrow v)$ we can use Lemma 3.3 to obtain that $i(p_5 \rightarrow p_6) \geq 3n - 5$. Since the unique arrow f from p_5 with $i(f) = 3n - 5$ has the wrong direction, we can further deduce that $i(p_5 \rightarrow p_6) \geq 3n - 6$. Thus $B_{n-2}(p)$ is well-defined and by Lemma 6.7 iii) we get that:



where $\beta_{n-2}(p, 5)$ is not matched with any arrow f having $u(f) \leq 3n - 6$. It follows quickly that $\beta_{n-2}(p, 5)$ is an unmatched cell and thus we have shown

$$\text{ZZ}(a, b) \cap I(3n) \stackrel{R}{\sim} \{p \in \text{ZZ}(a, b) \mid p = \llbracket_{n-2} B_{n-2}(p)\}. \quad (53)$$

Similarly, repeatedly using Lemmas 6.9 and 6.10 one proves that

$$ZZ(a, b) \cap \bigcup_{l=1}^{3n-6} I(l) \stackrel{R}{\sim} \{p \in ZZ(a, b) \mid p = B_{n-2}(p)\} \quad (54)$$

$$ZZ(a, b) \cap I(3n-2) \stackrel{R}{\sim} \{p \in ZZ(a, b) \mid p = \diamond_{n-2} B_{n-2}(p) \diamond_{n-2}^{-1}\} \quad (55)$$

$$ZZ(a, b) \cap I(3n-4) \stackrel{R}{\sim} \{p \in ZZ(a, b) \mid p = \nabla_{n-2} B_{n-2}(p) \overline{\nabla}^{-1}\}. \quad (56)$$

Now combining Relations 52, 53, 54, 55 and 56 yields

$$\begin{aligned} ZZ(a, b) &= \left(ZZ(a, b) \cap \bigcup_{l=1}^{3n-6} I(l) \right) \cup (ZZ(a, b) \cap I(3n-4)) \\ &\quad \cup (ZZ(a, b) \cap I(3n-2)) \cup (ZZ(a, b) \cap I(3n)) \\ &\stackrel{R}{\sim} \{p \in ZZ(a, b) \mid p \in \{B_{n-2}(p), \llbracket_{n-2} B_{n-2}(p), \diamond_{n-2} B_{n-2}(p) \diamond_{n-2}^{-1}, \nabla_{n-2} B_{n-2}(p) \overline{\nabla}^{-1}\}\} \\ &= ZZ(a, b) \cap A_n. \end{aligned}$$

For showing that $ZZ(\mathbf{c}_n(a), \mathbf{c}_n(b)) \stackrel{R}{\sim} ZZ(\mathbf{c}_n(a), \mathbf{c}_n(b)) \cap \text{im } \Phi_n$ one analogously verifies

$$ZZ(\mathbf{c}_n(a), \mathbf{c}_n(b)) \cap \bigcup_{l=1}^{n-6} I(l) \stackrel{R}{\sim} \{p \in ZZ(\mathbf{c}_n(a), \mathbf{c}_n(b)) \mid p = B_{n-2}(p)\} \quad (57)$$

$$ZZ(\mathbf{c}_n(a), \mathbf{c}_n(b)) \cap I(3n+12) \stackrel{R}{\sim} \{p \in ZZ(\mathbf{c}_n(a), \mathbf{c}_n(b)) \mid p = \llbracket_{n+2} \diamond_n \llbracket_{n-2} B_{n-2}(p) \diamond_n^{-1}\} \quad (58)$$

$$ZZ(\mathbf{c}_n(a), \mathbf{c}_n(b)) \cap I(3n+10) \stackrel{R}{\sim} \{p \in ZZ(\mathbf{c}_n(a), \mathbf{c}_n(b)) \mid p = \diamond_{n+2} \llbracket_n \diamond_{n-2} B_{n-2}(p) \diamond_{n-2}^{-1} \diamond_{n+2}^{-1}\} \quad (59)$$

$$ZZ(\mathbf{c}_n(a), \mathbf{c}_n(b)) \cap I(3n+8) \stackrel{R}{\sim} \{p \in ZZ(\mathbf{c}_n(a), \mathbf{c}_n(b)) \mid p = \nabla_{n+2} \nabla_n \nabla_{n-2} B_{n-2}(p) \nabla_{n-1}^{-1} \nabla_{n+1}^{-1} \overline{\nabla}^{-1}\}. \quad (60)$$

The subpaths B_{n-2} in the right-hand side of Relations 57-60 belong in their respective graphs $G_{r,n+4}$. These graphs $G_{r,n+4}$ are isomorphic to graphs $G_{s,n}$ of Relations 53-56 via graph isomorphisms Λ . It follows that the paths in the right-hand side of Relations 57-60 are precisely those of $\text{im } \Phi_n$.

One can also see that for all $l \in 3n-5, \dots, 3n+6, 3n+7, 3n+9, 3n+11$

$$ZZ(\mathbf{c}_n(a), \mathbf{c}_n(b)) \cap I(l) = \emptyset.$$

by using Lemma 6.8. Combining all of this together yields:

$$ZZ(\mathbf{c}_n(a), \mathbf{c}_n(b)) \stackrel{R}{\sim} ZZ(\mathbf{c}_n(a), \mathbf{c}_n(b)) \cap \text{im } \Phi_n.$$

The secondary case $a = v.001010001$ is proven similarly: Relations

$$ZZ(a, b) \cap \bigcup_{l=1}^{3n-6} I(l) \stackrel{R}{\sim} \{p \in ZZ(a, b) \mid p = B_{n-2}(p)\} \quad (61)$$

$$ZZ(a, b) \cap I(3n-1) \stackrel{R}{\sim} \{p \in ZZ(a, b) \mid p \in \{\overline{\nabla} \nabla_{n-3} B_{n-3}(p) \nabla_{n-2}^{-1}, \overline{\nabla} \llbracket_{n-3} B_{n-3}(p) \overline{\nabla}^{-1}\}\} \quad (62)$$

$$ZZ(a, b) \cap I(3n-2) \stackrel{R}{\sim} \{p \in ZZ(a, b) \mid p = \overline{\llbracket} \diamond_{n-3} B_{n-3}(p) \diamond_{n-3}^{-1}\} \quad (63)$$

$$ZZ(a, b) \cap I(3n-3) \stackrel{R}{\sim} \{p \in ZZ(a, b) \mid p = \llbracket_{n-3} B_{n-3}(p)\} \quad (64)$$

yield $ZZ(a, b) \stackrel{R}{\sim} ZZ(a, b) \cap A_n$ and $ZZ(a, b) \cap I(3n-8) = \emptyset$ by Lemma 6.8. For the codomain,

relations

$$ZZ(\mathbf{c}_n(a), \mathbf{c}_n(b)) \cap \bigcup_{l=1}^{n-6} I(l) \stackrel{R}{\sim} \{p \in ZZ(\mathbf{c}_n(a), \mathbf{c}_n(b)) \mid p = B_{n-2}(p)\} \quad (65)$$

$$ZZ(\mathbf{c}_n(a), \mathbf{c}_n(b)) \cap I(3n+11) \stackrel{R}{\sim} \{p \in ZZ(\mathbf{c}_n(a), \mathbf{c}_n(b)) \mid p \in \{\bar{\nabla} \nabla_{n+1} \nabla_{n-1} \nabla_{n-3} B_{n-3}(p) \nabla_{n-2}^{-1} \nabla_n^{-1} \nabla_{n+2}^{-1}, \bar{\nabla} \llbracket_{n+1} \Diamond_{n-1} \llbracket_{n-3} B_{n-3}(p) \Diamond_{n-1}^{-1} \bar{\nabla}^{-1}\rrbracket\}\} \quad (66)$$

$$ZZ(\mathbf{c}_n(a), \mathbf{c}_n(b)) \cap I(3n+10) \stackrel{R}{\sim} \{p \in ZZ(\mathbf{c}_n(a), \mathbf{c}_n(b)) \mid p = \llbracket \Diamond_{n+1} \llbracket_{n-1} \Diamond_{n-3} B_{n-3}(p) \Diamond_{n-3}^{-1} \Diamond_{n+1}^{-1} \rrbracket\} \quad (67)$$

$$ZZ(\mathbf{c}_n(a), \mathbf{c}_n(b)) \cap I(3n+9) \stackrel{R}{\sim} \{p \in ZZ(\mathbf{c}_n(a), \mathbf{c}_n(b)) \mid p = \llbracket_{n+1} \Diamond_{n-1} \llbracket_{n-3} B_{n-3}(p) \Diamond_{n-1}^{-1} \rrbracket\} \quad (68)$$

yield $ZZ(\mathbf{c}_n(a), \mathbf{c}_n(b)) \stackrel{R}{\sim} ZZ(\mathbf{c}_n(a), \mathbf{c}_n(b)) \cap \text{im } \Phi_n$ whereas $ZZ(\mathbf{c}_n(a), \mathbf{c}_n(b)) \cap \bigcup_{l=3n-5}^{3n+8} I(l) = \emptyset$. \square

7 Matchings on small braids: a numerical investigation

As a test set for our numerical examination, we consider knots up to 12 crossings (12 included). For this set of knots we obtain their (highly non-unique) braid diagrams from KnotInfo [LM25] and call this set of 2977 diagrams \mathcal{B} . By running an exhaustive search we obtain the following.

Numerical Result 7.1. *For 2976 out of 2977 braid diagrams $B \in \mathcal{B}$, the graphs $G(\Psi[B], M_{\text{gr}})$ are acyclic. For exactly one braid diagram $\text{BD}(12_{n784}) \in \mathcal{B}$ the graph $G(\Psi[\text{BD}(12_{n784})], M_{\text{gr}})$, contains directed cycles. Those cycles are of length 12 or longer and the graph $G(\Psi[\text{BD}(12_{n784})], M_{\text{gr}})$ contains no cycles of length strictly less than 12.*

The exceptional braid diagram $\text{BD}(12_{n784}) \in \mathcal{B}$ has 5 strands and 14 crossings and is defined as

$$\text{BD}(12_{n784}) = \sigma_1^{-1} \sigma_4^{-1} \sigma_2^{-1} \sigma_3 \sigma_2 \sigma_4^{-1} \sigma_3 \sigma_3 \sigma_2 \sigma_2 \sigma_1^{-1} \sigma_4^{-1} \sigma_3 \sigma_2.$$

By removing crossings from Γ through trial and error, we find a smaller braid diagram Γ with 10 crossings such that $G(\Psi[\Gamma], M_{\text{gr}})$ also contains an analogous directed cycle and

$$\Gamma = \sigma_1^{-1} \sigma_4^{-1} \sigma_3 \sigma_2 \sigma_3 \sigma_3 \sigma_2 \sigma_2 \sigma_1^{-1} \sigma_4^{-1}.$$

Additionally the cycle is unique in $G(\Psi[\Gamma], M_{\text{gr}})$ and due to its more reasonable size, we can depict it along side Γ in Figure 15:

To numerically measure the effectiveness of discrete Morse theory, we compare the sizes of de-looped complexes $\Psi[B]$ to Morse complexes $M_{\text{gr}}\Psi[B]$, $M_{\text{lex}}\Psi[B]$ and to the minimal complexes. We limit our test set to $\mathcal{B} \setminus \{\text{BD}(12_{n784})\}$ since the greedy matching does not generate a sensible complex on the exceptional braid diagram.

Given a braid B , we write $\min[B] = \min\{\dim_{\text{Kom}}(C) \mid C \simeq [B]\} \in \mathbb{Z}_{\geq 0}$. There are a number of programs which compute integral Khovanov homology of link diagrams using Bar-Natan's algorithm and therefore internally compute $\min[B]$. However (at least without minor tweaking), most of them do not offer inputs and outputs for braid/tangle diagrams as opposed to complete links. As a subsidiary for $\min[B]$, we compute $\min([B]; \mathbb{F}_2)$ which is the minimal size of the complex when taken with \mathbb{F}_2 coefficients and which can be readily computed with `kht++` [Zib25].

It is easy to see that $\min([B]; \mathbb{F}_2) \leq \min[B]$ and since odd torsion seems to be quite rare in Khovanov homology of complete links it seems reasonable to assume that $\min([B]; \mathbb{F}_2)$ is a good estimate for $\min[B]$. A summary of these results can be seen in Table 1 and a more detailed list of the results and the software generated them can be found in [Kel25].

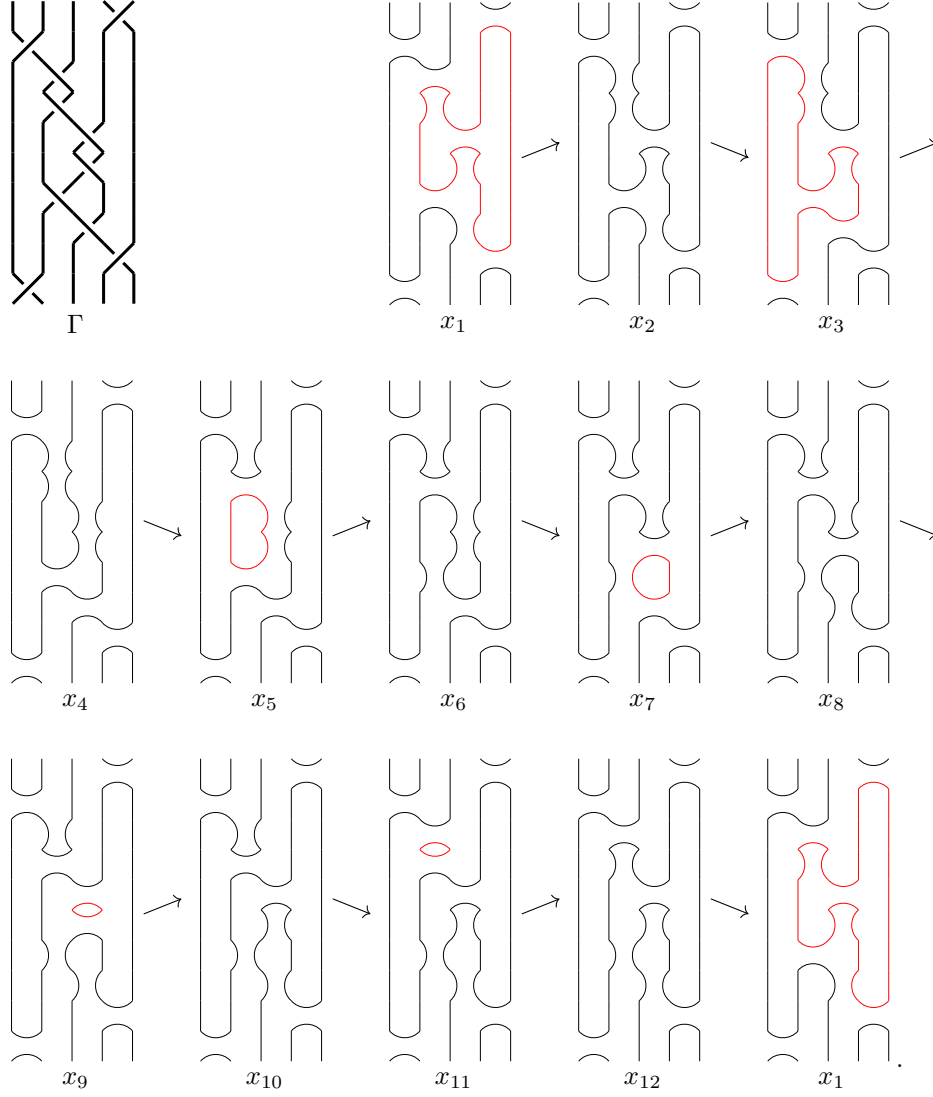


Figure 15: The braid diagram Γ and the unique cycle $x_1 \rightarrow \cdots \rightarrow x_{12} \rightarrow x_1$ of length 12 in the graph $G(\Psi[\Gamma_2], M_{\text{gr}})$

$\mathcal{B} \setminus \{\text{BD}(12_{n784})\}$	$\min(\llbracket B \rrbracket; \mathbb{F}_2)$	$M_{\text{gr}}\Psi[B]$	$M_{\text{lex}}\Psi[B]$	$\Psi[B]$
total cell count	2720982	3217752	7632284	226444836
ratio of total cell count to total cell count of minimal complexes	1.00	1.18	2.80	83.22
minimality obtained	2976/2976	871/2976	396/2976	0/2976

Table 1: A summary of sizes of various complexes for the test set $\mathcal{B} \setminus \{\text{BD}(12_{n784})\}$ of 2976 braid diagrams. On the first row containing numbers, the sum of minimizers $\sum_B \min(\llbracket B \rrbracket; \mathbb{F}_2)$ as well as the sums $\sum_B \dim_{\text{Kom}}(-)$ for different complexes of B are displayed. The second numerical row displays ratios in the row above and the last row displays the number of cases where the Morse complexes end up being minimal. It is noteworthy that the complexes $M_{\text{lex}}\Psi[B]$ obtain minimality exactly when B is an alternating braid diagram. The greedy complexes $M_{\text{gr}}\Psi[B]$ obtain minimality in 475 non-alternating braid diagrams in addition to the 396 alternating ones.

Appendix A: $\text{Kh}^{i,j}(T(4, -n))$ in lowest and highest degrees

This appendix is devoted to five tables presenting the even, unreduced integral Khovanov homology of negative 4-strand torus links in the lowest and highest non-trivial homological degrees. In combination, Figures 1, 16 and 17 describe non-vanishing homology groups $\text{Kh}^{i,j}(T(4, -n))$ for every $i \in \mathbb{Z}$ and $n \geq 28$ whenever such nontrivial groups exist. To save space in the large tables, the symbols \oplus are omitted, e.g., $\mathbb{Z} \mathbb{Z}_2^4 \mathbb{Z}_4$ denotes $\mathbb{Z} \oplus (\mathbb{Z}/2\mathbb{Z})^4 \oplus \mathbb{Z}/4\mathbb{Z}$.

	$-8n$									$-8n + 10$
$-24n + 24$										\mathbb{Z}
										$\mathbb{Z}^4 \mathbb{Z}_2$
								\mathbb{Z}	\mathbb{Z}	$\mathbb{Z} \mathbb{Z}_2^4 \mathbb{Z}_4$
								$\mathbb{Z}^4 \mathbb{Z}_2$	$\mathbb{Z}^5 \mathbb{Z}_2$	$\mathbb{Z} \mathbb{Z}_2^5 \mathbb{Z}_4$
						\mathbb{Z}	\mathbb{Z}	$\mathbb{Z} \mathbb{Z}_2^4 \mathbb{Z}_4$	$\mathbb{Z}^2 \mathbb{Z}_2^2 \mathbb{Z}_4$	$\mathbb{Z} \mathbb{Z}_2$
						$\mathbb{Z}^4 \mathbb{Z}_2$	$\mathbb{Z}^5 \mathbb{Z}_2$	$\mathbb{Z} \mathbb{Z}_2^2 \mathbb{Z}_4$	$\mathbb{Z}_2 \mathbb{Z}_4$	
					\mathbb{Z}	\mathbb{Z}	$\mathbb{Z}^4 \mathbb{Z}_4$	$\mathbb{Z} \mathbb{Z}_2^2 \mathbb{Z}_4$	\mathbb{Z}	
					$\mathbb{Z}^4 \mathbb{Z}_2$	$\mathbb{Z}^5 \mathbb{Z}_2$	$\mathbb{Z} \mathbb{Z}_2$	\mathbb{Z}_2		
			\mathbb{Z}	\mathbb{Z}	$\mathbb{Z}_2^3 \mathbb{Z}_4$	$\mathbb{Z}_2 \mathbb{Z}_4$				
			$\mathbb{Z}^3 \mathbb{Z}_2$	$\mathbb{Z}^4 \mathbb{Z}_2$	\mathbb{Z}					
		\mathbb{Z}	\mathbb{Z}	\mathbb{Z}_2^3	\mathbb{Z}_2					
$-24n + 2$	\mathbb{Z}^3	\mathbb{Z}^3								
$-24n$	\mathbb{Z}^2									

(a) For $n \geq 7$ the unreduced Khovanov homology $\text{Kh}^{i,j}(T(4, -4n))$ for homological degrees $i \leq -8n + 10$.

	$-8n - 4$									$-8n + 6$
$-24n + 10$										\mathbb{Z}^2
									\mathbb{Z}	$\mathbb{Z}^2 \mathbb{Z}_2^2 \mathbb{Z}_4$
								\mathbb{Z}^2	$\mathbb{Z}^3 \mathbb{Z}_2^2$	$\mathbb{Z} \mathbb{Z}_2^2 \mathbb{Z}_4$
								\mathbb{Z}	$\mathbb{Z}^2 \mathbb{Z}_2^2 \mathbb{Z}_4$	$\mathbb{Z} \mathbb{Z}_2$
							\mathbb{Z}^2	$\mathbb{Z}^3 \mathbb{Z}_2^2$	$\mathbb{Z} \mathbb{Z}_2^2 \mathbb{Z}_4$	
						\mathbb{Z}	$\mathbb{Z} \mathbb{Z}_2^2 \mathbb{Z}_4$	$\mathbb{Z} \mathbb{Z}_2^2 \mathbb{Z}_4$	$\mathbb{Z}_2 \mathbb{Z}_4$	
						\mathbb{Z}^2	$\mathbb{Z}^3 \mathbb{Z}_2^2$	$\mathbb{Z} \mathbb{Z}_2$	\mathbb{Z}_2	
				\mathbb{Z}	$\mathbb{Z} \mathbb{Z}_2 \mathbb{Z}_4$	$\mathbb{Z}_2 \mathbb{Z}_4$				
			\mathbb{Z}	$\mathbb{Z}^2 \mathbb{Z}_2^2$	\mathbb{Z}					
		\mathbb{Z}	$\mathbb{Z} \mathbb{Z}_2$	\mathbb{Z}_2						
$-24n - 10$	\mathbb{Z}	$\mathbb{Z} \mathbb{Z}_2$								
$-24n - 12$	\mathbb{Z}^2									

(b) For $n \geq 7$ the unreduced Khovanov homology $\text{Kh}^{i,j}(T(4, -4n - 2))$ for homological degrees $i \leq -8n + 6$.

	$-4n - 1$	$-4n$						$-4n + 6$
$-12n + 13$								\mathbb{Z}
								$\mathbb{Z} \mathbb{Z}_2 \mathbb{Z}_4$
						\mathbb{Z}	$\mathbb{Z}^2 \mathbb{Z}_2$	$\mathbb{Z} \mathbb{Z}_2^2 \mathbb{Z}_4$
						$\mathbb{Z} \mathbb{Z}_2 \mathbb{Z}_4$	$\mathbb{Z}^2 \mathbb{Z}_2^2 \mathbb{Z}_4$	$\mathbb{Z} \mathbb{Z}_2$
					\mathbb{Z}	$\mathbb{Z}^2 \mathbb{Z}_2$	$\mathbb{Z} \mathbb{Z}_2 \mathbb{Z}_4$	$\mathbb{Z}_2 \mathbb{Z}_4$
				$\mathbb{Z}_2 \mathbb{Z}_4$	$\mathbb{Z} \mathbb{Z}_2^2 \mathbb{Z}_4$	\mathbb{Z}		
		\mathbb{Z}	$\mathbb{Z}^2 \mathbb{Z}_2$	$\mathbb{Z} \mathbb{Z}_2$	\mathbb{Z}_2			
		\mathbb{Z}_4	$\mathbb{Z}_2 \mathbb{Z}_4$					
$-12n - 3$	$\mathbb{Z} \mathbb{Z}_2$	\mathbb{Z}						
$-12n - 5$	\mathbb{Z}_2							

(c) For $n \geq 14$ the unreduced Khovanov homology $\text{Kh}^{i,j}(T(4, -2n - 1))$ for homological degrees $i \leq -4n + 6$.

Figure 16: For $n \geq 28$ the unreduced integral Khovanov homology $\text{Kh}^{i,j}(T(4, -n))$ in the lowest non-trivial homological degrees. Outside the marked entries the homology vanishes for $i \leq -8n + 10$, $i \leq -8n + 6$ and $i \leq -4n + 6$ respectively.

References

- [Ali19] Akram Alishahi. “Unknotting number and Khovanov homology”. English. In: *Pac. J. Math.* 301.1 (2019), pp. 15–29.
- [AD19] Akram Alishahi and Nathan Dowlin. “The Lee spectral sequence, unknotting number, and the knight move conjecture”. English. In: *Topology Appl.* 254 (2019), pp. 29–38.
- [BCD25] Aninda Banerjee, Apratim Chakraborty, and Swarup Kumar Das. *A spanning tree model for Khovanov homology, Rasmussen’s s-invariant and exotic discs in the 4-ball*. 2025. arXiv: 2504.02625 [math.GT].
- [Bar05] Dror Bar-Natan. “Khovanov’s homology for tangles and cobordisms.” eng. In: *Geometry & Topology* 9 (2005), pp. 1443–1499.
- [Bar06] Dror Bar-Natan. “Fast Khovanov Homology Computations”. In: *Journal of Knot Theory and Its Ramifications* 16 (July 2006).
- [BGM09] Dror Bar-Natan, Jeremy Green, and Scott Morrisson. *JavaKh-v2*. URL: <https://github.com/geometer/JavaKh-v2>. Sept. 2009.
- [Ben17] M. Benheddi. *Khovanov Homology of Torus Links: Structure and Computations*. 2017.
- [Cha+22] Alex Chandler et al. “Torsion in thin regions of Khovanov homology”. In: *Canadian Journal of Mathematics* 74.3 (2022), pp. 630–654.
- [For98] Robin Forman. “Morse Theory for Cell Complexes”. In: *Advances in Mathematics* 134.1 (1998), pp. 90–145.
- [Fre+10] Michael H. Freedman et al. “Man and machine thinking about the smooth 4-dimensional Poincaré conjecture”. In: *Quantum Topology* 1.2 (June 2010), pp. 171–208.
- [Gil12] William Gillam. “Knot homology of $(3,m)$ torus knots”. In: *Journal of Knot Theory and its Ramifications* 8 (July 2012).
- [GOR13] Eugene Gorsky, Alexei Oblomkov, and Jacob Rasmussen. “On Stable Khovanov Homology of Torus Knots”. In: *Experimental Mathematics* 22.3 (July 2013), pp. 265–281.
- [HS24] Kyle Hayden and Isaac Sundberg. In: *Journal für die reine und angewandte Mathematik (Crelles Journal)* 2024.809 (2024), pp. 217–246.
- [HM19] Matthew Hogancamp and Anton Mellit. *Torus link homology*. 2019. arXiv: 1909.00418 [math.GT].
- [ILM21] Damian Iltgen, Lukas Lewark, and Laura Marino. *Khovanov homology and rational unknotting*. 2021. arXiv: 2110.15107 [math.GT].
- [ILR93] J.M. Isidro, J.M.F. Labastida, and A.V. Ramallo. “Polynomials for torus links from Chern-Simons gauge theories”. In: *Nuclear Physics B* 398.1 (June 1993), pp. 187–236.
- [Kel25] T. Kelomäki. *Code and data to accompany this paper*. https://github.com/Stobelius/DMT_Khovanov/. Accessed: 20.07.2025. 2025.
- [Kel24] Tuomas Kelomäki. *Discrete Morse Theory for Khovanov Homology*. 2024. arXiv: 2306.11186 [math.GT].
- [Kho00] Mikhail Khovanov. “A categorification of the Jones polynomial”. In: *Duke Mathematical Journal* 101.3 (2000), pp. 359–426.
- [Lee05] Eun Soo Lee. “An endomorphism of the Khovanov invariant”. In: *Advances in Mathematics* 197.2 (2005), pp. 554–586.
- [LL16] Lukas Lewark and Andrew Lobb. “New quantum obstructions to sliceness”. In: *Proceedings of the London Mathematical Society* 112.1 (Feb. 2016), pp. 81–114.
- [LMZ24] Lukas Lewark, Laura Marino, and Claudius Zibrowius. *Khovanov homology and refined bounds for Gordian distances*. 2024. arXiv: 2409.05743 [math.GT].
- [LS14] Robert Lipshitz and Sucharit Sarkar. “A Khovanov stable homotopy type”. In: *Journal of the American Mathematical Society* 27.4 (Apr. 2014), pp. 983–1042.

- [LM25] Charles Livingston and Allison H. Moore. *KnotInfo: Table of Knot Invariants*. URL: knotinfo.math.indiana.edu. May 2025.
- [Mal24] Leonardo Maltoni. “Reducing Rouquier complexes”. In: *Proceedings of the London Mathematical Society* 129.1 (June 2024).
- [Man18] Andrew Manion. “The Khovanov homology of 3-strand pretzels, revisited”. In: *New York Journal of Mathematics* 24 (2018), pp. 1076–1100.
- [MO08] Ciprian Manolescu and Peter Ozsvath. *On the Khovanov and knot Floer homologies of quasi-alternating links*. 2008. arXiv: 0708.3249 [math.GT].
- [MU21] Leonardo de Moura and Sebastian Ullrich. “The Lean 4 Theorem Prover and Programming Language”. In: *Automated Deduction – CADE 28*. Springer International Publishing, 2021, pp. 625–635.
- [Nao06] Gad Naot. “The universal Khovanov link homology theory”. English. In: *Algebr. Geom. Topol.* 6 (2006), pp. 1863–1892.
- [ORS13] Peter S Ozsváth, Jacob Rasmussen, and Zoltán Szabó. “Odd Khovanov homology”. In: *Algebraic & Geometric Topology* 13.3 (Apr. 2013), pp. 1465–1488.
- [Pic20] Lisa Piccirillo. “The Conway knot is not slice”. In: *Annals of Mathematics* 191.2 (Mar. 2020).
- [PL16] Krzysztof Putyra and Wojciech Lubawski. “Mirror links have dual odd and generalized Khovanov homology”. In: *Algebraic & Geometric Topology* 16.4 (2016), pp. 2021–2044.
- [Ras10] Jacob Rasmussen. “Khovanov homology and the slice genus”. In: *Inventiones mathematicae* 182.2 (Sept. 2010), pp. 419–447.
- [Ras15] Jacob Rasmussen. “Some differentials on Khovanov–Rozansky homology”. In: *Geometry & Topology* 19.6 (Dec. 2015), pp. 3031–3104.
- [Ren24] Qiuyu Ren. “Lee filtration structure of torus links”. In: *Geometry & Topology* 28.8 (Dec. 2024), pp. 3935–3960.
- [Sch25a] Dirk Schütz. *KnotJob*. URL: <https://www.maths.dur.ac.uk/users/dirk.schuetz/knotjob.html>. May 2025.
- [Sch25b] Dirk Schütz. *On the Khovanov homology of 3-braids*. 2025. arXiv: 2501.11547 [math.GT].
- [Skö06] Emil Sköldberg. “Morse Theory from an Algebraic Viewpoint”. In: *Transactions of the American Mathematical Society* 358.1 (2006), pp. 115–129.
- [Sto07] Marko Stošić. “Homological thickness and stability of torus knots”. In: *Algebraic & Geometric Topology* 7.1 (Mar. 2007), pp. 261–284.
- [Sto09] Marko Stošić. “Khovanov homology of torus links”. In: *Topology and its Applications* 156.3 (Jan. 2009), pp. 533–541.
- [Tur06] Paul Turner. “Calculating Bar-Natan’s characteristic two Khovanov homology”. In: *Journal of Knot Theory and Its Ramifications* 15.10 (2006), pp. 1335–1356.
- [Tur08] Paul Turner. “A spectral sequence for Khovanov homology with an application to $(3, q)$ -torus links”. In: *Algebraic & Geometric Topology* 8.2 (2008), pp. 869–884.
- [Weh08] S. Wehrli. “A spanning tree model for Khovanov homology”. In: *Journal of Knot Theory and Its Ramifications* 17.12 (Dec. 2008), pp. 1561–1574.
- [Zib25] Claudius Zibrowius. *kht++*, a program for computing Khovanov invariants for links and tangles. URL: <https://cbz20.raspberrypi.com/code/khtpp/docs/>. May 2025.